SURFACE AND INTERPHASE STUDIES OF THE ADHESION OF A SILOXANE-MODIFIED-POLYIMIDE COATING ON METALS

by

Tingdong Lin

Thesis submitted to the Faculty of the
Virginia Polytechnic Institute and State University
in partial fulfillment of the requirements for the degree of

MASTER OF SCIENCE

in

Chemistry

APPROVED:

Dr. J. P. Wightman, Chairman

Dr. J. G. Dillard

Dr. J. G. Mason

DECEMBER, 1990

BLACKSBURG, VIRGINIA

ABSTRACT

SURFACE AND INTERPHASE STUDIES OF THE ADHESION

OF A SILOXANE-MODIFIED-POLYIMIDE COATING ON METALS

by

Tingdong Lin

Committee Chairman: James P. Wightman

Chemistry

This research focused on the surface modification and interfacial profile studies of a siloxane modified polyimide, BDS [BTDA (3,3',4,4'-benzophenonetetracarboxylic dianhydride) - DDS (3,3'-diaminodiphenyl sulfone) - PSX (polydimethylsiloxane) copolymer], used as a coating material. The BDS coating surface can be modified by pretreatment in an alkaline solution. This surface pretreatment etched away the top siloxane surface layer, activated the surface by exposing and creating polar functional groups, particularly carboxylic acid groups, and roughened the surface. These changes on the coating surface significantly improved the wettability and the strength of the bond between the coating surface and a polar adhesive. Interfacial composition profiles were obtained from angular dependent X-ray photoelectron spectroscopy and Auger electron spectroscopy. Two kinds of interphases were found near the bond line of the coating/metal substrate. One was a component gradient interphase which was formed by component segregation of the BDS copolymer. The component gradient was different on different metal oxide surfaces with the siloxane interfacial excess in the order of Al > Ti > Zn. The relative acidities of the metal oxide surfaces were characterized by poly(vinyl

chloride) adsorption tests which were quantified by XPS measurements. The relative acidities were found in the order of Al > Ti > Zn. Therefore, the cause for the BDS component segregation was suggested to be the influence of acid-base interactions between components of the BDS copolymer and the metal surface oxides. The other kind of interphase was a polymer-metal oxide mixture interphase which formed on penetration of the BDS copolymer solution into porous aluminum surfaces.

ACKNOWLEDGEMENTS

I would like to express my utmost gratitude to my major adviser Dr. J. P. Wightman. His constant guidance, support and encouragement led to the establishment of my self confidence and ability. His combination of strictness in scientific study and kindness in human life showed me a good example of a scientific career.

I would like to thank Dr. J. G. Mason for his helpful guidance and encouragement. I would like to thank Dr. J. G. Dillard for serving as a committee member and for helpful discussions.

I would like to thank the National Science Foundation Science and Technology Center for financial support.

I would like to thank Dr. D. A. Dillard and Mr. G. Anderson for helping with the peel test.

I would like to thank Dr. J. E. McGrath and Mr. T. H. Yoon for the supply of BDS polymer needed for this research.

I would like to thank Mr. T. F. Cromer for his never-ending patience in helping me in surface analysis. I would also like to thank Mr. Paul Vail for helping with the DSC measurement.

I would like to thank Cathy at the Material Engineering Shop for helping me in metal grinding. I would like to thank individuals at the Physics Shop, Chemistry Glass Shop and Chemistry Electronics Shop for assistance in machining, glassware making and electronic equipment repair.

I would especially like to thank two senior graduate students in my research group, Francis and Pascal for their helpful discussions and constant assistance. I would like to thank all fellow graduate students currently in my research group for their support.

I would like to thank my wife, Yanmei, for her understanding of the time required to finish this project. I would also like to thank my new born daughter Virginia for her cooperation during the time for thesis preparation.

TABLE OF CONTENTS

LIST OF FIGURES

LIST OF SCHEMES

LIST OF TABLES

I. INTRODUCTION

An enormous effort has been made on the development of high performance structural adhesives to meet the demands in the aerospace and electronics industries [1-4]. Attention usually has been directed at the improvement of bulk properties such as thermoxidative stability [5] and processibility [6]. However, if a material is to be used as an adhesive, not only bulk properties but also surface and interface properties of the material must be considered. This is especially the case for some coating materials used in the electronics industry [7]. The coatings are required to have good bulk properties such as ductility and modulus. Such coatings must also show good adhesion to substrates and to other adhesives.

Even if a material has good bulk properties but not good surface or interface properties, it may not be used as a coating. A siloxane modified polyimide which was used in this research may serve as an example.

The siloxane modified polyimide BDS [BTDA (3,3',4,4'-benzophenonetetracarboxylic dianhydride) - DDS (3,3'-diaminodiphenyl sulfone) - PSX (polydimethylsiloxane) copolymer] was developed for use in the electronics industry [8]. Its molecular structure is demonstrated in Scheme I. Its bulk properties such as thermoxidative stability, processibility, and ductility are excellent [9]. However, its surface and interface properties may present problems. Therefore, surface and interface studies on this polymer are needed.

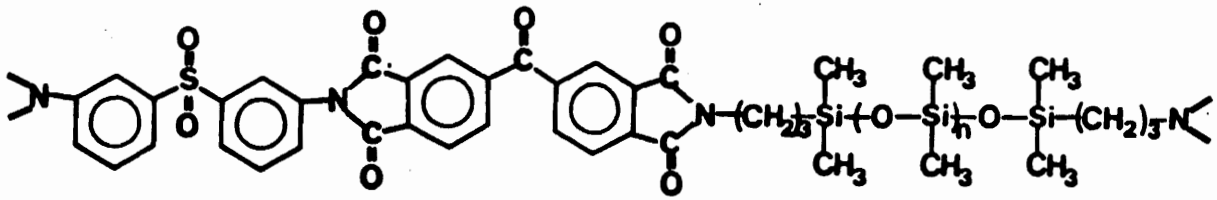

n=15

DDS BTDA PSX

Scheme I. The molecular structure of BDS copolymer.

The surface study should be addressed when the polymer is used as a coating. The BDS copolymer coating formed from solution is usually siloxane enriched on the surface [9] and this surface may be difficult to adhere to metal substrates or other adhesives because the siloxane component has a low surface free energy. Fortunately, there are strong indications that adhesion properties of a polymer film surface can be improved through surface modification [10-11]. Therefore, surface modification of the BDS polymer coating may improve its adhesion properties. However, this kind of research has not been done for this material.

The interface study should also be addressed when the polymer forms a coating on a metal substrate. Two major issues should be raised in the interface studies: wetting of the substrate by the polymer coating and component distribution at the polymer/metal substrate interface. Substrate wetting may be a problem because a polymeric solution is usually viscous. This wetting is even more severe if the substrate is rough or porous [12]. Component distribution of the copolymer against metal surfaces may play an important role in adhesion such as in determining bond strength and durability. There are two kinds of segments in the BDS polymer chain: one is the siloxane flexible segment and the other is the imide rigid segment. The distribution of the two kinds of segments at an interface may affect energy dissipation in adhesion failure and so affect adhesion strength [13]. The distribution may be different on different metal substrates and so lead to different adhesion outcomes. These two major issues should be understood when the material is considered for use as a coating material in the electronics industry. There is no relevant literature addressing these issues for this kind of material.

Surface and interface studies on siloxane modified polyimides are not only practically but also theoretically important. It is expected that these studies may help to understand adhesion phenomena.

The term "adhesion" has different meanings in different research communities. Mittal described adhesion in terms of three categories: basic adhesion, thermodynamic adhesion and practical adhesion [14].

Basic adhesion is the result of the atomic or molecular bonding forces acting between surfaces. This definition is of limited usefulness since it is not yet possible to either directly measure or calculate such quantities, although much progress has been made in theoretical modeling and in development of an atomic force microscope in recent years [15].

The thermodynamic adhesion definition uses the classical Dupre formulation which gives the thermodynamic work of adhesion (Wa),

$$Wa = \gamma_1 + \gamma_2 - \gamma_{12} \qquad [1]$$

where γ_1 and γ_2 are the surface free energies of the two separated materials before bonding, respectively; γ_{12} is the interfacial free energy. The surface free energies and the interfacial free energy should be different for different compositions of the two materials and so should the work of adhesion. However, there is still a lack of studies on the direct relation between the composition of material surfaces and the work of adhesion in bonding.

Practical adhesion is defined as experimentally testable adhesion which is described in terms of bond strength. "Bond strength" is the measured force or work required to separate the two materials. A question that should be asked is, what is the relation between the work of adhesion and the actual adhesion strength. Generally, adhesion strength increases with an increase in the work of adhesion [16-19]. However, the adhesion strength does not have to be linearly related to the work of adhesion [20] because of two reasons in a practical adhesive joint. The first is that a practical adhesion test is affected by extrinsic factors such as manner of loading, stress concentrations, plastic relaxation, and the elasto-plastic behavior of the materials. Thus, a test for adhesion strength is related to the work of adhesion but it can not directly yield values of the latter unless all other factors are known [20]. The second reason is that the definition of the thermodynamic adhesion itself is valid only if there is a physically distinct interface formed between the components, i.e., no molecular interdiffusion. In practice, an adhesive bond line is not a "interface" which is a two dimensional concept. Instead, it is a three dimensional region which has been termed an interphase [21]. This region incorporates all the material from some point in the bulk adhesive toward and through the actual boundary between the adhesive and the adherend to the point where the local properties approach those of the bulk adherend.

Interphases can be classified into two categories: one is the interphase formed by the influence of two materials on each other but with no mass transfer across the bond line boundary. Examples for this kind of interphase include the cross-link density gradient of an adhesive at a bond line [22]. The second kind of

interphase is formed by mass transfer across the bond line boundary such as polymer interdiffusion [23-24] and adhesive penetration into porous metal oxide surfaces [25-30]. Unfortunately, there are very few reports on mechanism studies for these two kinds of interphases, perhaps because of the limited size (in the range of hundreds of nanometers in thickness) and location of the interphase which do not fulfill conventional surface technique requirements [31].

In this research, studies of adhesion of a coating on metal substrates were conducted. These studies included three objectives. The first objective was to confirm that surface pretreatment of the BDS polymer coating in an alkaline solution could change the surface properties and these changes could have a direct relation to adhesion. The second objective was to confirm that the component distribution of the BDS copolymer at the polymer/metal interface is influenced by the metallic oxide and in turn the formation of the interphase. The third objective was to confirm that the BDS polymer solution can wet or penetrate porous metal surfaces such as aluminum and therefore make it possible for the formation of the polymer/metal oxide interphase.

II. LITERATURE REVIEW

2.1. Adhesion Theories

The term "adhesion" has different meanings to different research communities. Qualitatively, it simply means the sticking together of two materials which may be similar or dissimilar [20]. The "science of adhesion" is the fundamental knowledge concerning the nature of the forces of attraction between bodies, determination of the magnitude of such intrinsic forces, and their relation to measured adhesive joint strengths [12]. The science of adhesion is a multi-disciplinary subject. The aspects needed to be considered in the science of adhesion include surface chemistry and physics, rheology, polymer chemistry and physics, stress analysis and fracture analysis. The mechanisms of adhesion are still not fully understood and many theories from different points of view are found in the literature [12]. Basically four mechanisms of adhesion have been proposed, namely,

a). mechanical interlocking;

b). diffusion theory;

c). electronic theory; and,

d). adsorption theory.

2.1.1. Mechanical interlocking

This theory proposes that the major source of intrinsic adhesion is from mechanical keying, or interlocking, of the adhesive into the irregularities of the

substrate surface [32-36]. This theory emphasizes the irregularities of substrates and the penetration of adhesives into the substrate surface. However, the attainment of good adhesion to smooth surfaces shows that this theory does not have general applicability.

Some researchers revised this theory as a combination of contributions from mechanical interlocking and surface force components [37-41]. This revision is further supported by the studies of adhesion strength enhancement through pretreatment of substrate surfaces [25-30].

2.1.2. Diffusion theory

This theory was proposed by Voyutskii [42]. It states that the intrinsic theory of adhesion of high polymers to themselves (autohesion), and to each other, is due to mutual diffusion of polymer molecules across the interface. This requires that the chain segments of the polymers possess sufficient mobility and are mutually soluble. Vasenin has adopted a more fundamental, theoretical approach to the diffusion theory and has related molecular characteristics of the polymer chain to measured joint strength [23,24,43]. However, some researchers have argued that the diffusion theory actually could be explained in terms of wetting kinetics in which intimate molecular contact is established between adhesive and substrate [44]. Some controversial results limited the application scale of the diffusion theory [45]. For instance, in the case of two polymers (adhesive and substrate) adhered together, if the solubility parameters of the polymers are dissimilar, or where one polymer is

highly crosslinked, is crystalline or is above its glass transition temperature, then inter-diffusion is unlikely to make an intrinsic contribution to adhesion.

2.1.3. Electronic theory

If the adhesive and substrate have different electronic band structures, there is likely to be some electron transfer on contact to balance Fermi levels. This transfer will result in the formation of a double layer of electrical charge at the interface. The electrostatic forces arising from such contact or junction potentials may contribute significantly to the intrinsic adhesion [46]. However, calculations from experimental results indicated that the contributions from these electrostatic forces for a typical adhesive joint are actually negligible compared to the contributions from van der Waals forces [47]. The applicability of this theory is thus limited.

2.1.4. Adsorption theory

The adsorption theory is the most generally accepted theory of adhesion [48-51]. This theory proposes that, provided sufficiently intimate intermolecular contact is achieved at the interface, the materials will adhere because of the forces acting between the atoms in the two surfaces. The most common such forces are van der Waals forces and are referred to as secondary bonds. In addition, chemisorption may well occur and thus ionic, covalent and metallic bonds may form at the interface. These types of bonds are referred to as primary bonds. Huntsberger [51] calculated the attractive forces between two planar bulk phases due solely to dispersion forces.

Even at a separation of one nanometer, the attractive force would be approximately 100 MPa which is considerably higher than the experimental strength of most joints.

The thermodynamic work of adhesion required to separate a unit area of two phases forming an interface may be related to the surface free energies by the Dupre equation. In the absence of chemisorption and interdiffusion, the reversible work of adhesion, Wa, in an inert medium may be expressed by equation [1] discussed previously. For the case of a liquid/solid interface, the Young-Dupre equation [52] can be expressed by

$$\gamma_{se} = \gamma_{sl} + \gamma_{lv}\cos\theta \qquad [2]$$

where θ is the contact angle, γ_{se}, γ_{sl} and γ_{lv} are the interfacial free energies of the solid/vapor, solid/liquid and liquid/vapor interfaces, respectively. The solid here is equilibrium with the saturated vapor of the liquid, and its interfacial free energy is different from the surface free energy of the "bare" solid (γ_s). By definition the equilibrium film pressure (π) is given by

$$\pi = \gamma_s - \gamma_{se} \qquad [3]$$

The bare solid means that there is no vapor of the liquid adsorbed on the solid. By combination of equations [1], [2] and [3], the work of adhesion can be related to contact angles as shown below,

$$Wa=\pi + \gamma_{lv}(1+\cos\theta) \quad [4]$$

If π = o, that is, if the difference between γ_s and γ_{se} is negligible which is a general case for polymer films, then

$$Wa = \gamma_{lv}(1+\cos\theta) \quad [5]$$

In terms of contributions to the work of adhesion, Fowkes et al. [53-59] proposed that the major contributions are from dispersive force and acid-base interaction

$$Wa = Wa^{d} + Wa^{ab} \quad [6]$$

where Wa^{d} and Wa^{ab} are the contributions from dispersive force and acid-base interaction, respectively.

In summary, the four theories of adhesion actually emphasize different aspects of adhesion. The electronic theory describes the contribution of electrostatic fields to adhesion which is only a portion of the attractive forces at the interface. The adsorption theory emphasizes the contribution of adhesion from the thermodynamic work of adhesion. The problem for the adsorption theory is that it assumes that the surfaces of the two materials are still distinguishable after bonding. In reality, the two surfaces may be destroyed and the consideration of contributions from the thermodynamic surface free energies may become irrelevant because other parts of the material under the original surfaces may now participate in bonding.

The mechanical interlocking and diffusion theories emphasize the contact between adhesives and substrates either at mechanical level or the molecular level but lack an explanation in terms of molecular force contributions.

All four theories discussed above do not consider a concept called the interphase. An interphase, as defined in the previous chapter, is a 'new-born baby' formed after bonding two materials together. This interphase may have different properties which do not correspond to either those of the two original surfaces or the bulk of the materials. An interphase is important because all load on an adhesive joint has to pass through it. Unfortunately, systematic studies on the interphase or on adhesion mechanisms arising from studies on the interphase are not found in the literature. Research has been reported only for a limited number of specific systems [31,60,61].

2.2. Surface Modification

According to the adsorption theory of adhesion, molecular interactions at the adhesive/substrate interface are the basis of adhesion strength. To improve adhesion for a polymer film to other materials, surface modification usually is needed. The purposes for polymer surface modification primary fall into three categories: cleaning, activating, and roughening.

During processing and handling of polymers, the surfaces can be easily contaminated with processing impurities such as mold release agents and oils. During storage of polymers or during formation of polymer surfaces, some low surface

tension components can segregate from the bulk in the surface. This process often leads to poor adhesion with coatings or adhesives applied to the polymer surfaces. Cleaning involves removal of low surface tension components from the polymer surface [62].

The purpose of activating is to obtain a more chemically reactive or physically polar surface for bonding. This usually can be obtained through the introduction of functional groups on the surface [62]. Roughening increases the surface area which should benefit adhesion.

Surface modification techniques of polymers can be divided into two major categories. One is a dry process which involves no solution in its pretreatment process. The other is a wet process in which the polymers are modified in chemical solutions.

2.2.1. Dry process

The dry process of polymer surface modification usually involves the application of an external exciting source which can be a plasma [11,63-65], a laser [66-67], UV exposure [68-69], ion [70,71], electron beam bombardment [72], or X-ray flux [73]. A commonly used exciting source is a plasma. The principal advantage of polymer surface modification by plasma treatment is experimental simplicity [74,75]. Inexpensive equipment can be used to generate a variety of plasmas and scale-up for industrial application is straight forward. The disadvantage, from an academic viewpoint, is that chemically well-defined surfaces

can not be designed and prepared. The technique is severe and plasma species (electrons, ions, and metastables) and UV radiation induce cascades of reactions involving homolytic bond cleavage, fragmentation, and cross-linking in the polymer surface. This disadvantage applies to the other exciting sources listed above.

There is evidence which indicates that the dry process, typically plasma pretreatment, may cause cross-linking or even forming a silica-like phase in a siloxane containing polymer surface [65]. This change on a polymer surface does not favor adhesion because diffusion of an adhesive into the silica-like phase is difficult. Diffusion of an adhesive into a polymer surface is very important in polymer adhesion [42]. The polymer used in the present research is a siloxane modified polyimide. It has the same problem when pretreated with plasma as described above [9]. This problem with the plasma pretreatment on the siloxane modified polyimide excludes the selection of a "dry process" for the surface pretreatment of the BDS polymer.

2.2.2. Wet process

The wet process for polymer surface modification involves the use of a chemical solution. This process can also be divided into two categories. The first one is to modify a polymer surface by introducing a coating on the surface. This includes polymer adsorption [76] and polymer surface graft polymerization [77-80]. The second one is to change or create functional groups on the polymer surfaces through chemical reaction in a solution. Among the modifications reported in the second category are oxidations, especially of polyethylene [81-89], reductions of

fluoropolymers [10, 90-92], sulfonations [93, 94], dehydrohalogenations [95, 96] and hydrolyses [7, 97, 98]. As an example, the surface hydrolysis of polyimide [7] will be discussed below.

2.2.3. Surface modification of polyimide

Lee et al [7]. recently reported the surface modification of poly(pyromellitic dianhydride-oxydianiline) (PMDA-ODA) through surface reaction in aqueous KOH or NaOH solution at room temperature. The reaction scheme is shown in Scheme II. The polyimide PMDA-ODA was converted into polyamate through an imide ring opening reaction. The polyamate was further acidified into polyamic acid. The XPS (X-ray photoelectron spectroscopy) spectra obtained at a 35° take-off angle clearly indicated these changes. Figure 1a is the C1s spectrum of the polyimide starting material, which had one peak for carbonyl, the highest binding energy peak at about 289 ev. Figure 1b, the spectrum of the polyamate, showed two peaks for carbonyl and is similar to Figure 1c, the spectrum of the polyamic acid. When the polyamic acid was re-cured (Figure 1d), the spectrum was the same as the starting material.

The external reflectance IR (ER-IR) spectra obtained at 37° IR beam incident angle and shown in Figure 2 also clearly indicated the changes on the polymer surface. The starting film was 870Å thick and the whole layer was modified. The important peaks were at 1740 cm^{-1} and 1381 cm^{-1} in Figure 2a. These are the peaks for the imide I and II bands [7]. These peaks disappeared after the polyimide was completely converted to polyamate. Two new pairs of peaks appeared in the polyamate spectrum shown in Figure 2b, at1668 cm^{-1} - 1540 cm^{-1} (amide I and II

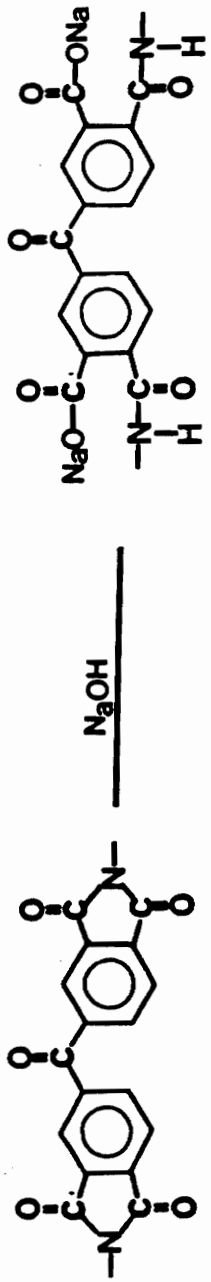

Scheme II. An illustration of imide reactions with bases [7].

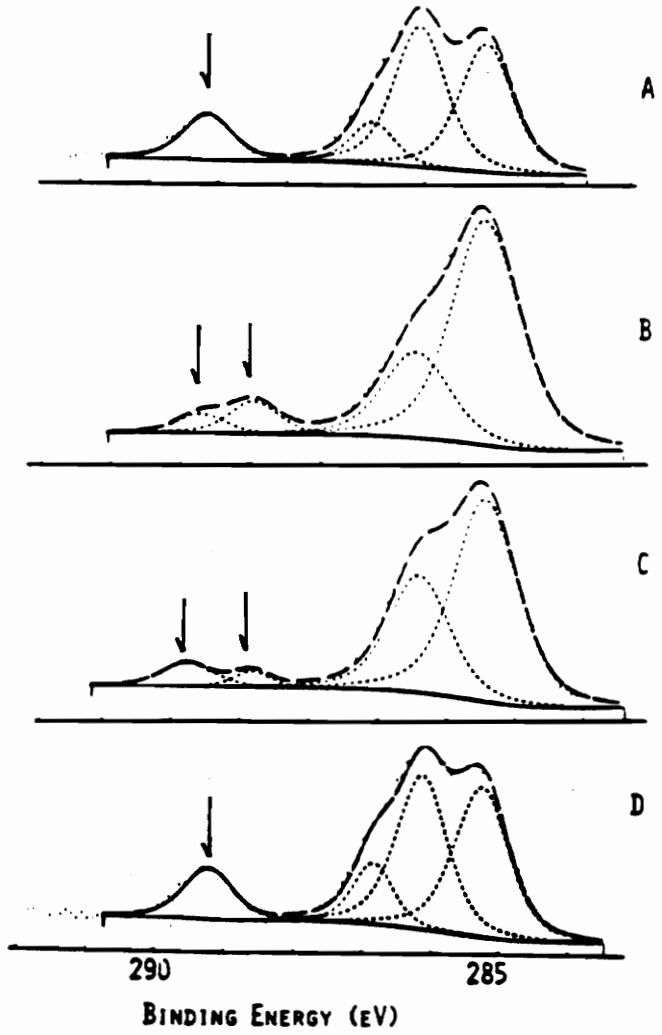

Figure 1. C1s XPS spectra of (a) PMDA-ODA starting material,(b) polyamate, (c) polyamic acid, and (d) re-cured polyimide [7].

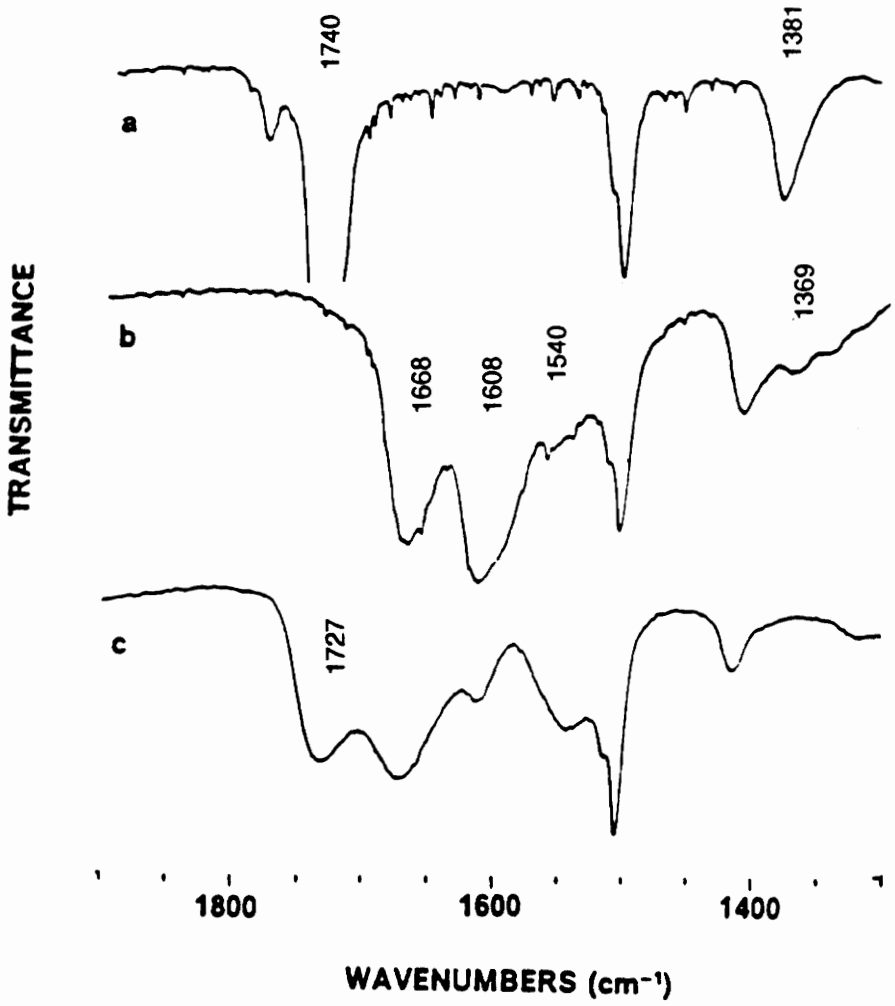

Figure 2. External reflectance IR spectra of (a) PMDA-ODA polyimide, (b) polyamate, (c) polyamic acid [7].

bands) and 1608 cm^{-1} - 1369 cm^{-1} (carboxylate asymmetric and symmetric stretching). When polyamate was converted into polyamic acid (see Fig. 2c), the two peaks for carboxylate almost disappeared and a new peak at 1727 cm^{-1} for the carbonyl of carboxylic acid appeared. The XPS and ER-IR spectra above clearly showed the surface reactions which occurred during surface modification.

Lee et al. [7] also researched surface selectivity of the modification and the relation between surface modification and adhesion. It was found that the surface modification of PMDA-ODA polyimide was surface selective. The modified layer was about 4 nm thick after pretreatment in 1.0 M KOH at 22°C for 2 minutes. Adhesion properties such as water contact angle and peel strength were improved significantly with the modification.

2.2.4. Evaluation methods used in polymer surface modification

Techniques commonly used in the evaluation of polymer surface modification include XPS [7], IRS (infrared spectroscopy) [7,86], SEM (scanning electron microscopy) [86], peel test [7], water contact angle measurement [7, 86, 87] and ellipsometry [7].

Three techniques which were extensively used in this research will be selectively discussed in the following three sections. They are angular dependent XPS which is derived from a conventional XPS, the peel test, and contact angle titration which is derived from a conventional contact angle measurement.

2.2.4.1. Angular dependent XPS

The so-called angular dependent XPS is a measurement in which the take-off angle between a sample surface and the emitted electron beam to the detector is varied so that the sampling depth is changed. This measurement is illustrated in Figure 3. The relation between the sampling depth (d) and the take-off angle θ [99] is given by

$$d = 3\lambda \sin(\theta) \qquad [7]$$

where the sampling depth is defined as the sample depth from which 95 % of the detected signal arises. The mean free path (λ) of the emitted electrons is dependent on the sample material and the kinetic energy of the photoejected electrons. By varying the take-off angle, a sample is measured at different depths from its surface and a surface profile can be obtained.

2.2.4.2. Peel test

Strip peel tests as illustrated in Figure 4 have been used to compare effects of surface preparations [100]. These comparisons are usually conducted by applying a constant rate loading to the specimen and recording the applied force P (force per unit width of the specimen) versus time. An average force after the specimen has reached a maximum load, is reported as the peel strength.

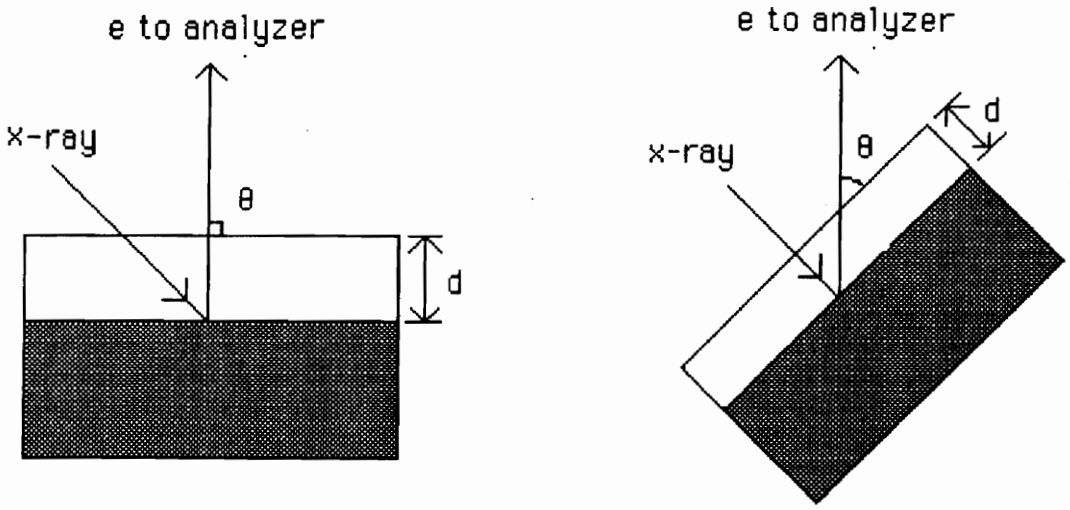

$$d = 3\lambda \sin\theta$$

d ___ sampling depth.
λ ___ electron mean free path.
θ ___ angle between the electron take-off beam and the sample surface.

Figure 3. An illustration of the XPS angular dependent technique.

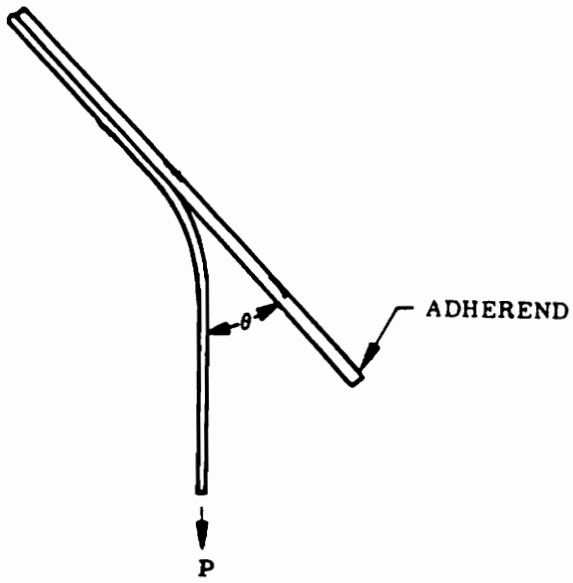

Figure 4. Schematic diagram of peel test specimen [101].

To relate the measured peel strength to the fracture energy which is directly related to the work of adhesion, four assumptions were made [101]

(1). The material is linearly elastic;

(2). The geometry, and therefore the energy stored within the region of large bending, does not change with peeled length;

(3). Debond lengths are long enough so that a portion of the peel specimen has no curvature; and,

(4). The base plate is mechanically rigid (no energy is stored in the plate).

A relation between the fracture energy (γ_a) and the peel strength (P) can be derived [101] as

$$\gamma_a = P\,[(1+\lambda)/2 - \cos\theta\,] \qquad [8]$$

If failure is primarily in the adhesive mode, γ_a approximately equals Wa (the work of adhesion). The term λ is the extension ratio in the zero curvature portion of the peeled strip and θ is the peel angle.

For a 180° peel test which is used in the present research, if a small extension is assumed ($\lambda \sim 1$), equation [8] can be rewritten as

$$P \approx \gamma_a/2 \approx Wa/2 \qquad [9]$$

Equation [9] is only an approximate relation. Some other factors should be considered in a more precise analysis [101].

2.2.4.3. pH contact angle titration

The pH contact angle titration technique was developed by Whitesides et al. [86, 87]. This technique was used to characterize the acidity of pretreated polymer film surfaces. Contact angle titration is similar to a conventional water contact angle measurement. The only difference is that the liquid droplet used in the contact angle titration is a buffer solution of specific pH instead of pure water. The polymer films used by Whitesides et al. were PE-COOH films obtained from pretreatment of polyethylene films with chromic acid solution [86]. Carboxylic acid groups were shown to be present on these films.

The question arises as to how contact angle measurements are sensitive to functional groups on a polymer film surface. Whitesides et al. made three assumptions for the measurements [86].

(i) The surface free energy consists of the sum of contributions from individual groups present at the solid surface and in direct contact with the liquid phase, namely

$$\gamma_{ls} = \Sigma\, \beta_j \gamma_{lsj} \qquad [10]$$

where β_j is the normalized fraction of a particular type of organic group j in the population of groups on the polymer surface in contact with the liquid phase. γ_{ls} is the interfacial free energy and γ_{lsj} is the value of γ_{ls} for a surface completely covered by the group j ($\beta_j = 1$).

(ii) The surface does not reconstruct on changing pH.

(iii) Changing in wetting of the surface with changes in pH are dominated by γ_{ls} . The interfacial free energy of liquid/vapor (γ_{lv}) and interfacial free energy of solid/vapor (γ_{sv}) can be considered to be independent of pH.

The first assumption means that γ_{ls} is determined only by the interaction of the liquid phase with the collection of groups on the exterior surface of the solid; groups in the subsurface region do not influence γ_{ls}. Evidence was presented showing that contact angle measurements can sense only the top 5 Å layer of the solid surface [85].

The second assumption may be difficult to justify in detail. However, from experimental results [88] and other reported results in the literature [102], in order to have significant reconstruction, the films need to be heated up to high temperature or put in water for tens of hours. Whitesides' experiments were always done within minutes. It was expected that the influence from reconstruction was negligible.

The third assumption was checked experimentally as illustrated in Figure 5 [87]. The contact angle of water on surfaces containing no ionizable groups (the upper four lines in Figure 5) is independent of pH. This means that γ_{lv} and γ_{sv} are independent of the pH of the contact liquids.

To evaluate the contact angle titration method, a series of experiments have been done which included tests of film stability, buffer concentration effect, and added salt effect [81-89]. Most importantly, parallel titration measurements have also been done with two independent methods: titration with ATR-IR (attenuated total reflectance infrared) and potentiometric measurements [86]. Results from the contact angle titration agreed very well with those from the two parallel titrations [86]. Whitesides et al. concluded that the contact angle titration method can be used for characterizing the physical-organic chemistry of organic surfaces with ionizable functional groups. The cause for contact angle changing with pH on the PE-COOH film surface is that the unionized species (PE-COOH) and ionized species (PE-COONa) on the film surfaces have a different interfacial free energy when contacted with water [86].

2.3. Properties of the BDS copolymer

2.3.1. Bulk properties

The BDS copolymer used in the present research is a randomly coupled segmented copolymer made from solution imidization [9]. Figure 6 [9] is a FTIR spectrum of a completely imidized (solution imidization for 24 hours at 160 °C)

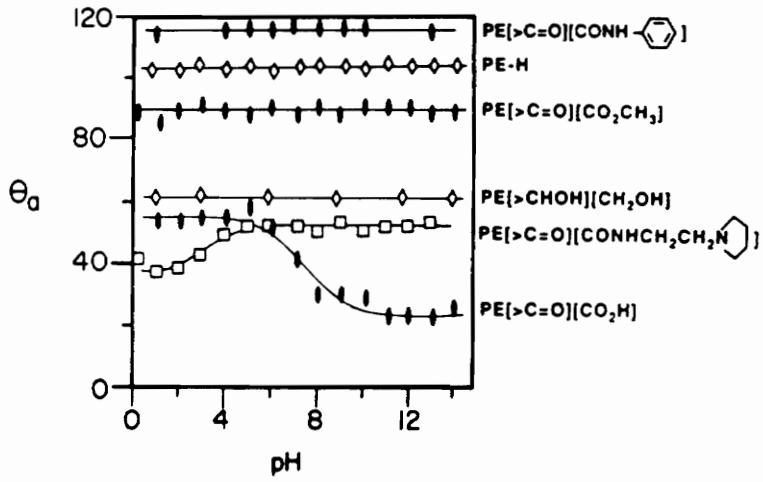

Figure 5. Advancing contact angle θa (obtained by using sessile drops) as a function of the pH of the drop for several derivatives of PE-COOH [87].

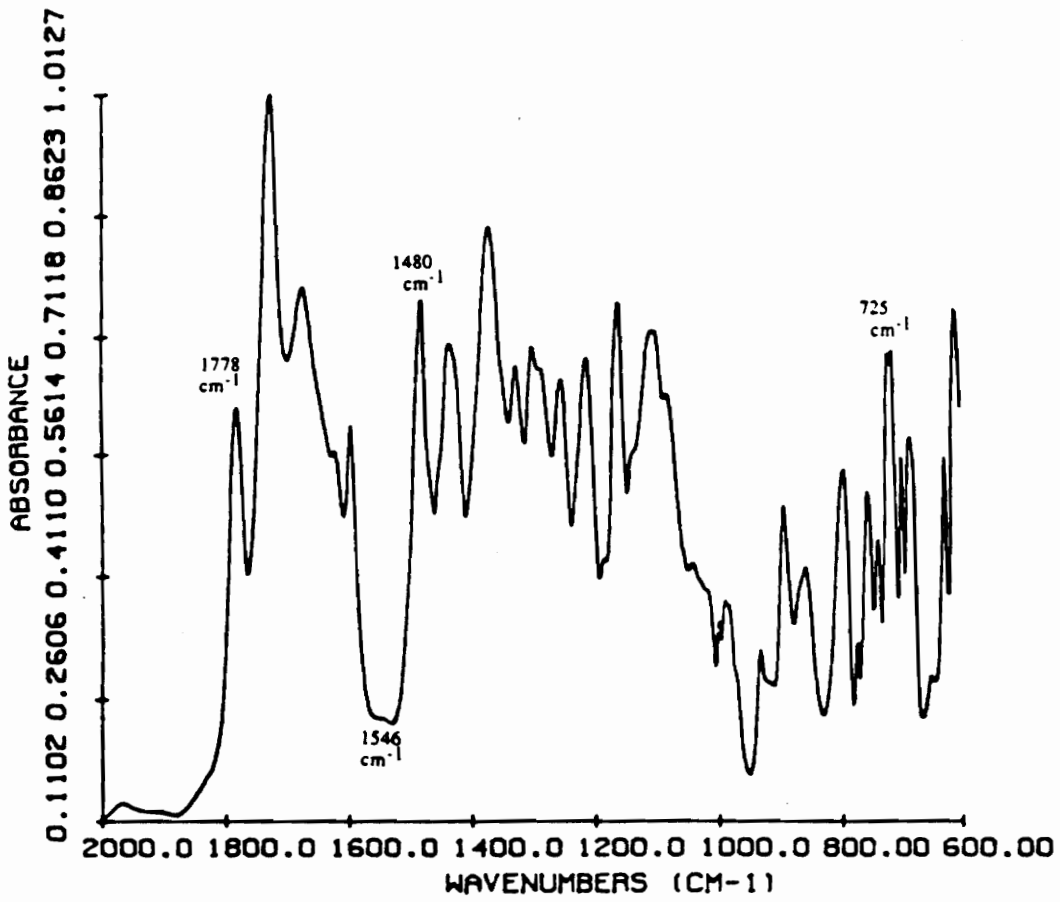

Figure 6. FTIR spectrum of poly(imide siloxane) [9].

BDS polymer. The FTIR spectrum [9] of a partially imidized (solution imidization for 20 minutes at 160 °C) BDS polymer (or polyamic acid) is shown in Figure 7. An intense peak originally present at 1546 cm^{-1} in the spectrum of polyamic acid (see Fig. 7) almost disappeared in the spectrum of polyimide (see Fig. 6). This shows that the imidization of the polyimide is almost complete. The absorption band assignments of the IR spectrum of the polyimide are listed in Table I [9].

The BDS is a copolymer. There are two kinds of dissimilar segments in the polymer chains. One is the siloxane segment and the other is an imide segment. Due to the dissimilarity of the two kinds of segments, microphase separation occurs in the bulk polymer [9].

Polyimides may have very high moduli but usually are brittle materials. Incorporating the siloxane segments into a polyimide can modify the polyimide and improve processibility and ductility [9]. The processibility improvement is indicated by the reduction of intrinsic viscosities which can be as much as 50 % [9]. Most significantly, the siloxane modified polyimide not only has a relatively high modulus but also has reasonable ductility if the siloxane content is around 10 wt% in the copolymer. Figure 8 and Table II are Instron tensile test results obtained at a cross-head speed of 5 mm/min. The slashed entries shown in Fig. 8 indicate the siloxane content (wt%) and the siloxane molecular weight. It is shown that tensile modulus of the poly(imide siloxane) with 10 wt% siloxane is around 2000 MPa which is comparable to that of polyimide without siloxane (the "control" sample), while the elongations at rupture, the indication of ductility, are 15 % to 25 % for the 10 wt% siloxane polyimide, which are higher than that of the non-siloxane

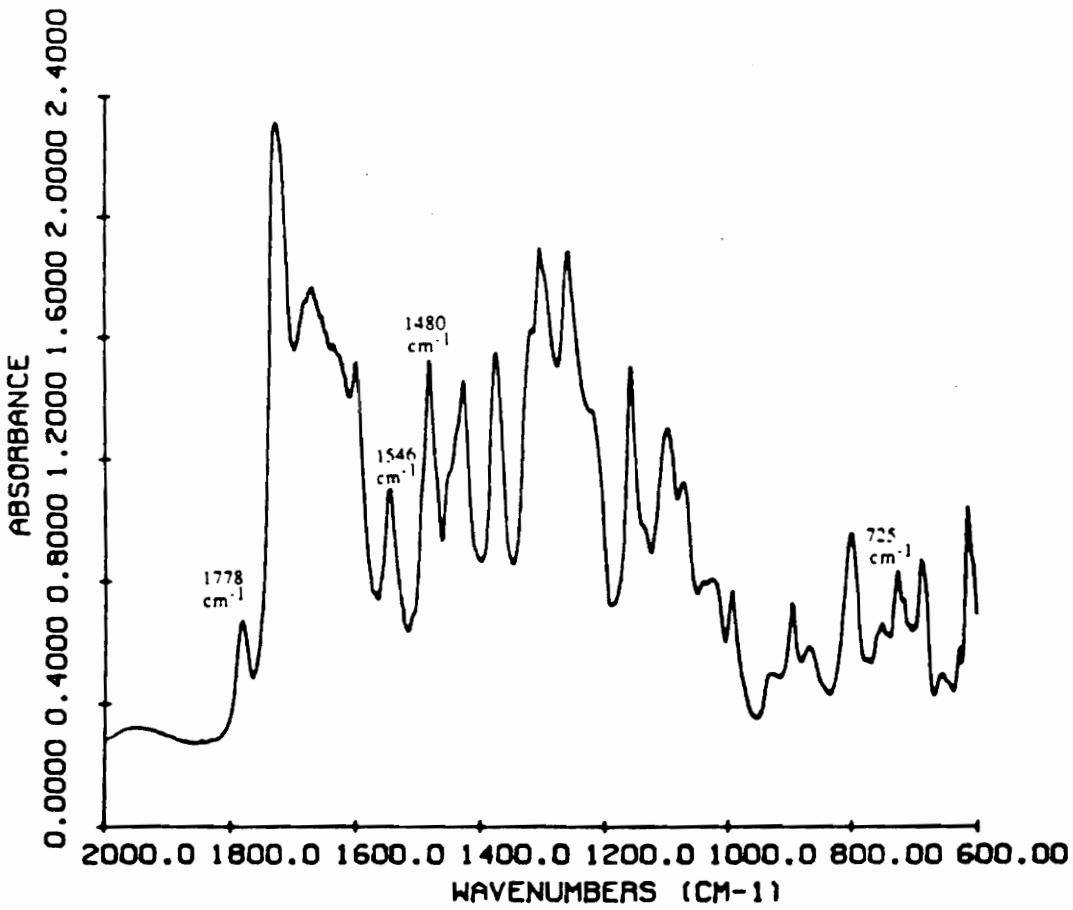

Figure 7. FTIR spectrum of a solution partial imidized poly(amic acid siloxane) [9].

Table I. FTIR assignments for poly(imide siloxane) [9].

Frequency (cm^{-1})	Assignment
1778	Imide C=O stretch vibration
1546	Coupling of C-N stretch and N-H deformation vibration
1480	Aromatic C-C stretch vibration
725	Imide band

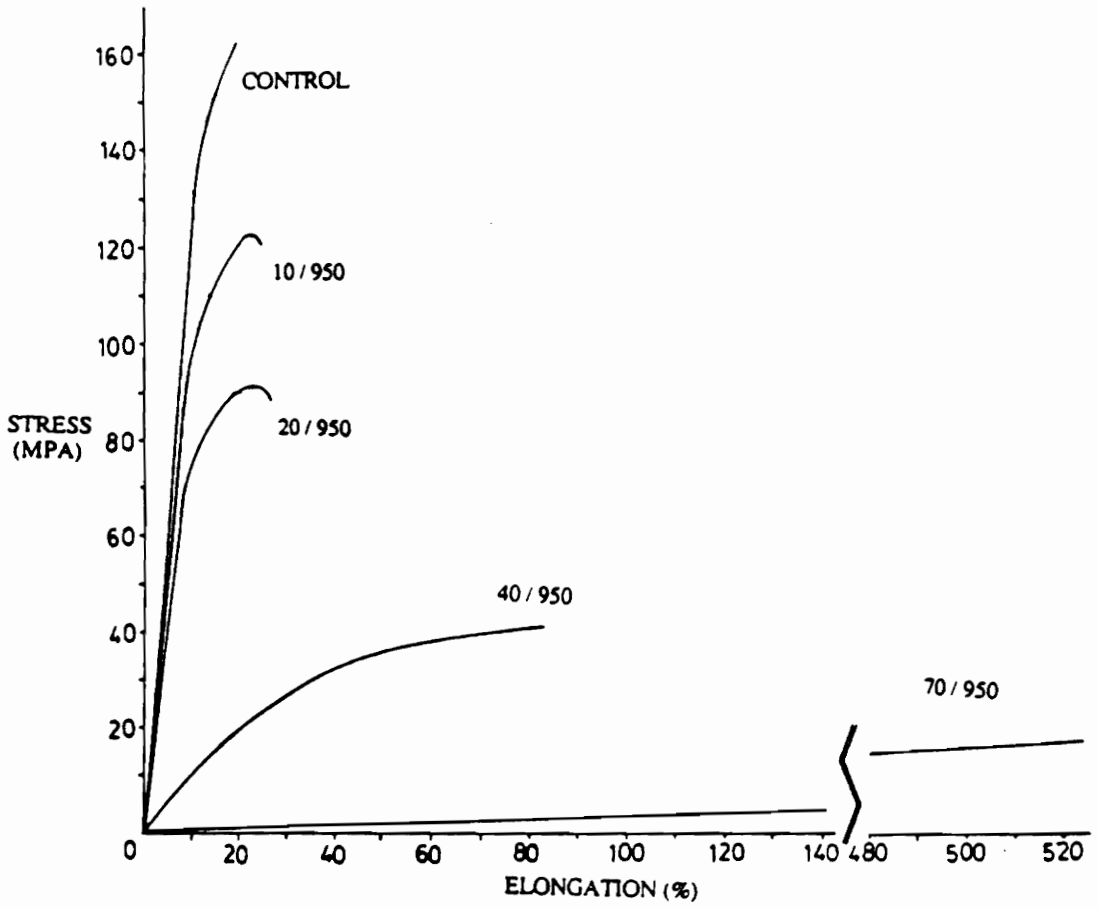

Figure 8. Stress-strain analysis of siloxane modified polyimides [9].

Table II. Mechanical properties of poly(imide siloxane) segmented copolymers (BTDA/3,3'-DDS based) [9].

PSX (Wt. % / Mn)	Tensile Strength (MPa)	Tensile Modulus (MPa)	Elongation to Break (%)
Control	170	2250	9
5 / 950	142	2110	10
10 / 950	118	1910	15
10 / 2100	120	1950	25
10 / 5000	123	1880	15
10 / 10000	125	2040	17
20 / 950	83	1300	25
20 / 2100	72	1330	23
20 / 5000	86	1340	20
40 / 950	44	470	45

polyimide (9%). The improvements of processibility and ductility also mean the improvement of wetting ability (lower viscosity) and bendability (high ductility) which is expected in coating materials used in electronics industry. In addition, the water resistance of the BDS copolymer is also excellent [9].

2.3.2. Surface properties

In siloxane-containing copolymers, the siloxane component is usually segregated to the polymer surface [103, 104]. This is also the case for the BDS copolymer [9]. The siloxane segment is enriched on film surfaces when the films were formed from solutions [9]. This surface property makes the copolymer have a high resistance to oxygen degradation because the oxidation of the top layer of siloxane converts the surface siloxane into a network-like, or inorganic ceramic-like silica which can prevent further oxygen degradation [9]. The problem is that enrichment of the siloxane component on the coating surface makes adhesion difficult. Thus, surface modification of the BDS coating is needed.

2.3.3. Selection of surface modification methods

The " dry process" method can not be used for surface modification of siloxane containing polymer for the reasons mentioned previously (section 2.2.1). The "wet process " or, solution pretreatment may be useful in the surface modification. The reason for saying this is based on the structure of the BDS copolymer. As shown in scheme I, the BDS copolymer is composed of imide and siloxane segments. The siloxane segments will be enriched on a coating surface formed from solution. The

backbone of the siloxane segment molecular chain is made of polar Si-O bonds. These bonds can react with acids or bases [105, 106]. The reaction of siloxane with bases is illustrated in Scheme III. This reaction can remove the surface siloxane segment. Further reaction can occur between the base solution and the BDS copolymer after the removal of the surface siloxane. This is the imide segment reaction. A typical reaction between the imide segments and the base solution is the imide ring opening which has been discussed previously and demonstrated in Scheme II (see section 2.2.3). This imide reaction will introduce carboxylic acid groups on the film surface and will activate the coating surfaces.

2.4. Studies of the Polymer/Metal Interphase

2.4.1. Characterization of metal surfaces

To study the polymer/metal interface and especially the influence of the metal surface on the polymer at an interface, the metal surface must be characterized. There are many techniques such as SEM, XPS and AES (Auger electron spectroscopy), available for characterization of metal surface morphology and composition. However, there are very few methods available for characterization of the acidity of metal surface oxides which is important in adhesion studies. Some methods are available for characterization of acidity of metal oxide powders [53-59, 107]. The major difficulty in quantifying the acidity of metal surfaces is that such surfaces generally have minimal surface area.

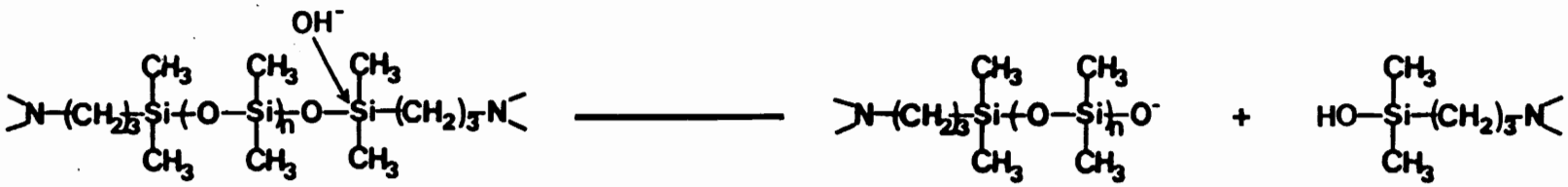

Scheme III. An illustration of siloxane reactions with bases [105].

Recently, Berger developed a method to quantify the acidity of a solid surface [108]. He used a four probe liquid method to measure a so-called quantity D which is related to surface acidity as

$$D = \Sigma[\gamma_S^p{}_{(\text{basic probe})}]^{1/2} - \Sigma[\gamma_S^p{}_{(\text{acidic probe})}]^{1/2} \qquad [11]$$

γ_S^p is the polar (or acid-base interaction) portion of the surface free energy of a solid obtained from contact angle measurements with the basic or acidic probe liquids. There are several problems with this method however. The meaning of the quantity D itself is not clear theoretically and the measurement of D is complicated. Another method proposed recently by Watts is an ion exchange measurement used in evaluating the IEPS (isoelectric point of the surface) of iron oxide [109]. By carrying out ion (K^+ or $HPO4^{2-}$) exchange experiments on iron coupons and monitoring the extent of uptake by XPS, a value of 10 for the IEPS was obtained. The problem is that the experiments were lengthy and some experimental procedures which might introduce error in the measurement have not been evaluated. Because of these deficiencies, new methods which are directed towards surface acidity and experimentally straightforward are needed.

2.4.2. Profile studies of interphases

The two major concerns for an adhesive joint are strength and durability. Consequently, those parameters which affect strength and durability are at the heart of adhesion science research today. These parameters include the physical properties of adhesives, the bulk and surface characteristics of adherends, and the nature of the

forces involved in bonding [31]. One of the recognized facts about an adhesive bond is that these parameters are all interrelated and can undergo changes once a bond joint is formed. These changes are thought to occur primarily at the bond line, i.e., the interface. The study of the interface then is a key issue for understanding failure mechanisms of an adhesive joint [31, 60, 61].

As discussed previously (see the Introduction section), a bond line actually is not an "interface" which is a two dimensional concept. Rather, it is an "interphase' which is a three dimensional "phase". The interphase plays an important role in adhesion and the experimental analysis of the interphase is a frontier area in adhesion research today.

The formation of an interphase may be complicated. As mentioned previously, there are two ways to form an interphase. One is mass transfer across the bond line and the other is component segregation induced by each of the two materials.

2.4.2.1. Interphase formation through component segregation

Component segregation at the air/polymer interface has long been known [110-114]. Thomas and co-workers used XPS angular dependent technique to study component segregation of polymer blends [113] and copolymers [111,112]. By varying the take-off angle of the emitted electrons and curve fitting the XPS spectrum to resolve photopeaks associated with different functional groups, the component profile across the air/polymer interface has been determined [111-

113]. Gradients in component distribution at the interface (or more properly in the interphase) were found.

However, these so-called "interfaces" actually are the surfaces of the polymer against air. If an interphase between a polymer and a metal is studied, the measurement will be very difficult because both the size and location of the interphase are not convenient for conventional surface techniques [31]. No research on the component segregation study at the polymer/metal interface has been reported even though the influence of metal surfaces on the cross-linking density at the interfaces has been emphasized [22].

2.4.2.2. Interphase formation through mass transfer

Interphase formation through mass transfer across the bond line has been extensively studied [31, 42, 60, 61, 115]. There are two typical kinds of interphase formation in this category. One is interphase formation from interdiffusion in polymer-polymer bonds [42]. The other is interphase formation from adhesive penetration into porous metal surfaces [31, 60, 61, 115]. These two kinds of interphases actually are backed by corresponding adhesion theories namely the interdiffusion theory and the mechanical interlocking theory, respectively. Interphase formation from interdiffusion is not related to the research here, so only interphase formation from penetration will be discussed briefly below.

Earlier research has been reported on the wetting of rough substrates by polymer liquids [116, 117]. Different models, such as "capillary" and "ink bottle",

of substrate surface topography were used in the penetration studies [116, 117]. The sizes of the models were in the range of microns. If the pore size of a porous metal surface is in the range of 100 Å which is in the size or mean gyration radius range of many polymer molecules, the penetration of polymers into the pores may become difficult kinetically and thermodynamically. The study of the penetration may also be difficult because of the small size (or depth) and the location of the interphase [31].

Recently, Nitschke used the Auger profile method to study interphases formed from adhesive primer penetration into porous aluminum surfaces made by PAA (phosphoric acid anodization) and CAA (chromic acid anodization) pretreatments [61]. Most of the metal was removed by mechanical grinding and chemical etching. Then the Auger technique was used to profile the primer-metal oxide interphase from the metal side. Figure 9 shows an example of such profile. It was found that this profile method can be used in interphase microanalysis and it was concluded that the porous oxide layers were completely invaded by the primer [61]. The primer Nitschke used was composed of small molecules. If a polymer was used, the conclusion might be different. Actually, there have been reports showing that the porous oxide morphology can act as a molecular sieve. Hence, only the low molecular weight fractions of the adhesive penetrate into the pores, while the large molecules collect above the surface, causing a layering within the polymer [118]. Even though a lot of research has been done on the influence of interphase formation from adhesive penetration into porous metal surface oxides on bond strength and durability [115, 119, 120, 121], only limited research has been done in the microstructure analysis of the interphases [31, 60-61, 122-127].

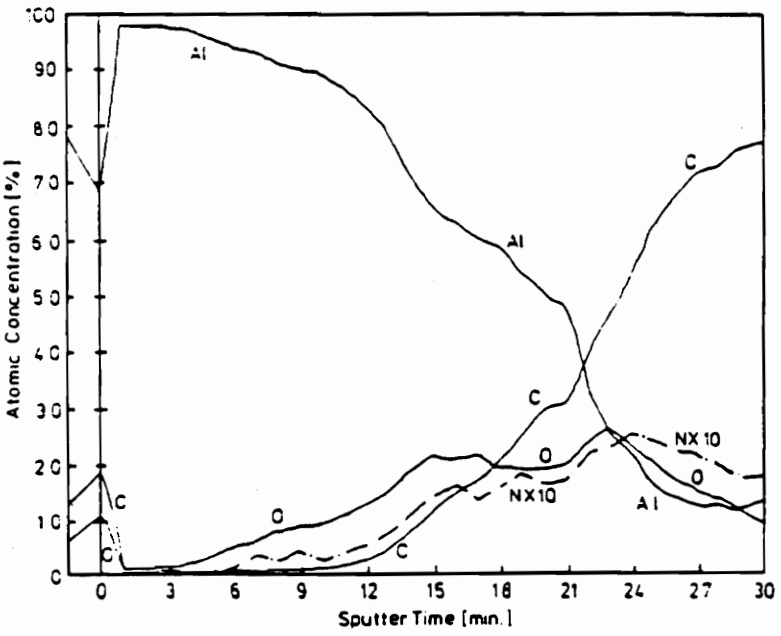

Figure 9. AES depth profile for a primed PAA oxide (N * 10) [61].

III. EXPERIMENTAL

3.1. Surface Modification

3.1.1. Materials

BDS polymer. BDS [BTDA (3,3',4,4'-benzophenonetetracarboxylic dianhydride) -DDS (3,3'-diaminodiphenyl sulfone) - PSX (polydimethylsiloxane) copolymer] powder was obtained from McGrath's laboratory [9]. The polysiloxane segment (Mw 1350 g/mol, with amino end groups) in the copolymer was 10 % by weight. The molecular weight of the polymer was about 50K g/mol. The lower Tg was -117°C. The upper Tg was measured with a Dupont 2100 DSC (differential scanning calorimeter) at a 10 °C/min. scan rate. The polymer was made through solution imidization and isolated in 50/50 weight percent water/methanol solvent.

NMP solvent. NMP (N-methyl-2-pyrrolidinone) was purchased from Aldrich and purified by distillation.

Supporting substrate plates. Ferrotype plates with a mirror-like surface finish, were obtained from Apollo Metals, Inc. These chrome plated steel plates were cut into 2.0*2.0 cm^2 samples for preparation of polymer coatings; those samples used in the peel tests were 2.0*6.0 cm^2.

Pretreatment solution. A 1.25M (~ 5 wt%) sodium hydroxide solution was used to pretreat the polymer surface. A.C.S. certified grade NaOH was obtained from

Fisher Scientific Co. The NaOH solution was prepared by dissolving 25.0 g NaOH in deionized water and diluting to 500.0 ml.

Contact angle titration solution. A 0.05 M sodium phosphate buffer was used as the contact angle titration solution. A.C.S. certified dibasic sodium phosphate ($Na_2HPO_4.7H_2O$) was obtained from Fisher Scientific Co.. Dibasic sodium phosphate (6.70 g) was dissolved in 500.0 ml deionized water to make the buffer solution. Buffer solutions at different pHs were obtained by adding concentrated HCl or NaOH solution to adjust to an approximate pH and then using dilute HCl acid or NaOH solution to finely adjust pH to the desired value. The pHs of the buffer solutions were measured with an Orion Research 701 digital pH meter. The volume change of the solution was very small (within 1 %) during the pH adjustment.

Adhesive tape. The adhesive tape used for peel tests was a commercial 3M Scotch pressure sensitive adhesive tape (1/2 in. width). The pressure sensitive adhesive was acrylate based and the support base material was polypropylene.

3.1.2. Polymer coating preparation

A glass plate was put in a vacuum oven and the oven was placed on an adjustable platform. The glass plate was levelled by finely adjusting the platform. Then the glass plate was taken out. The 2.0×2.0 cm^2 Ferrotype plates were placed on the glass plate. Three drops of the 3.0 wt% BDS solution in NMP were placed on each metal plate and spread over the whole plate using a glass rod. The glass plate was put in the oven again and the samples were dried under vacuum (~ 1 torr) at room

temperature for 7 hours and then 85 °C for another 24 hours. The coating thickness was about 10 microns which was determined by SEM analysis. In addition, peel test samples were prepared on 2.0*6.0 cm^2 plates. All coatings prepared as described above were annealed for one hour under argon at 220 °C.

3.1.3. Coating surface pretreatment

The coatings on the Ferrotype plates prepared above were pretreated in a 1.25 M NaOH solution bath at 30 ± 1 °C for 1 to 10 minutes, washed with deionized water for 3 minutes, put in a 0.01 M dilute HCl solution for 1 minute and rinsed with deionized water and kept in deionized water for 10 minutes. The samples were then taken out and blown with argon to remove all visible water from the coating surfaces and further dried under argon at room temperature for one hour.

3.1.4. Contact angle measurement

Contact angles of the coating surfaces pretreated above were measured with deionized water at room temperature. Figure 10 is a diagram for the contact angle measurement. The instrument used was a Rame Hart 100 goniometer. A 10 μl water droplet was placed on the coating surface and the contact angle was taken between the first and third minute.

In the contact angle pH surface titration studies, all procedures were the same as above except that the 0.05 M dibasic sodium phosphate buffer solutions with different pH values were substituted for deionized water.

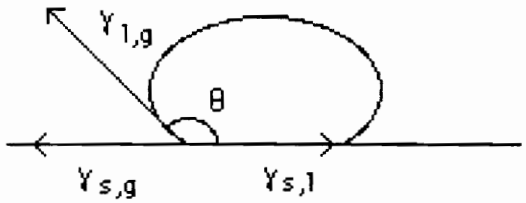

$$\gamma_{s,g} = \gamma_{1,g} \cos(\theta) + \gamma_{s,l}$$

θ — contact angle

$\gamma_{s,g}$ — interfacial tension of solid/gas

$\gamma_{1,g}$ — interfacial tension of liquid/gas

$\gamma_{s,l}$ — interfacial tension of solid/liquid

Figure 10. A schematic diagram for the contact angle measurement.

3.1.5. Peel tests

Pretreated coatings on 2.0*6.0 cm^2 Ferrotype plates were adhered to 3M Scotch adhesive tape. The samples were stored for 20 hours at room temperature for relaxation. Then 180° peel tests were made with an Instrumentors Inc. SP-102B-3M90 slip/peel tester. The peel rates were 1 and 3 in./min. The peel test is illustrated in Figure 11.

3.1.6. Spectroscopy measurements

3.1.6.1. XPS measurements

X-ray photoelectron spectroscopy (XPS) was used for composition measurements of the coating surfaces. A typical measurement was made at a 45° take-off angle. The angular dependent technique was used in the surface analysis. The technique is illustrated in Figure 3 (see the previous chapter). The sampling depth (d) can be calculated from equation [7] as discussed previously. The take-off angles were 15°, 35° and 75° in a typical profile measurement. The instrument was a Perkin Elmer 5300 XPS spectrometer. All operations were done under the following conditions: $MgK\alpha_{1,2}$ X-ray source, pressure < $6.0*10^{-7}$ torr and X-ray power of 400 w at 15 kv. Quantification for XPS data was made using the standard sensitivity parameters provided with the instrument operation software.

3.1.6.2. SEM measurements

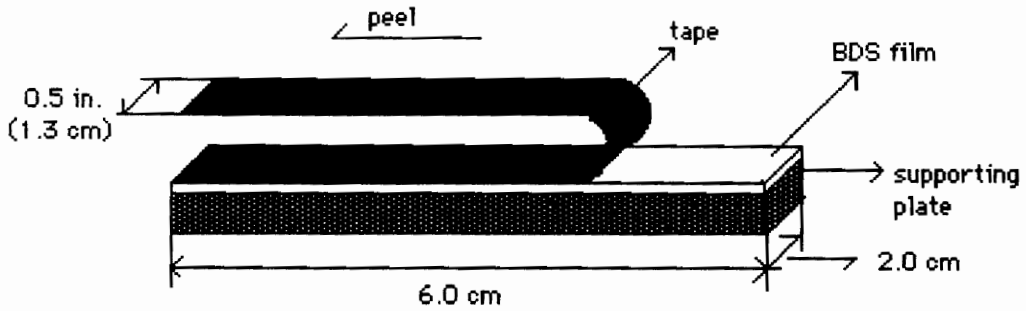

Figure 11. A schematic diagram for the 180° peel test.

Scanning electron microscopy (SEM) photomicrographs were obtained on an ISI-SX-40 scanning electron microscope. The polymer coatings were coated with gold (~100 Å) before the SEM measurements.

3.1.6.3. ATR-IR measurements

Attenuated total reflectance infrared (ATR-IR) spectra of the coatings were obtained on a Nicolet 5DXB FT-IR spectrometer with an ATR cell. A schematic diagram of the ATR cell is shown in Figure 12. A coating on a supporting plate was attached to an KRS-5 IRE (internal reflection element) by clamping the IRE and the sample (with coating side facing the IRE) together with two pieces of plates (not shown in Figure 12) of the ATR cell. The infrared beam incident angle was 60°. All other procedures of the ATR-IR measurements were the same as conventional IR measurements.

3.2. Interphase Studies

3.2.1. Materials

The BDS polymer and NMP solvent were the same as used in the surface modification section.

Aluminum, titanium and zinc were used as adherend substrates. Aluminum foil was obtained from Aldrich Co.. The foil thickness was 0.25 mm; purity was

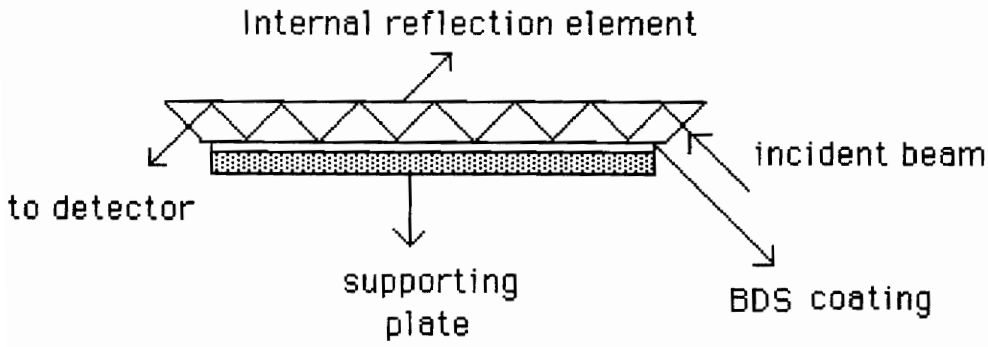

Figure 12. A schematic diagram for the ATR-IR sample set-up.

99.99%. The foil was cut into 2.0*2.0 cm^2 samples which were used without further polishing. Titanium foil had a purity of 99.7% and was 0.89 mm thick. Zinc foil had a purity of 99.9% and was 0.62 mm thick. Titanium and zinc foils were both obtained from AESAR Johnson Matthey, Inc. and were both cut into 2.0*2.0 cm^2 plates and polished to a 0.5 μm surface finish.

All the metal plates were solvent cleaned by vapor-recycled extraction in hexane for 24 hours. The plates were then heated in an oven for two hours at 100 °C. The plates as removed from the oven were used within an hour. A.C.S. certified grade hexane used in the extraction was obtained from Fisher Scientific Co.

A solution of PVC (poly(vinyl chloride)) in THF (tetrahydrofuran) was used in the characterization of acidity of the metal oxide surfaces. PVC was obtained from BF Goodrich Co. and had a molecular weight of 43 K g/mol. A.C.S. certified grade THF was obtained from Fisher Scientific Co.

Teflon TFE plastic sheet was used as an internal reference material in the XPS measurement of acid/base characterization. The Teflon sheet (0.005 ± 0.0003 in. thick) was obtained from Read Plastics, Inc. and had a continuous service temperature 500 °F. The sheet was cleaned with acetone.

3.2.2. Characterization of the metal surfaces

3.2.2.1. SEM and XPS characterization

Surface morphology and composition of the metal surfaces were analyzed using SEM and XPS. The measurement procedures for SEM and XPS have been described above. The take-off angle for the XPS measurements was 45°.

3.2.2.2. Characterization of surface acidity

The surface acidity of the metal oxide surfaces was characterized by PVC solution adsorption tests. A 0.01 wt% solution of PVC in THF was used. The solvent cleaned metal plates were dipped in the 0.01 wt% PVC solution for 15 minutes to attain equilibrium [55], taken out and immediately blown with argon to remove all visible solution. The samples were further dried in an oven at 120 °C for two hours before XPS measurements.

The sample setup for XPS measurements of the adsorption test is illustrated in Figure 13. A thin Teflon sheet was cut to make a straight edge and placed on the sample with a piece of double sided stick tape. The edge of the Teflon sheet was focused at the maximum magnification of the microscope in the XPS sample chamber and was adjusted to the central mark of the microscope. XPS measurements were run at 45° take-off angle. The XPS sampling area was 1.0*3.0 mm as shown in Figure 13. The reference Teflon sheet was kept on the same side (for instance, the left side) and the edge of the sheet was kept as perpendicular as possible to the line of the mark for all sample measurements. The total acquisition time per sample was 2.7 minutes. The same Teflon sheet was used as the reference material for all the sample measurements (three measurements for each of the three metals). The atomic ratio of chlorine to fluorine was taken as equal to the relative amount of PVC adsorption.

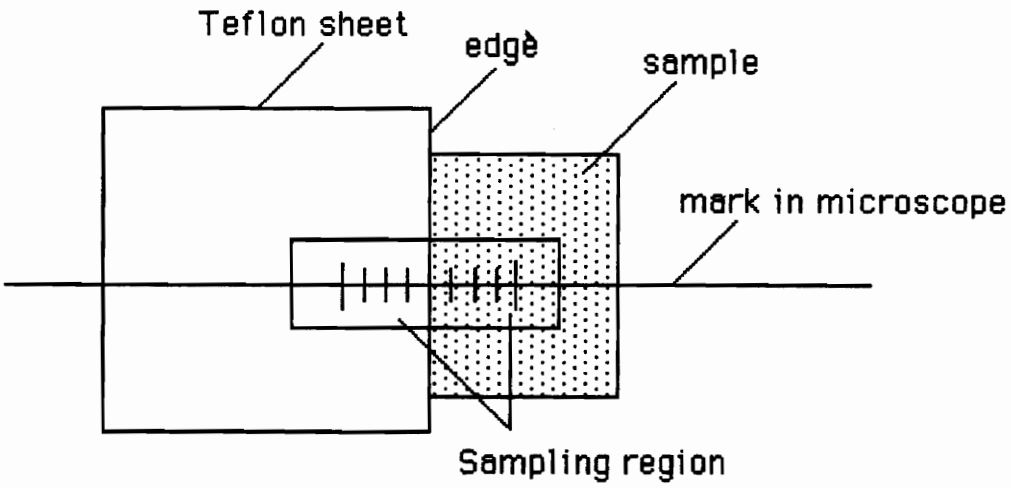

Figure 13. The sample set-up for XPS measurements in the PVC adsorption test.

3.2.3. Sample preparation for component segregation studies

The metal plates after solvent cleaning and oven drying were coated using a similar procedure described in section 3.1.2. The difference was that after the samples were dried in the vacuum oven and taken out, the samples were not annealed. Rather, the samples were put in 50 °C water for less than 5 minutes, taken out, wipe-dried and the polymer coatings were tape-stripped off from the metal substrates. The polymer side of the interface was profiled with the XPS angular dependent technique and the metal side of the interface was also analyzed with XPS at a 45° take-off angle.

3.3. Interphase Study II: Polymer Penetration

3.3.1. Materials

The sodium hydroxide solution used here was described in section 3.1.1. Sodium dichromate and 85 wt % phosphoric acid were A.C.S. certified. Concentrated (98.0 wt%) surfuric acid was reagent grade. All the reagents were obtained from Fisher Scientific Co..

The iodine solution used in dissolving metal was prepared by adding 20 g of iodine to 100 ml of dry methanol. The iodine was reagent grade and the methanol was A.C.S. certified grade. Both chemicals were obtained from Fisher Scientific Co..

3.3.2. Sample preparation

Phosphoric acid anodization (PAA) was used in preparation of porous aluminum surfaces. The PAA procedure [128] is described as follows. The aluminum plates were first degreased by extraction in hexane for 24 hours. The plates were then cleaned with a 5 wt% NaOH solution at 70 °C for 7 minutes and deoxidized with a dichromate solution of 16 g solution dichromate, 160 g 98.0 wt% concentrated sulfuric acid, and 480 g H_2O at 70 °C for 10 minutes. The plates were then rinsed in deionized water for 3 minutes and finally were anodized in a beaker containing 10 wt% phosphoric acid solution [prepared by adding 69.5 ml of H_3PO_4 (85 wt%) to 1000 ml of deionized water] at room temperature in two different ways. The first way was to keep the anodizing current density constant at 6.5 mA/cm^2 and anodizing for 20 minutes. The second way was to keep the anodizing voltage constant at 30 v and anodizing for 5 minutes. The major apparatus used for anodization was a Sorensen DCR 150-6B power supply. As soon as the current was turned off, the samples were taken out and rinsed in deionized water for 15 minutes and then dried in an oven at 80 °C for 30 minutes. The dried samples must be used within 120 minutes.

The aluminum plates with porous surfaces prepared above were coated with 3.0 wt% BDS solution and dried in a vacuum oven as described in section 3.2.3. After drying, the coated samples were annealed under argon at 220 °C for one hour.

3.3.3. Cross-section analysis

The cross-section of porous aluminum surface oxide layer was obtained by notching on one side of the aluminum plate, cooling in liquid nitrogen, and bending as it was cold. The cross-section was coated with gold and examined in a SEM.

3.3.4. AES interphase profile

A typical procedure for preparing a sample for AES (Auger electron spectroscopy) interphase profile is described below. A sample prepared as described in section 3.3.2 was embedded in a cold curing epoxy with the polymer coating facing the epoxy. Most of the aluminum metal was ground away. The sample was put in the iodine solution (see section 3.3.1) to further dissolve away the metal. The dissolution took no longer than 20 minutes to prevent possible swelling of the polymer by methanol. The sample was then rinsed with methanol, dried and coated with a thin layer of gold.

The samples prepared according to the above procedure were AES profiled by argon ion sputtering in a Perkin-Elmer PHI 610 scanning Auger microprobe. The samples were set so that the surface was 45° relative to the incident beam. The AES instrument was operated with the beam voltage at 3.0 kv and the beam current at 0.030 μA with the pressure $< 6*10^{-6}$ torr. The argon sputter gun was operated at 4 kv and an ion current density of 20 $\mu A/mm^2$ at a pressure of $15*10^{-3}$ torr. Quantification of AES data was made using the standard sensitivity parameters provided with the instrument operation software. The absolute sputter rate (or depth) was not obtained from calibration because of the complexity of interphase

sputtering [31, 61]. Instead, the relative sputter depth was presented in terms of sputter time for relative comparison.

IV. RESULTS AND DISCUSSION: PART I

MODIFICATION OF POLYMER SURFACES

4.1. Initial Surface of the BDS Polymer Coating

The BDS copolymer is composed of two kinds of segments which have two characteristic values of Tg; the lower Tg at -117 °C is for the siloxane segments [9]; the upper Tg at 233 °C as indicated in the DSC spectrum shown in Figure 14 for the imide segments. The structure of the BDS copolymer is shown in Scheme I. BTDA is a joint component through which PSX or DDS component units are connected to form linear chains of the polymer. Component distribution of the copolymer at the coating surface can be determined from the relative percentage of PSX and DDS. Silicon and sulfur are antained in the chain units of PSX and DDS in the copolymer, respectively. This distribution can also be expressed as the relative atomic concentration of silicon (Si at%) referenced to silicon and sulfur as shown below.

$$\text{Si at\%} = [\text{Si}/(\text{Si} + \text{S})]*100\% \qquad [12]$$

where Si and S are the atomic concentrations of silicon and sulfur obtained from XPS measurements, respectively.

To determine an elemental profile, one important concern is the sampling depth difference for different elements such as Si and S. Here, the sampling depth (d) is directly proportional to the mean free path (λ) of the emitted electrons (see equation [7]). The λ term has the following relation to the kinetic energy of the

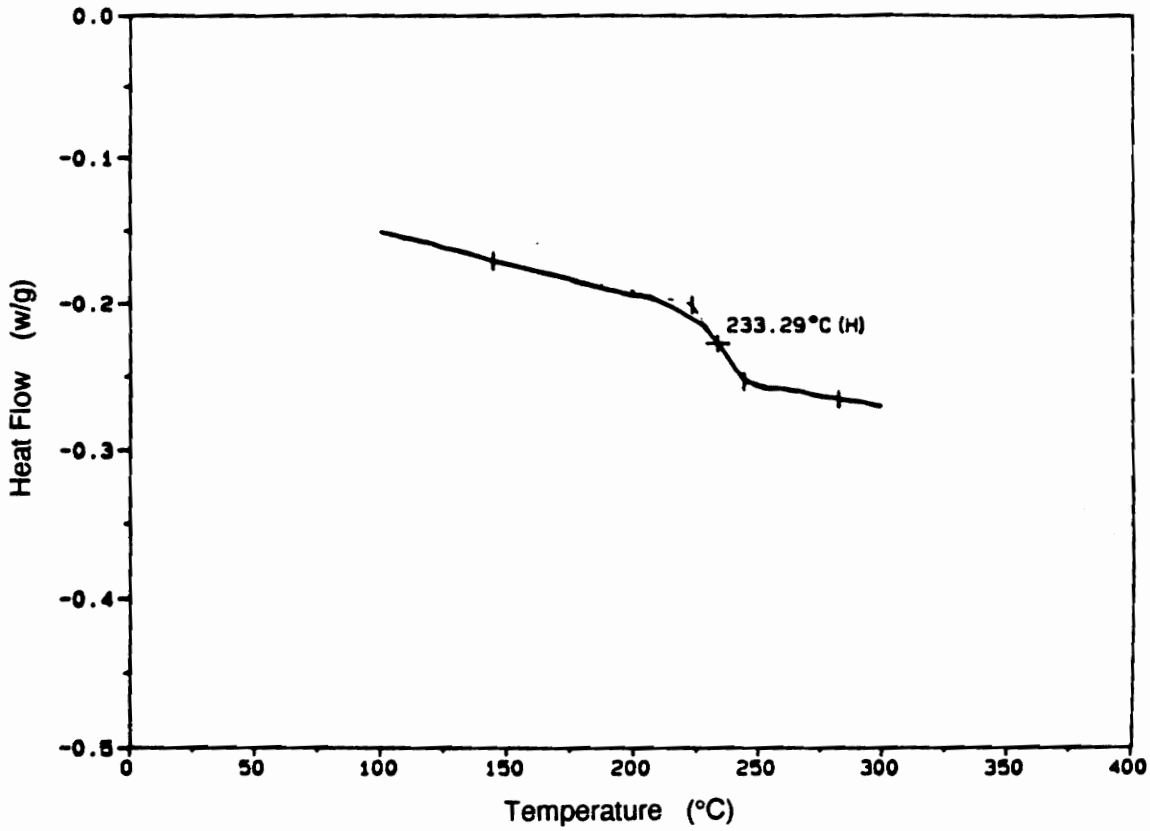

Figure 14. DSC spectrum of the 10 % siloxane modified polyimide.

emitted electrons which is different for different elements (or from the same element but for different energy levels) [129-132]:

$$\lambda = kE^{p} \qquad [13]$$

where E is the kinetic energy of the ejected electrons. The terms "k" and "p" are constants depending on the sample. For organic materials, there are several theoretically and experimentally estimated values for p ranging from 0.5 to 1.0 [129-132]. A value of unity [129] was selected in the estimation of the sampling depth difference between Si and S. The corresponding k value selected was 0.03 [129]. The kinetic energies of emitted photoelectrons for Si and S are 1151 ev and 1086 ev, and the calculated λ values are 34 Å and 33 Å, respectively. This means the maximum sampling depth ($d = 3\lambda$) is 102 Å and 99 Å for Si and S, respectively. The maximum relative variation of the sampling depths between these two elements is within 5%. It is expected that variation of the elemental composition profile caused by the difference of the sampling depth between Si and S is negligible.

Figure 15 shows the surface XPS angular dependent spectra for Si and S of the BDS coating formed from solution. The normalized spectra show that the intensity of the Si peak decreases with increasing take-off angle, i.e., decreases with increasing sampling depth. By contrast, the intensity of the S peak increases with increasing sampling depth. The quantitative results of the surface profile analysis can be seen in Figure 16. The relative atomic concentration of Si is everywhere > 80 % which is much higher than the bulk concentration (43.2%) within the top 100 Å of the coating surface. The 100 Å thickness corresponds to the maximum value of the

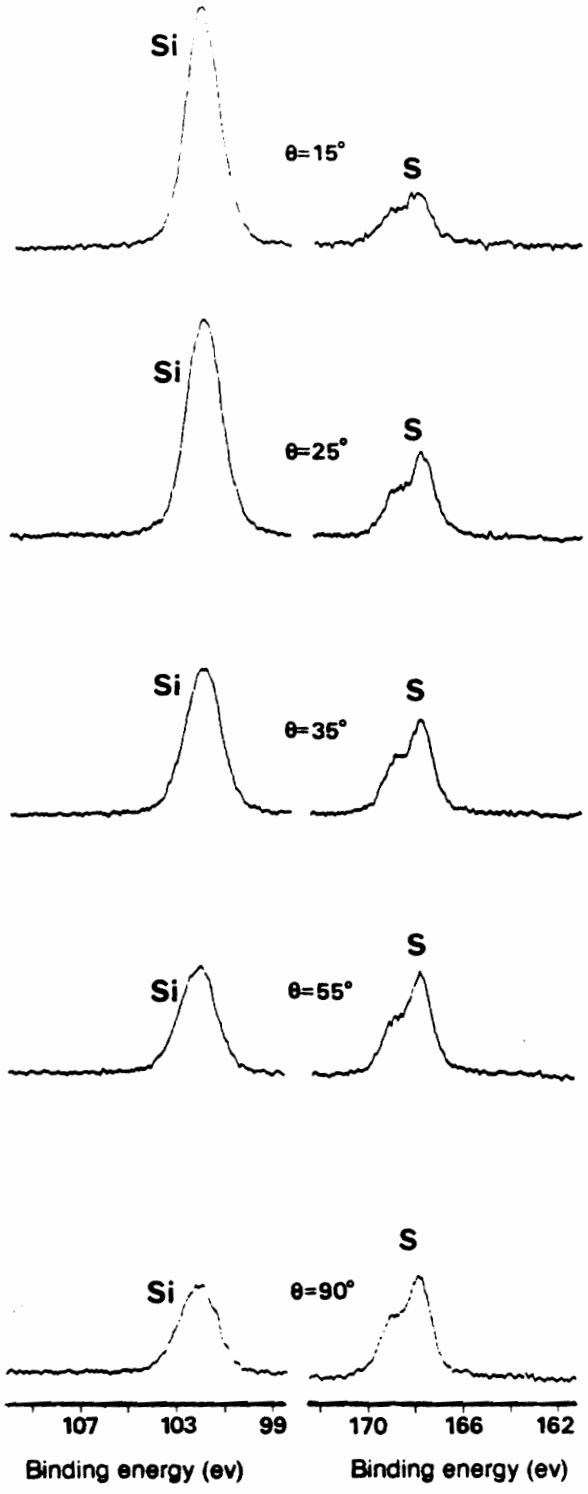

Figure 15. XPS angular dependent spectra of BDS coating surfaces.

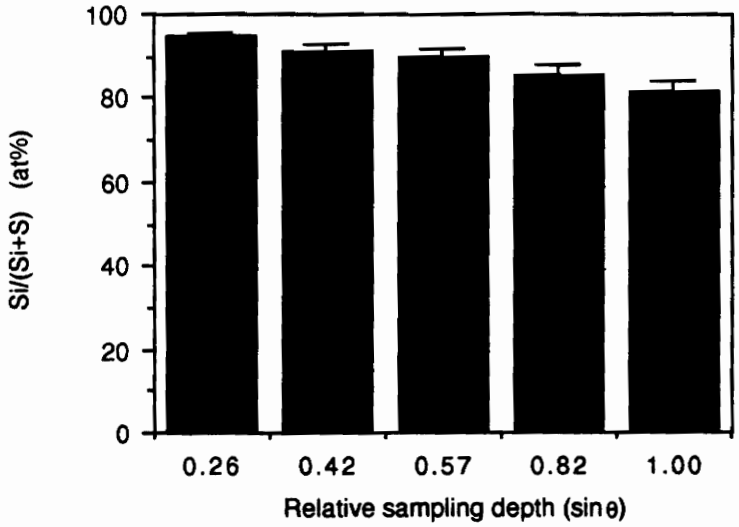

Figure 16. Surface profile of the BDS polymer coatings.

relative sampling depth in Figure 16 and is estimated from other reported results for organic materials [129]. These results are in agreement with results reported in the literature [9]. There is a top layer of siloxane on the coating surface. Because siloxane has a low surface free energy estimated to range from 17 to 22 erg/cm^2 [9], it is reasonable to predict that the top layer of siloxane on the coating surface will make the surface hydrophobic and poor in terms of adhesion when the coating is bonded to a polar adhesive. Surface modification may solve this problem.

4.2. Surface Property Changes in Surface Modification

The possible major changes of the surface after pretreatment in 1.25 M NaOH solution at 30 °C may be surface etching and chemical structure changes.

4.2.1. Surface etching

As discussed previously, the siloxane backbone , which is composed of Si-O bonds, can be broken by base reactions (Scheme III). These reactions may etch away the top siloxane layer of the coating surface. Figure 17 shows the relation between the relative atomic concentration of silicon at the coating surface (15° take-off angle in XPS measurements) and pretreatment time. The silicon concentration decreased quickly during the first 5 minutes of the pretreatment and then the rate decreased. The decrease in silicon concentration means the etching and removal of surface siloxane segments. The silicon concentrations obtained at different sampling depths (35° and 75° take-off angles, see Figure 18) showed the similar trends of the

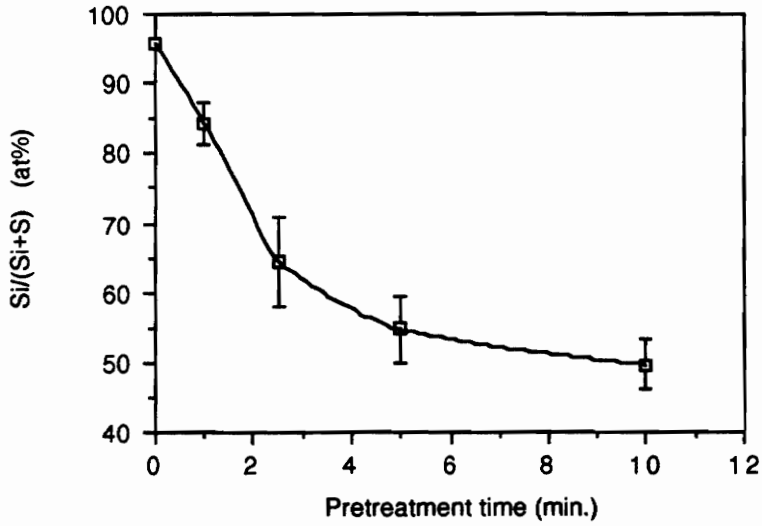

Figure 17. Surface silicon atomic concentration changes with pretreatment time.

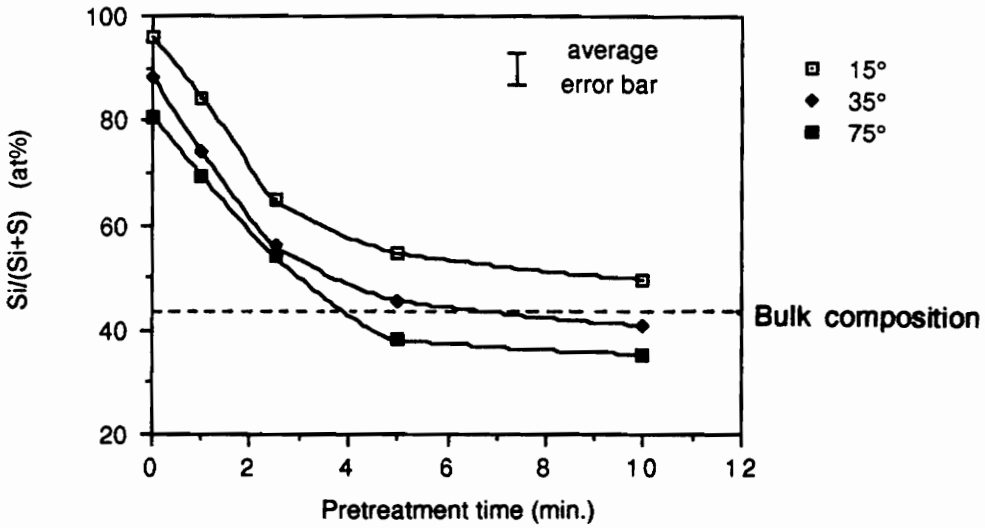

Figure 18. Silicon profiles across BDS coating surfaces pretreated for different periods of time.

silicon concentration decrease. These XPS results support the point that etching of the surface siloxane occurred during the solution pretreatment.

Another interesting point is that in the slower rate regions obtained at different sampling depths (the region within the 5 and 10 minute pretreatment time for the curves obtained at 15°, 35° and 75° take-off angles in Fig.18), the curves do not converge. This means there is still a gradient of silicon composition on the coating surface after the 5 to 10 minute pretreatment. The siloxane content was still higher at the top surface (15° take-off angle) than that below the surface (35° and 75° take-off angles). However, the top siloxane layer of the coating after the 10 minute pretreatment is expected to be very thin because the profile at 35° take-off angle has already reached the bulk composition (43.2 %) indicated by the dashed line in Fig.18.

The etching of the coating surfaces can be further confirmed by SEM analysis. Figure 19 shows the SEM photographs of the non-treated and the 10-minute pretreated coating surfaces. The non-treated coating surface is very smooth while the pretreated coating surface shows considerable roughness. This is even more apparent at higher magnification as shown in Figure 20. These results indicated that the etching of the BDS coating surface not only removed the siloxane layer, but also increased the roughness of the surfaces. An increase in surface roughness is favored in adhesion.

4.2.2. Chemical structure changes

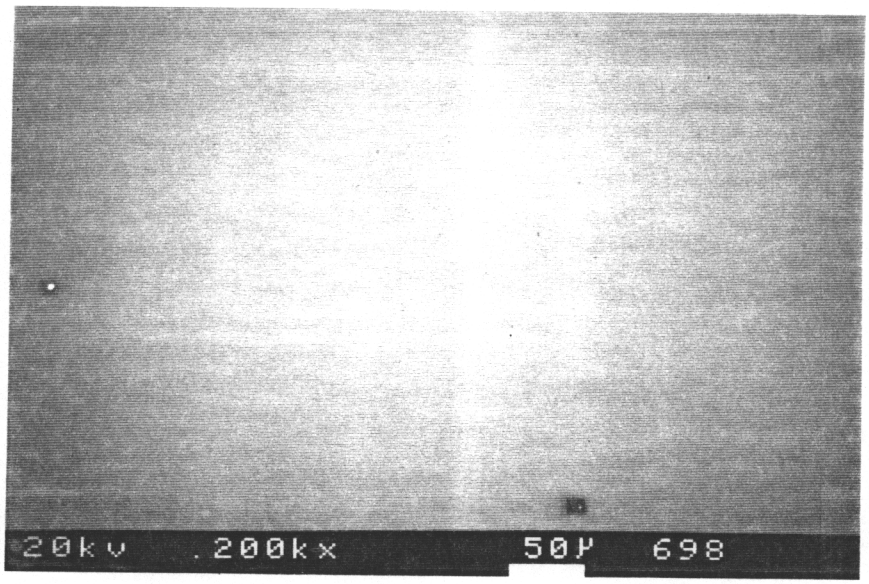

a

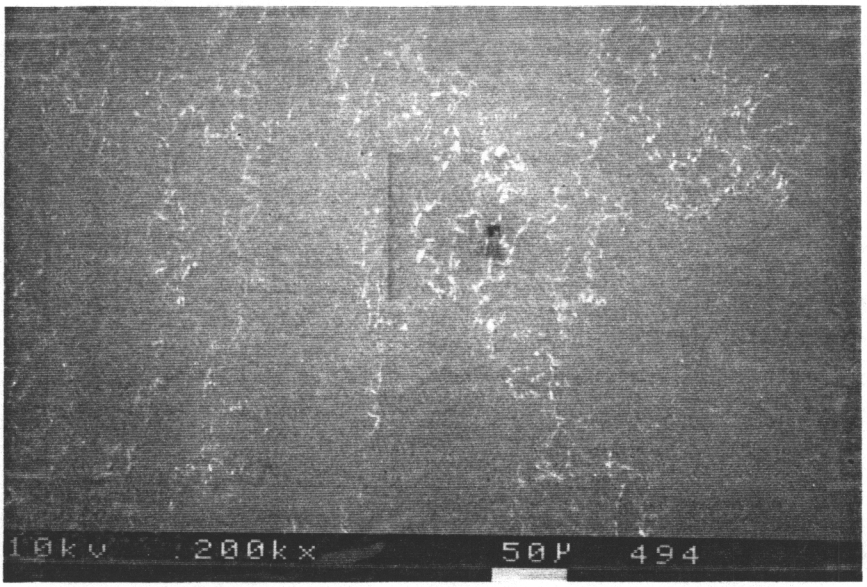

b

Figure 19. SEM photographs of the BDS coating surfaces (200X).
a. non-treated; b. 10-minute pretreated.

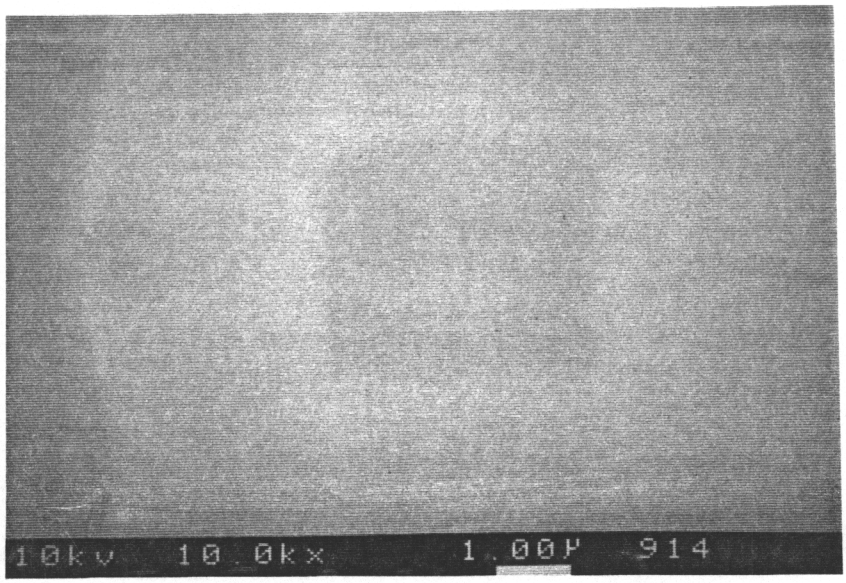

a

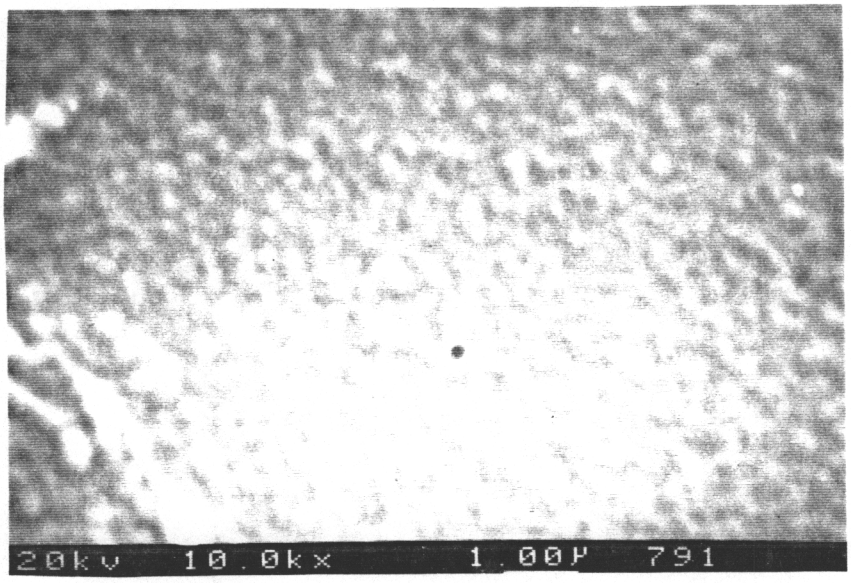

b

Figure 20. SEM photographs of the BDS coating surfaces (10kX).
a. non-treated; b. 10-minute pretreated.

After removal of the top siloxane layer of the BDS coating, the imide segments of the polymer are exposed and available for reaction. The imide reaction with a base solution is primarily an imide ring opening reaction which was discussed previously and shown in Scheme II [7]. The created carboxylic acid groups (after neutralization) should improve the adhesion properties of the surfaces. In order to confirm the occurrence of the imide reaction, pH contact angle titration, ATR-IR, and XPS measurements were conducted.

4.2.2.1. pH contact angle titration

pH contact angle titration is a method developed by Whitesides et al. [86] which was discussed in Chapter II. The contact angle will be dependent on pH only for the case of polymer surfaces on which there are ionizable functional groups such as carboxylic acid groups. If there are carboxylic acid groups on the pretreated BDS coating surfaces, the contact angles measured on the surfaces should be also pH dependent.

Whitesides et al. [86, 87] have evaluated the pH contact angle titration method. In order to confirm the reliability of the method used in the measurement on the BDS surfaces, several experiments were conducted. Table III shows the measured contact angle for different buffer concentrations at pH 8 on a 10-minute-pretreated BDS coating surface. It is shown that the contact angle decreased slightly with increasing buffer concentration. However, the contact angle change is negligible when the buffer concentration approached 50 mM. A concentration of 50 mM (0.05M) was used in the pH contact angle titration measurements in this research.

Table III. The effect of buffer concentration on contact angle.

Concentration (mM)	Contact angle (degree)
0.05	61.8 ± 0.9
0.5	59.5 ± 0.6
5.0	58.1 ± 0.8
50.0	57.6 ± 1.9

Figure 21 shows the dependence of contact angles on measurement time for a 10 minute pretreated BDS coating surface. It is shown that at low pH (pH 2), the contact angle does not change with measurement time over 10 minutes. At high pH (pH 13), the contact angle does not change with measurement time over 5 minutes after equilibrium is reached in about 0.5 minute. After 5 minutes, the contact angle starts to decrease with time. This may due to a slow reaction between the buffer solution and the coating surface. All contact angles were measured between the first and third minutes in the contact angle titration measurements.

Figure 22 shows the contact angle titration curves for a non-treated and a 10 minute pretreated coating surface. The contact angle does not change with pH on the non-treated coating surface. This means that there are no ionizable functional groups on the non-treated surface. In addition, the constant contact angle on the non-treated surface with pH also means that the surface free energy of the contact liquid does not change with pH significantly as indicated by Whitesides et al.[86]. The dependence of contact angle on pH for the 10 minute pretreated coating surface shows a typical titration curve observed in acid-base titration. This indicates that there are ionizable acid or base functional groups on the pretreated surface. The contact angle dependence on pH shown in Figure 23 was also obtained on other coating surfaces pretreated for different time. These results further confirm the point that there are ionizable acid or base functional groups on the pretreated surfaces.

4.2.2.2. ATR-IR analysis

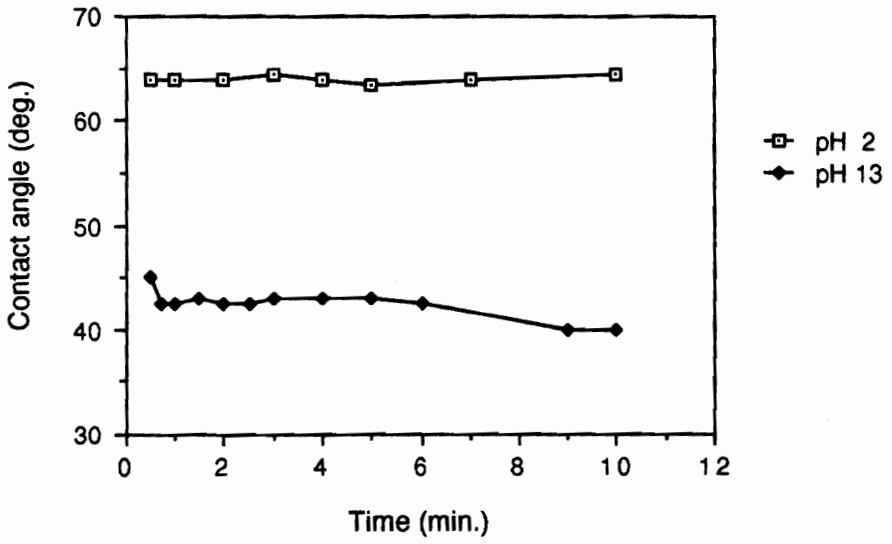

Figure 21. Dependence of contact angle on measurement time.

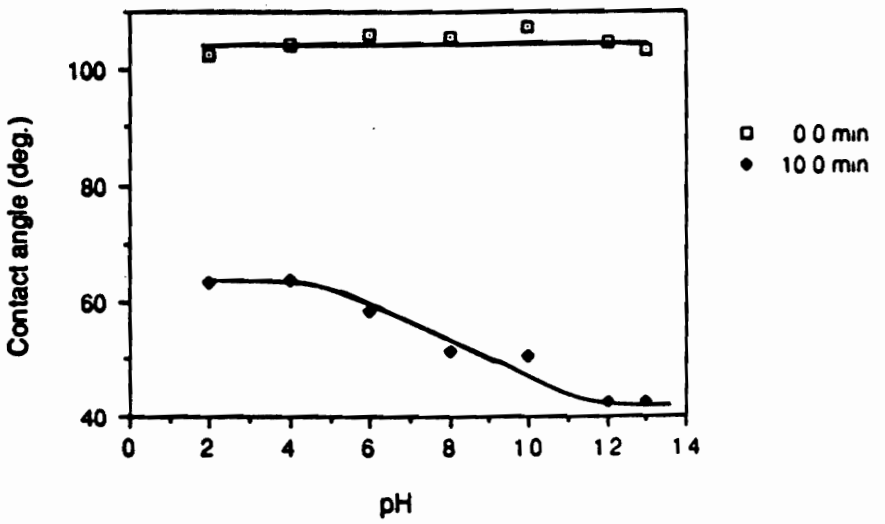

Figure 22. Relation of contact angle and pH for non-treated and pretreated coating surfaces.

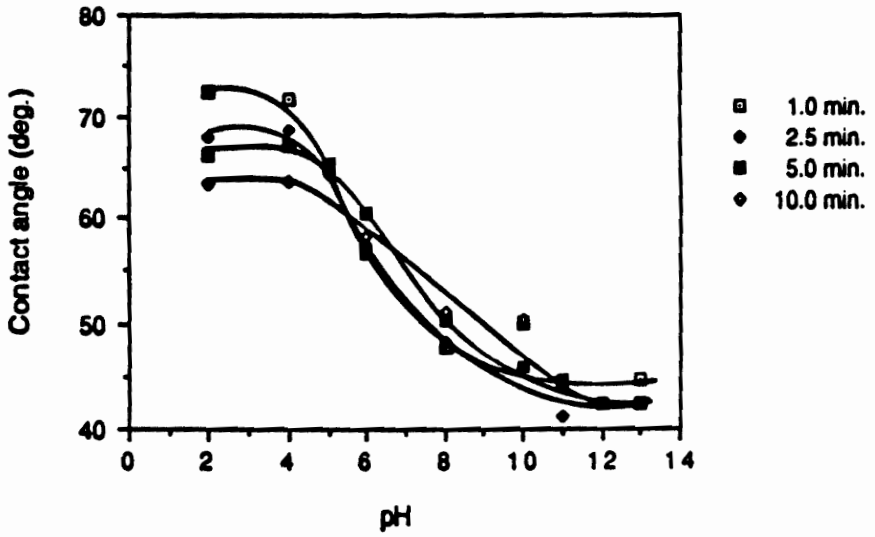

Figure 23. Dependence of contact angle on pH for pretreated BDS coatings.

Figure 24 shows the ATR-IR spectra of the BDS coatings obtained at a 60° IR beam incident angle. Figure 24a and 24b are spectra of a 10-minute pretreated and a non-treated coating, respectively. A small peak at 1548 cm^{-1} for the non-treated BDS coating was assigned to the C-N-H asymmetric stretching mode [133]. This peak was also found in poly(amic acid) intermediates in the synthesis of the BDS copolymer (see Fig. 7). The appearance of this peak indicates that there is a small amount of poly(amic acid) presented in the starting material. After 10 minute surface pretreatment, the peak was enhanced significantly. This enhancement indicates that the imide ring opening on the coating surface is significant.

4.2.2.3. XPS analysis

Figure 25 shows the curve fitted XPS carbon spectra of the coating surfaces. The spectra were obtained at a 15° take-off angle. The spectrum for the non-treated coating surface shows four peaks for carbon, C_6H_x (benzene ring), CHx (hydrocarbon), CN (imide) and O=C-N (imide). After 10 minute pretreatment, a considerable carbonyl peak was seen and a new but small peak for carboxylic acid appeared. The quantitative results from the curve fitted spectra are summarized in Tables IV and V. Table IV shows the curve fitted results presented in area %. Table V shows the results in atom % which were calculated from the area % data showed in Table IV and the composition data of the BDS surfaces. The composition for the non-treated coating is C- 56.0, O-24.7, Si-17.2 at%; for the 10-minute pretreated coating is C-73.5, O-19.6, Si 2.2 at%. It is shown that the concentration of carbonyl groups is increased 10 times on the coating surface after a 10 minute pretreatment. This result further confirms the removal of the top siloxane layer and

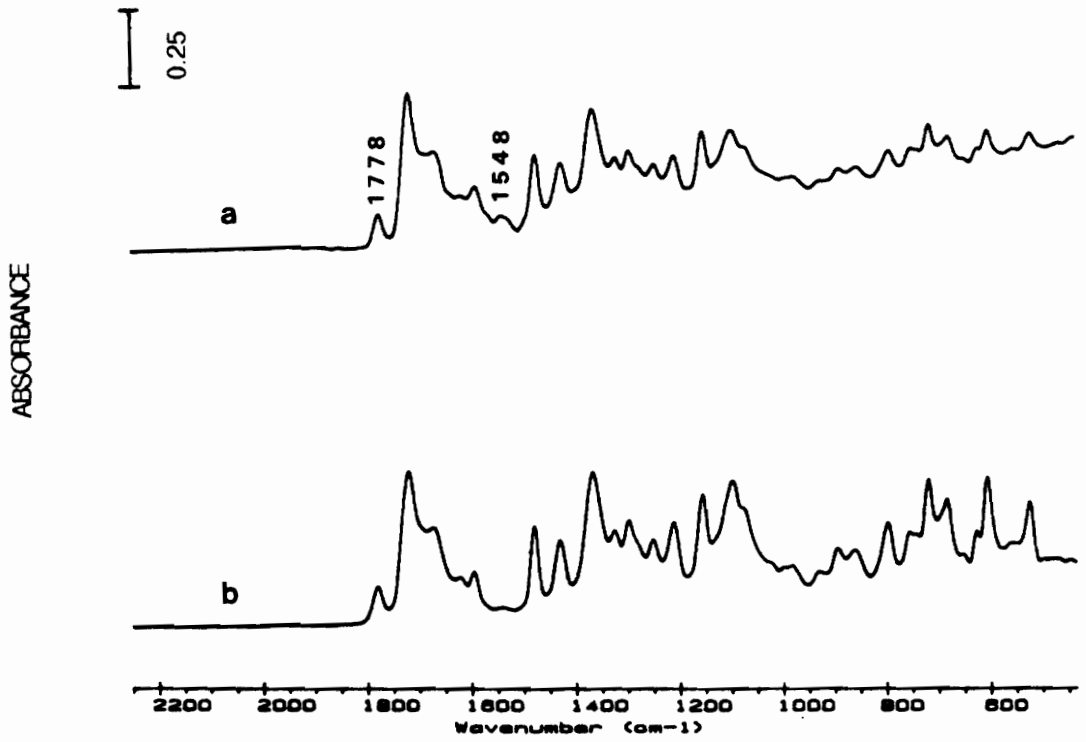

Figure 24. ATR-IR spectra of the BDS coatings.
a. pretreated; b. non-treated.

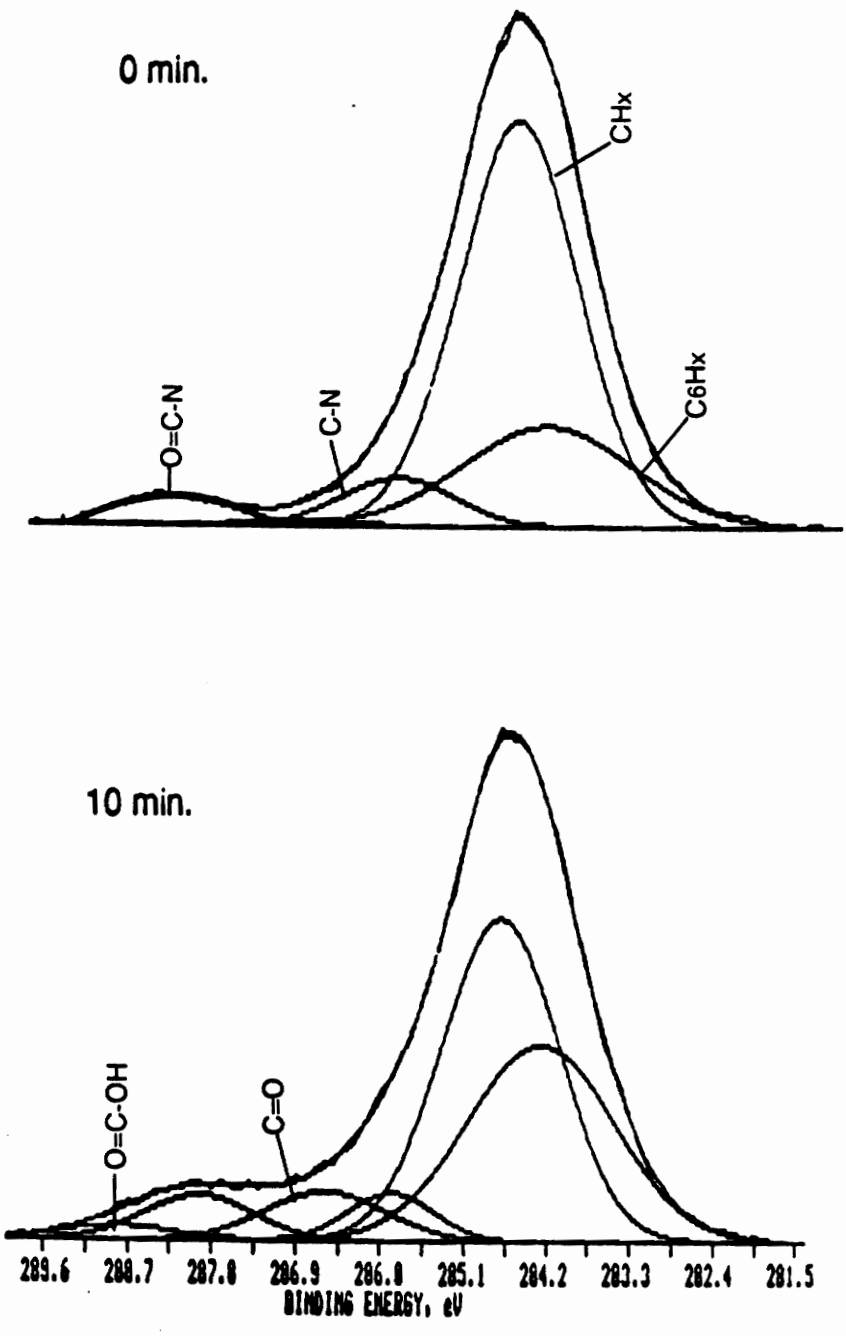

Figure 25. Curve fitted XPS carbon spectra of BDS coatings.

Table IV. XPS curve fitted results (in area percentage) of BDS coatings.

	Non-treated coatings		Pretreated coatings	
Core level	BE (ev)	Area[a] (%)	BE (ev)	Area[b] (%)
C1s				
-C6Hx-	284.6	23.1	284.6	34.6
CHx	285.0	64.1	285.0	45.2
C-N	286.2	7.3	286.2	5.0
O=C	287.2	0.9	287.0	7.2
O=C-N	288.5	4.6	288.2	6.0
O=C-OH	—	—	289.1	2.0
O1s				
O=S=O	531.2	4.1	531.3	16.2
O=C	532.1	11.7	532.1	55.7
O-Si(CH3)2-O	532.7	65.7	533.0	13.7
O-Si(CH3)(O)-O	533.3	18.6	533.3	5.0
H-O-C=O	—	—	534.0	9.4
Si2p				
O-Si(CH3)2-O	101.0	78.4	101.0	75.5
O-Si(CH3)(O)-O	101.9	21.6	102.0	24.5

a. The average of the Best Estimate of Standard error is 1.5.

b. The average of the Best Estimate of Standard error is 1.8.

Table V. XPS curve fitted results (in atom percentage) of BDS coatings.

	Non-treated coatings		Pretreated coatings	
Core level	BE (ev)	Atom[a] (%)	BE (ev)	Atom[b] (%)
C1s				
-C6Hx-	284.6	12.9	284.6	25.4
CHx	285.0	35.9	285.0	33.2
C-N	286.2	4.1	286.2	3.7
O=C	287.2	0.5	287.0	5.3
O=C-N	288.5	2.6	288.2	4.4
O=C-OH	—	—	289.1	1.5
O1s				
O=S=O	531.2	1.0	531.3	3.2
O=C	532.1	2.9	532.1	10.9
O-Si(CH3)2-O	532.7	16.2	533.0	2.7
O-Si(CH3)(O)-O	533.3	4.6	533.3	1.0
H-O-C=O	—	—	534.0	1.8
Si2p				
O-Si(CH3)2-O	101.0	13.5	101.0	1.7
O-Si(CH3)(O)-O	101.9	3.7	102.0	0.5

a. The Average of the Best Estimate of Standard error is 1.4.

b. The average of the Best Estimate of Standard error is 1.6.

thus the exposure of polar groups on the surfaces after the pretreatment. More interestingly, the carboxylic acid groups, which are not seen on the non-treated surface, are present on the pretreated surfaces. This further confirms the creation of carboxylic acid groups on the coating surface after the surface pretreatment.

The curve fitted results from the carbon and oxygen spectra correlate well as seen in Table V. For instance, for the non-treated surface, the atomic concentration obtained from carbon spectrum for C=O is 3.1 at% (equals to [(0.5 at%)C=O + (2.6 at%)O=C-N]) which is very close to the value of 2.9 at% from the oxygen spectrum.

In addition, information about the siloxane can also be obtained from the curve fitted results. There are two kinds of siloxane structure in the coating, namely, O-Si(CH_3)$_2$-O (Si binding energy 101 ev) and O-Si(CH_3)(O)-O (Si binding energy 102 ev). The mole ratio (about 3) of these two kinds of species is constant for the non-treated and pretreated coating surfaces. This means that the solution pretreatment etches away the siloxane but does not lead to other significant side reactions such as cross-linking.

The above evidence indicates that imide rings of the BDS copolymer were opened and carboxylic groups were introduced on the solution pretreated coating surfaces. This change, in addition to the siloxane etching and surface roughening, should have an influence on adhesion.

4.3. Adhesion Property Change in the Surface Modification

4.3.1. Contact angle changes

A major concern of the adhesion properties of an adherend is its wettability by adhesives. Wettability of an adherend by polar adhesive liquids usually is evaluated by the wettability of the adherend by water. This can be done through water contact angle measurements.

Figure 26 shows the change in water contact angle with pretreatment time. When the BDS coatings were pretreated in 1.25 M NaOH solution at 30 °C for 10 minutes, the contact angle decreased significantly from the initial value of 103° to near 60° at the end of the 10 minute pretreatment. The high initial contact angle of 103° is consistent with the hydrophobic nature of the BDS coating surface formed from solution. The decrease of the contact angle with polar liquid water indicates the increase of hydrophilicity of the surface and so the increase of the wettability of the surface by polar adhesives. The hydrophilicity increase of the BDS coating surfaces should improve the adhesion between the polymer coating and polar adhesives. This concept was investigated using the peel test described in the following section.

4.3.2. Peel strength changes

A 3M Scotch pressure sensitive adhesive tape was selected as a representative adhesive to make the peel test. The adhesive on the commercial tape is acrylate based. Figure 27 is a wide scan XPS spectrum (obtained at 45° take-off angle) of the tape adhesive. It is shown that this tape contains only carbon and oxygen. The percentage of carbon and oxygen is listed in Table VI. Figure 28 and 29 show the narrow scan

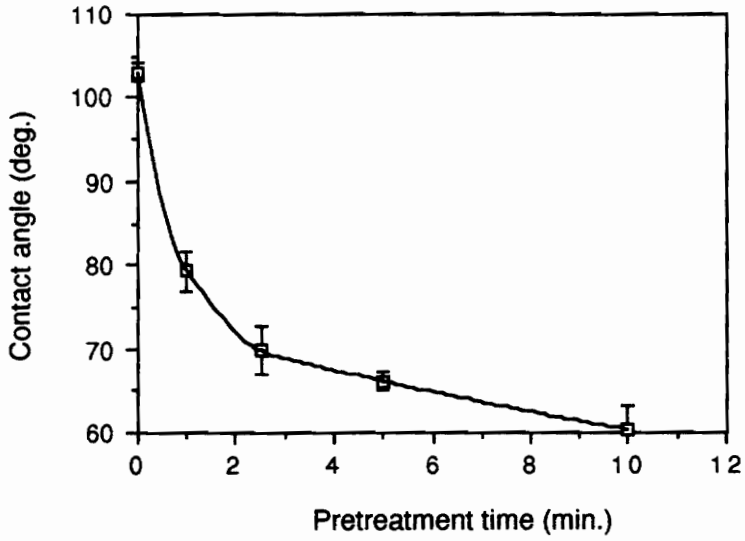

Figure 26. Relation of contact angle and pretreatment time.

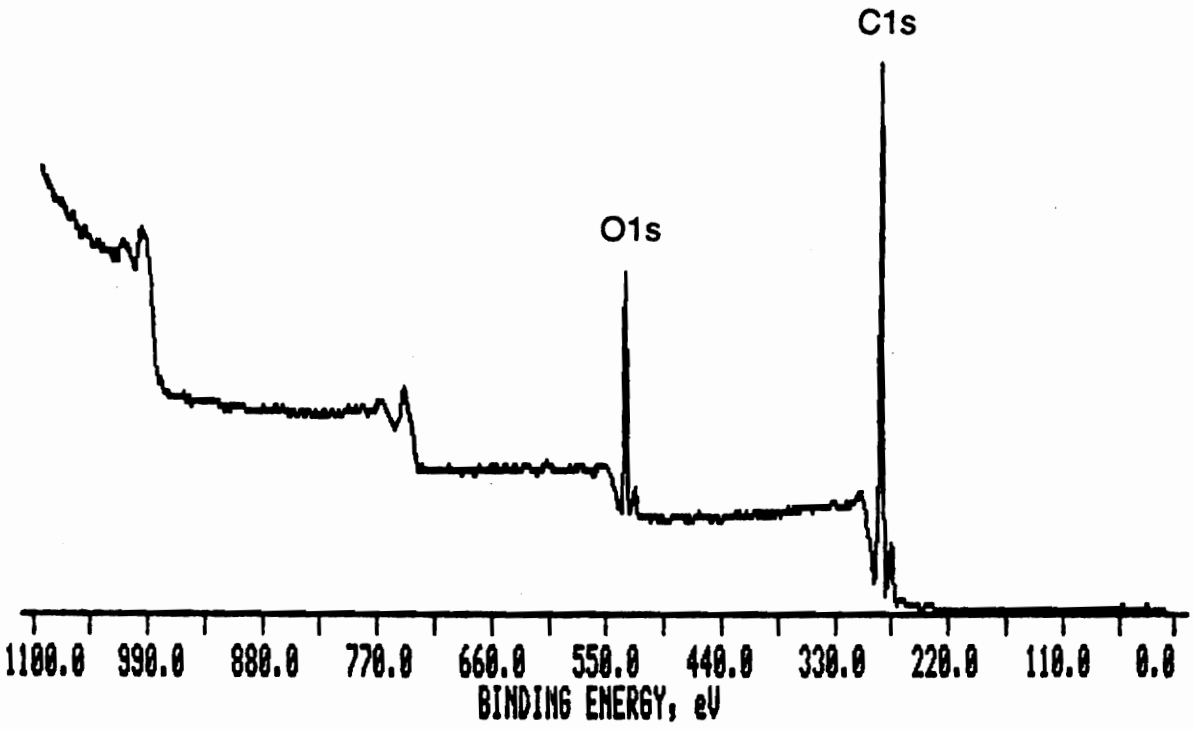

Figure 27. A wide scan XPS spectrum of the adhesive in the 3M Scotch tape.

Table VI. Atomic composition of the adhesive in the 3M Scotch tape.

Element	Atom%
C	84.2 ± 1.2
O	15.8 ± 0.8

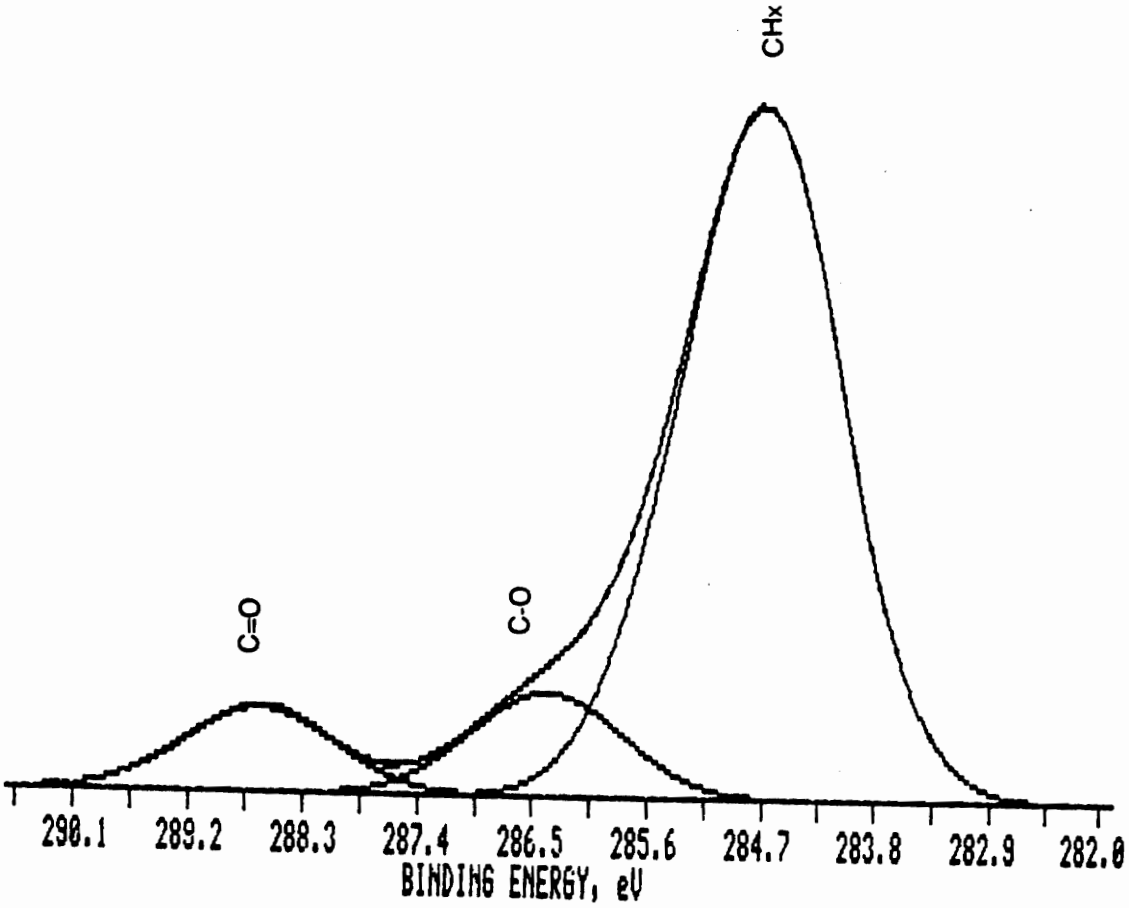

Figure 28. A narrow scan XPS spectrum of carbon in the adhesive of the 3M Scotch tape.

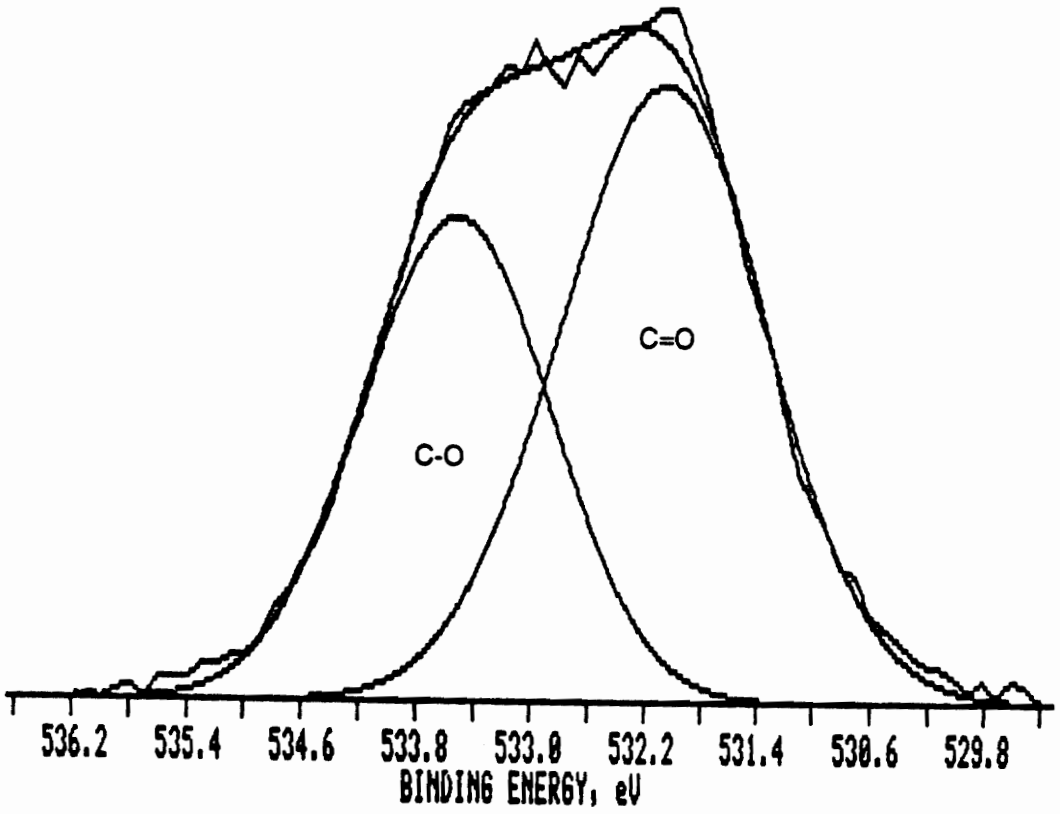

Figure 29. A narrow scan XPS spectrum of oxygen in the adhesive of the 3M Scotch tape.

XPS spectra for carbon and oxygen, respectively. Instead of a single peak, overlapped multiple peaks are observed for both carbon and oxygen. These multiple peaks suggest the existence of multiple functional groups such as carbonyl and carboxylic acid groups on the adhesive. Table VII summarizes the curve fitted results. It is shown that both C=O groups (may include carbonyl and carboxylic acid groups) and C-O groups are present in the tape adhesive. These assignment were further confirmed by ATR-IR analysis. Figure 30 shows the IR spectra obtained at 60° IR beam incident angle. Figure 30a was obtained from the tape treated with 0.01 M NaOH solution, Figure 30b was obtained from the initial tape and Figure 30c was obtained by subtraction of Fig. 30b from Fig. 30a. The peak at 1733 cm^{-1} clearly shows the existence of carbonyl groups and the peak at 1162 cm^{-1} indicates the existence of C-O bonds. Two new peaks appear at 1570 cm^{-1} and 1410 cm^{-1} after the tape was treated with dilute NaOH (Fig. 30c). These two peaks are assigned to the symmetric and asymmetric stretching modes of COO^- [134]. These new peaks are taken as evidence of the existence of carboxylic acid groups on the tape.

Before peel test results are presented, failure modes of an adhesive bond in a test should be discussed first. There are two kinds of failure modes, namely, adhesive failure which is failure at the bond line between the adhesive and the adherend; cohesive failure which is failure within the adhesive layer. The failure mode can often be identified by XPS analysis. Table VIII shows the XPS analysis results on failure surfaces produced during the peel test. The BDS coatings were pretreated in 1.25 M NaOH solution at 30 °C for 10 minutes and the take-off angle in XPS measurement was 15°. Comparing the composition of the BDS coating surfaces before applying the tape adhesive and after peeling-off the tape, for an adhesive failure

Table VII. XPS curve fitted results of the adhesive in the 3M Scotch tape.

Core level	BE (ev)	Area[a] (%)	Atom[b]%
C1s			
CHx	284.7	79.9	67.3
O-C	286.4	11.0	9.3
O=C	288.5	9.1	7.7
O1s			
O=C	532.1	58.6	9.3
C-O	533.5	41.4	6.5

a. The average of the Best Estimate of Standard Error is 1.5.

b. The average of the Best Estimate of Standard Error is 1.0.

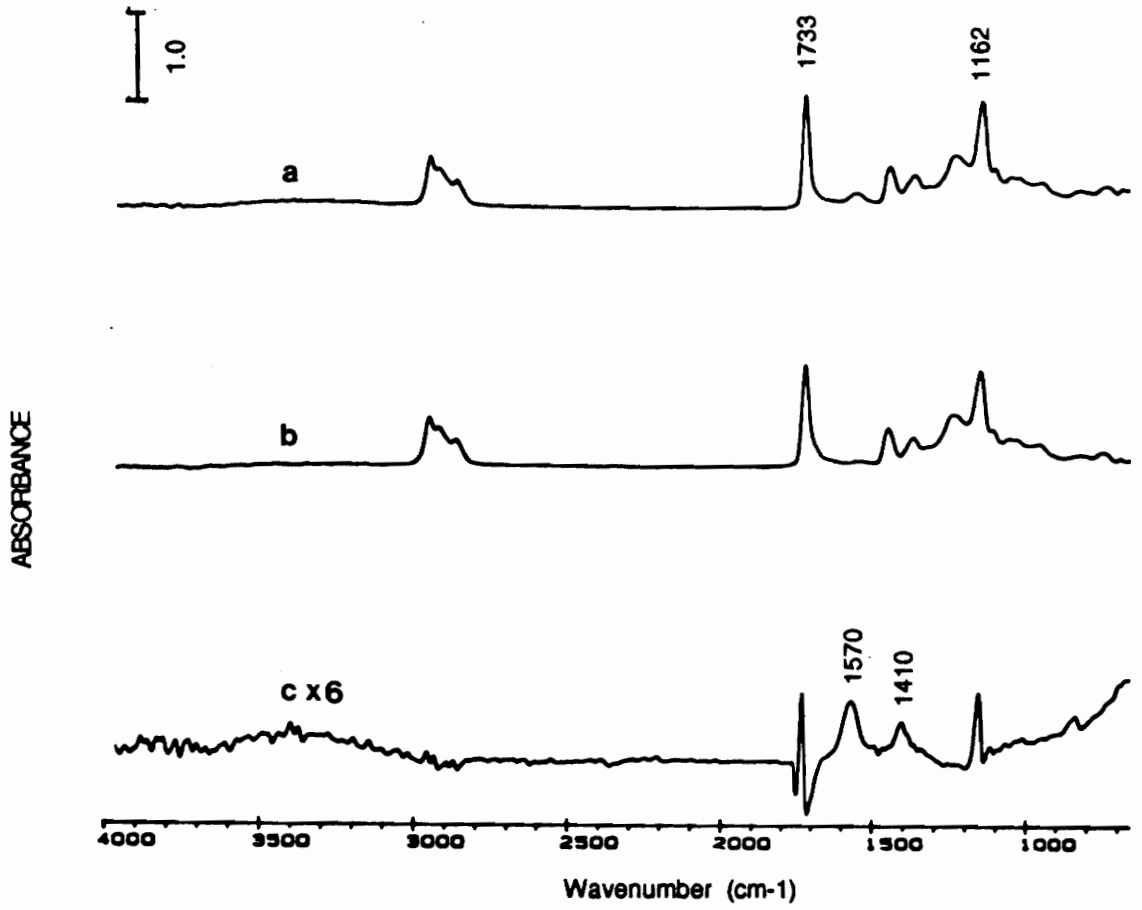

Figure 30. ATR-IR spectra of the adhesive in the 3M Scotch tape.
a. treated with 0.01 M NaOH solution; b. original tape; c. (a-b).

Table VIII. XPS analysis of failure surfaces in peel tests*.

	C %	O %	Si %	S %	N %
BDS side					
before**	74.4	19.3	2.2	1.7	2.5
after***(a)	77.9	17.4	0.7	1.8	2.2
after(c)	85.1	14.5	0.3	0.2	0.0
tape side					
before	84.2	15.8	0.0	0.0	0.0
after	84.1	15.7	0.2	0.0	0.0

* The Best Estimates of the Standard Errors for all data are within 1.5.

** Before the adhesive tape was applied.

*** After the adhesive tape was peeled off.

(a) --- adhesive failure, (c) ---- cohesive failure.

mode, the composition change is very small even though there is indication that some siloxane fragments had transfered from the BDS surface to the tape. However, for cohesive failure, the changes of composition on the BDS surfaces are significant as judged by changes in Si, S and N. This cohesive failure mode actually can be identified by visibly observing the adhesive remaining on the BDS coating surfaces.

Table IX shows peel test results obtained using a peel rate of 1.0 in/min. It is shown that peel strength increased with pretreatment time. This indicates that the surface pretreatment does improve adhesion of the BDS coating surfaces. The problem is that the failure mode changed from adhesive failure to adhesive-cohesive mixed mode failure when the surface pretreatment time increased. As discussed previously, only for adhesive failure is there a direct relation between peel strength and the work of adhesion. Therefore, a 1.0 in/min peel rate is not proper for the evaluation of the BDS surface pretreatment.

When the peel rate was changed to 3.0 in/min, the failure mode for all samples was adhesive failure which satisfied the evaluation requirement. Figure 31 shows the relation between peel strength and pretreatment time. It is clearly indicated that peel strength increased significantly with increasing pretreatment time. After 10 minute pretreatment, the peel strength increased three times. This result clearly indicates that the solution pretreatment can significantly improve the adhesion properties of the BDS coating surfaces.

4.3.3. Relation between surface properties and adhesion properties

Table IX. Peel strength for coatings at different pretreatment time.

Pretreatment time (min.)	Peel strength (10^2 g/in.)	Failure mode
0.0	2.72 ± 0.42	adhesive
1.0	3.86 ± 0.68	adhesive
2.5	4.33 ± 0.44	mixed mode
5.0	7.08 ± 0.81	mixed mode
10.0	79.8 ± 6.6	mixed mode

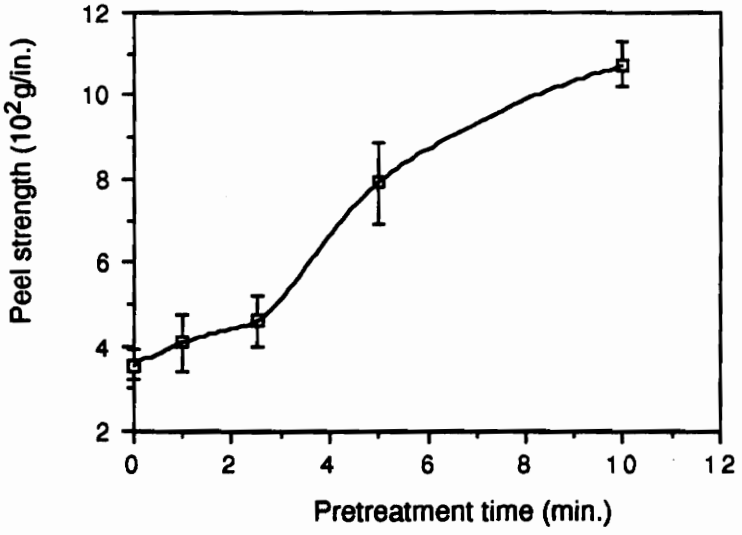

Figure 31. Relation of peel strength and pretreatment time.

The improvements in wettability and adhesion of the BDS coating surface with polar adhesives may result from the removal of the top siloxane layer, the creation of carboxylic acid groups, and the increase of roughness on the BDS coating surface. To distinguish contributions from these individual changes is difficult. However, all of these changes are apparently related to the composition changes on the coating surfaces. Therefore, the relation between the surface composition and the adhesion properties may give some insight as to the cause of the improvement in adhesion due to the surface pretreatment.

Figure 32 shows the relation between silicon concentration of the surface, peel strength, and work of adhesion. The work of adhesion (Wa) was calculated from the water contact angle data by equation [5]. The surface free energy of water used in the calculation was 72.0 mN/m [135]. The peel strengths were obtained at a peel rate of 3.0 in/min. It is shown that both the peel strength and work of adhesion increased with a decrease of the surface silicon concentration. It is interesting that the curves of peel strength and work of adhesion are not symmetric. At the beginning of the surface pretreatment (the data points for high silicon concentrations), peel strength increased slightly with a decrease of silicon concentration. while work of adhesion increased sharply. Thus, the changes in peel strength and work of adhesion are not equivalent. This difference can be seen more clearly in Figure 33 which shows the relation between the peel strength and the work of adhesion of water/BDS coating surfaces. It is assumed that the work of adhesion between the tape and the BDS coating surface is proportional to the measured work of adhesion between water and the BDS coating surface. Theoretically, the peel strength should then be linearly related to the work of adhesion as measured from the water contact angle. A slope of

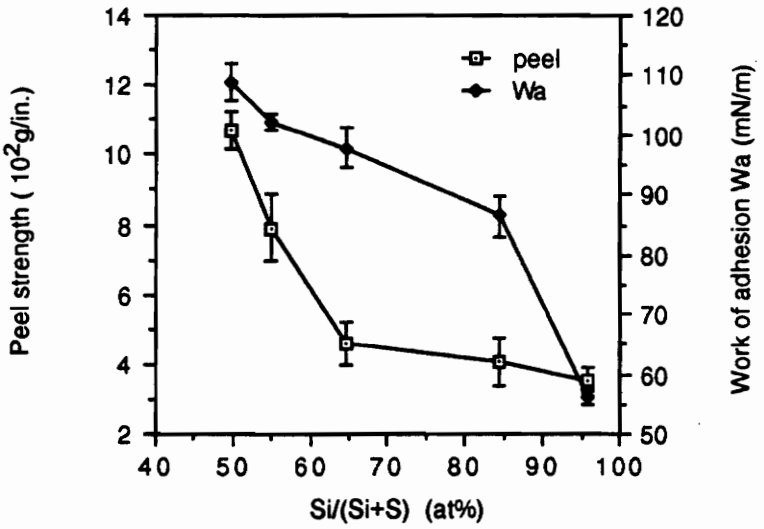

Figure 32. Peel strength and work of adhesion change with siloxane concentration on the coating surfaces.

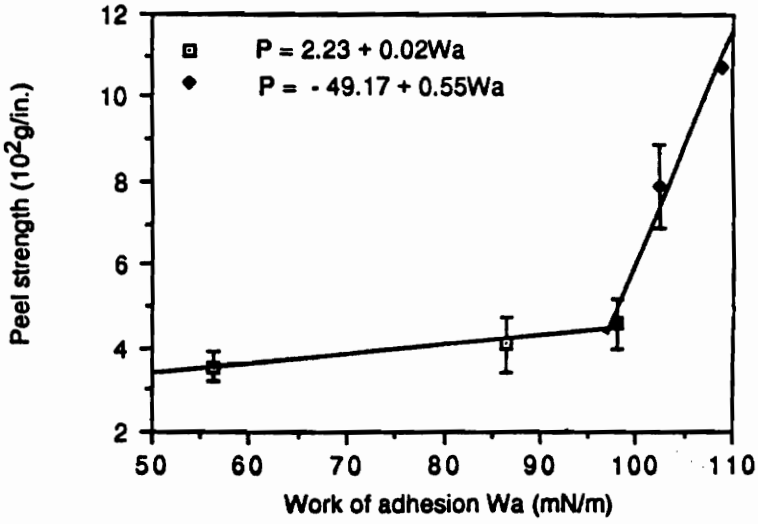

Figure 33. Relation between peel strength of the tape/coating and work of adhesion of water/coating.

0.5 would be expected. However, in Figure 33, in the early stage of the pretreatment (low work of adhesion), peel strength is almost independent of the work of adhesion (with a slope of only 0.02); while at the later stage of the pretreatment (high work of adhesion), the peel strength has a linear relation to the work of adhesion with a slope of 0.55 which is very close to the theoretical value. It is suggested that at the beginning of the pretreatment, because the etching of the surface is inhomogeneous (see the SEM photograph in Fig. 20), an "island-like" surface is created. The behavior of the island-like surface is such that even though the silicon concentration of the whole surface decreased significantly with increasing pretreatment time, the top of the "islands" are still covered with a layer of siloxane. The peel test only senses the top of the "islands". Hence the peel strength increased slowly with the decrease of silicon concentration at the beginning. However, water as a liquid, can wet the "island like" surface better than the adhesive on the 3M Scotch tape. In addition, the roughness increase of the surface may also improve the wetting by water. Therefore, the work of adhesion measured from water contact angle increased significantly in the beginning stage. In the later stages of the surface pretreatment, the top siloxane layer of the BDS coating surface was almost completely removed. Thus, the decrease of silicon concentration with pretreatment time was less (see Fig. 17). The important event for the surface in this stage is that the surface was further activated with the creation of carboxylic acid groups through imide ring opening. The peel test, like water contact angle measurement, can sense the whole surface. Therefore, the peel strength increased consistently with the work of adhesion.

V. RESULTS AND DISCUSSION: PART II

THE BDS COPOLYMER/METAL INTERPHASES

BDS copolymer is a two component copolymer. It may form two kinds of interphases with metal surface oxides. One is a component gradient interphase formed by component segregation at the polymer/metal bond line. The other one is a polymer-metal oxide mixture interphase formed by polymer penetrating into a porous metal oxide surface.

5.1. Interphase Formed from Component Segregation

5.1.1. Characterization of metal surfaces

5.1.1.1. SEM characterization

A polymer surface, obtained by peeling-off a coating from a metal substrate, must be smooth to be used in profiling with the XPS angular dependent technique. This requires that the surface of the metal substrate is also smooth. Metal substrates used in this study were aluminum, titanium and zinc. Figures 34 to 36 show the SEM photographs of the metal substrate surfaces. The metal surfaces are relatively smooth. This qualitative analysis suggests that the requirement for the substrate surfaces used in the copolymer component segregation study may be met.

5.1.1.2. Acidity of the metal substrate surfaces

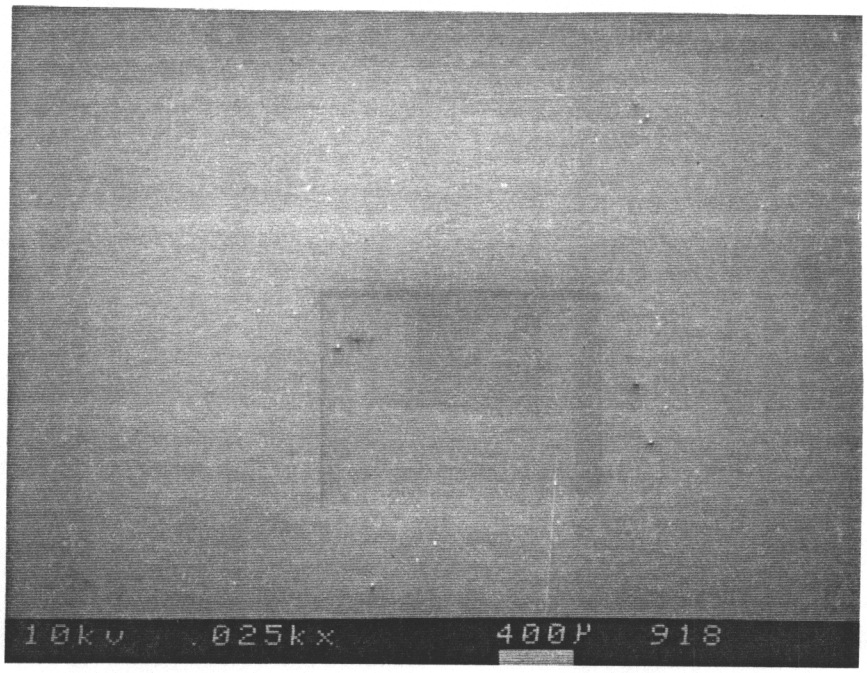

Figure 34. A SEM photograph of the aluminum substrate used for the studies of BDS component segregation.

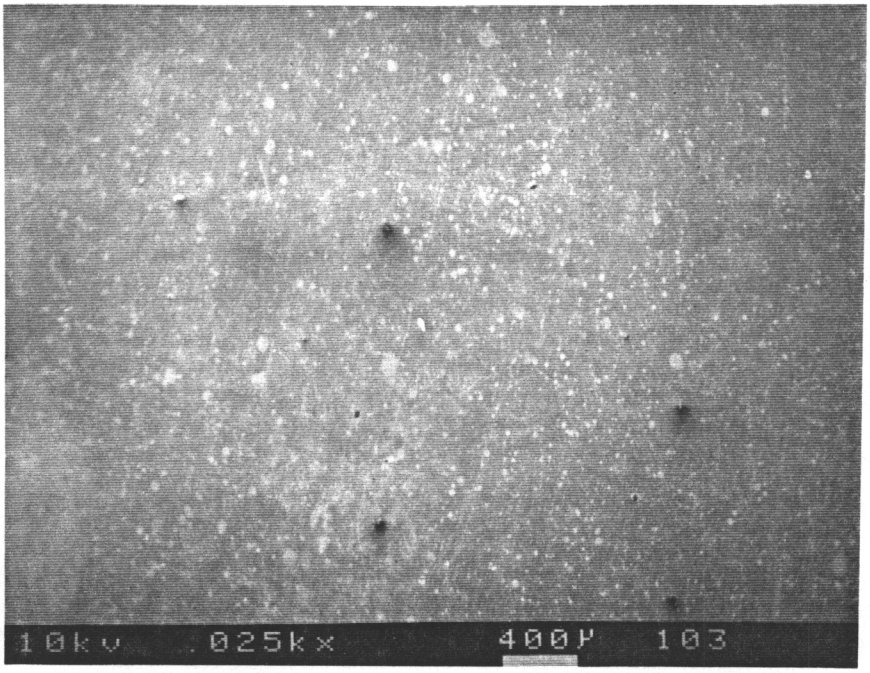

Figure 35. A SEM photograph of the titanium substrate used for the studies of BDS component segregation.

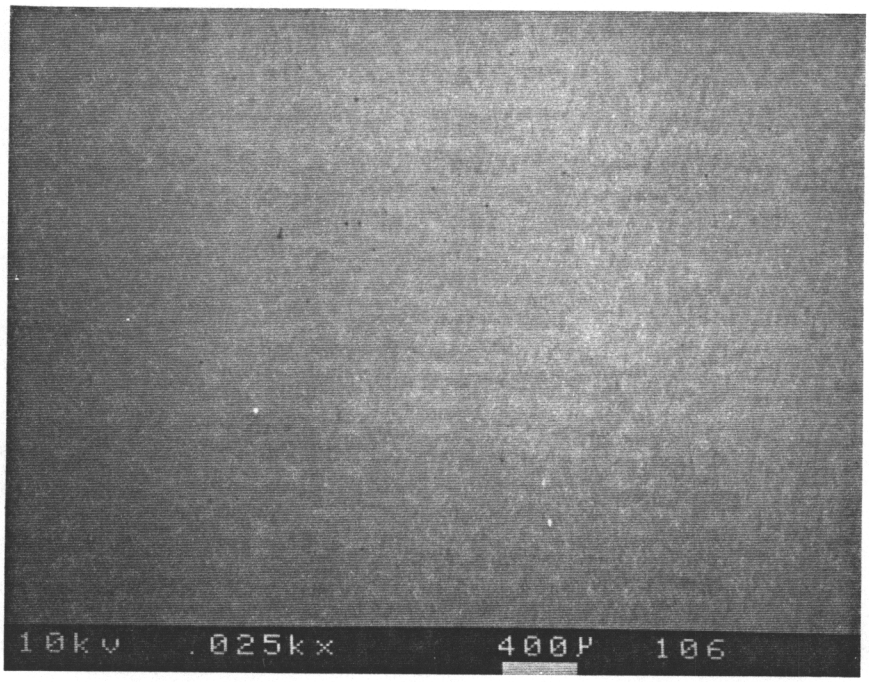

Figure 36. A SEM photograph of the zinc substrate used for the studies of BDS component segregation.

(a). Evaluation of the PVC adsorption test

The relative acidity of the metal substrate surfaces was evaluated by a PVC adsorption test. PVC has been used as an acidic probe in evaluating the acidity of metal oxide powers [55]. However, the PVC adsorption test here in which the PVC adsorbed on a metal surface from a solution was quantified by XPS measurement is a new method. It should be evaluated. The evaluation included the stability of the reference material (Teflon), stability of PVC polymer adsorbed on the metal surfaces and possible reactions other than acid/base interactions between PVC and the metal surfaces. Other factors such as measurement reproducibility will also be discussed.

Stability of the reference material

Table X shows the composition of a Teflon sheet under X-ray exposure in the XPS chamber for different periods of time. It is shown that within 27.5 minutes, the composition of Teflon is not changed distinguishably. Usually, a single XPS measurement for a sample from the PVC adsorption test took 2.7 minutes. Three samples per metal and a total 9 samples for the three metals were measured with the same reference Teflon sheet. The total X-ray exposure time for the reference sheet was then about 25 minutes which is less than the certified 27.5 minutes. Therefore, the stability of the reference material under X-ray exposure during XPS measurement is insured.

Stability of PVC adsorbed on the metals

Table X. X-ray exposure tests of Teflon reference sheets.

Exposure time (min.)	Atomic concentration (%)*				
	C	O	Si	Cl	F
0.0	45.3	2.5	0.0	0.5	51.5
16.5	47.3	2.7	0.0	0.3	49.6
27.5	46.5	2.3	0.0	0.4	50.9

* The Best Estimates of Standard Errors for all data are within 1.5.

Table XI shows the ratio of chlorine from PVC adsorbed on aluminum plates to fluorine from the reference Teflon sheet. The PVC adsorption was conducted in 0.1 wt% PVC solution for 15 minutes. The dried adsorption samples were quantified by XPS measurements at 45° take-off angle with the internal reference (Teflon sheet). It is concluded that the Cl/F ratio did not change with exposure time within 6 minutes. A typical XPS measurement took 2.7 minutes. This means within the XPS measurement time, the loss of PVC under X-ray exposure in the XPS instrument chamber is negligible. In addition, from the data in Table XI, the maximum deviation (the best estimate of the standard error) is 0.012 which represents 7 % relative deviation. This is the evaluation for the reproducibility.

Reactions other than acid/base interaction

There have been reports which indicated that PVC may react with some metal oxides at high temperature [136]. If there are reactions other than the acid/base reaction, the adsorption results may not evaluate the acidity of the metal surfaces. The evidence for reaction was concluded from changes in the chlorine XPS spectrum [136]. Figure 37 is an XPS chlorine spectrum of the PVC polymer used in the adsorption test. Figure 38 is a typical chlorine spectrum of PVC adsorbed on the metal surface in the adsorption tests. It is concluded from shape similarity that there is no change in the chlorine spectrum when the PVC is adsorbed on metal substrate surfaces. This indicates that there is no significant reaction between PVC and the metal surfaces other than acid/base reaction. Figure 39-41 are the XPS spectra of aluminum, titanium and zinc with adsorbed PVC on the surfaces, respectively. These

Table XI. The effect of x-ray exposure on Cl/F ratio in PVC adsorption tests.

Exposure time (min.)	Cl/F ratio
0.0	0.158 ± 0.012
3.0	0.153 ± 0.008
6.0	0.160 ± 0.010

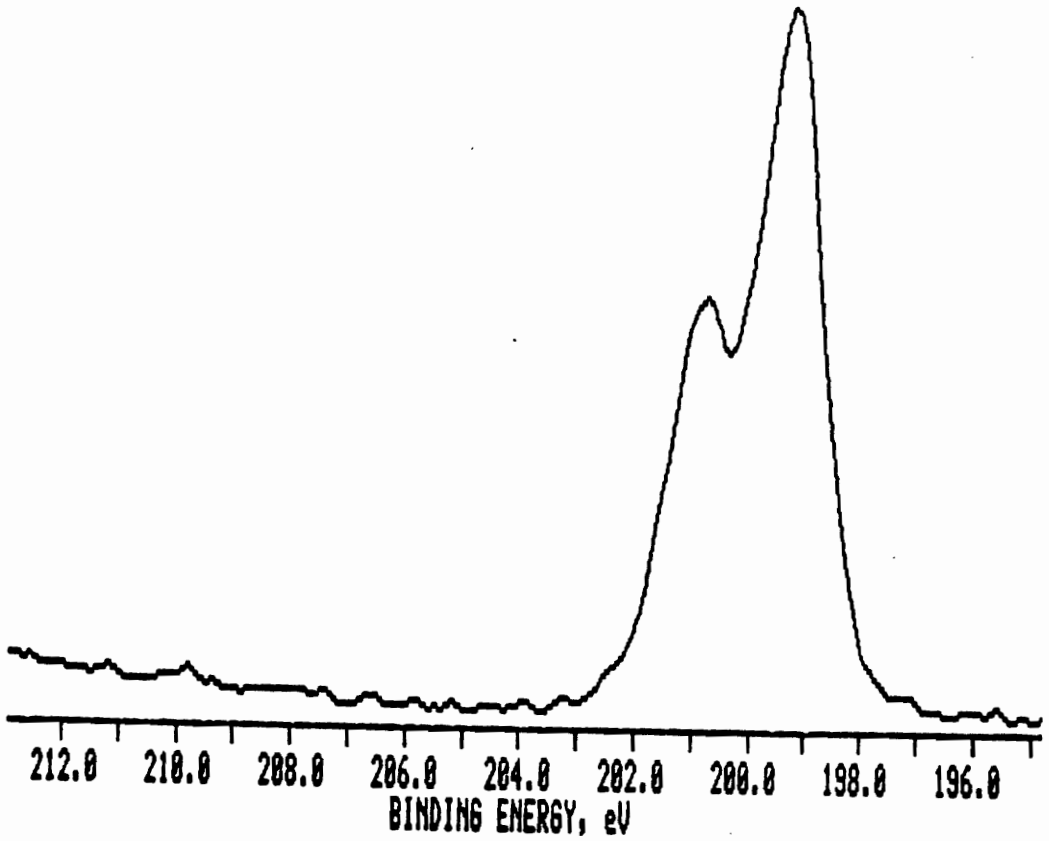

Figure 37. A narrow scan XPS spectrum of chlorine in the PVC polymer used in adsorption tests.

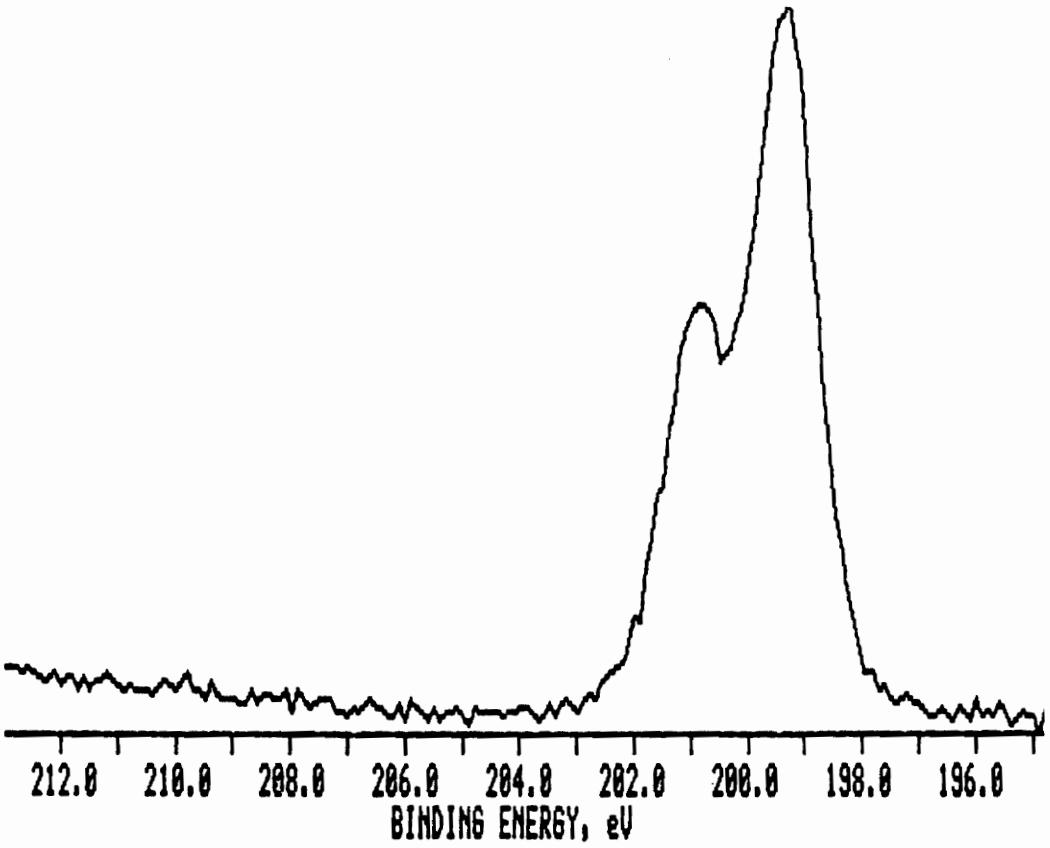

Figure 38. A typical narrow scan XPS spectrum of chlorine of the PVC polymer adsorbed on the metal surfaces.

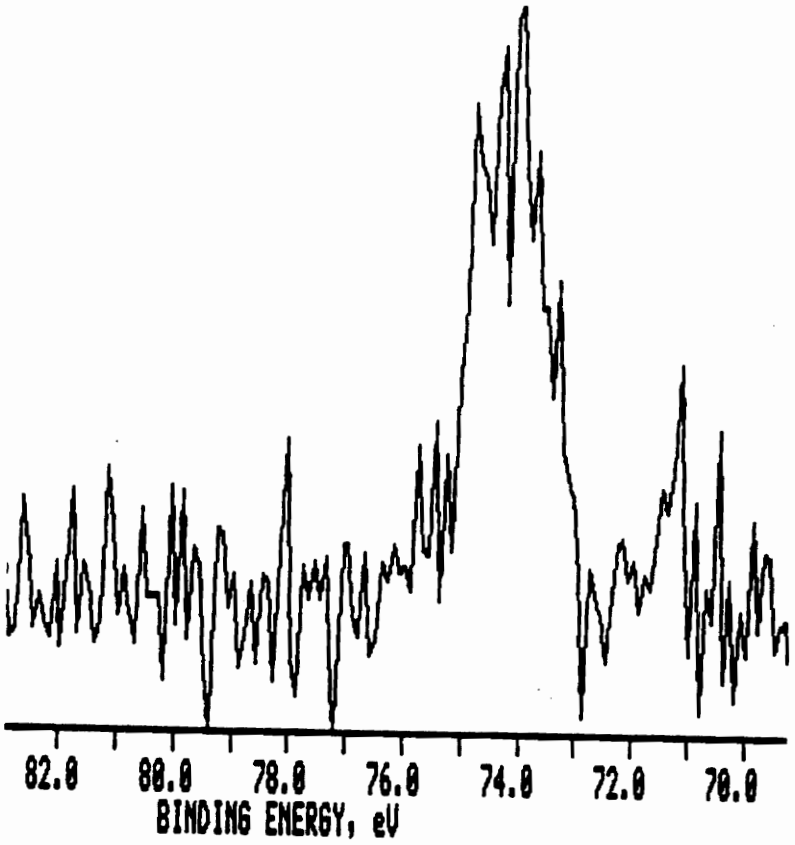

Figure 39. A narrow scan XPS spectrum of aluminum on a PVC-adsorbed aluminum surface.

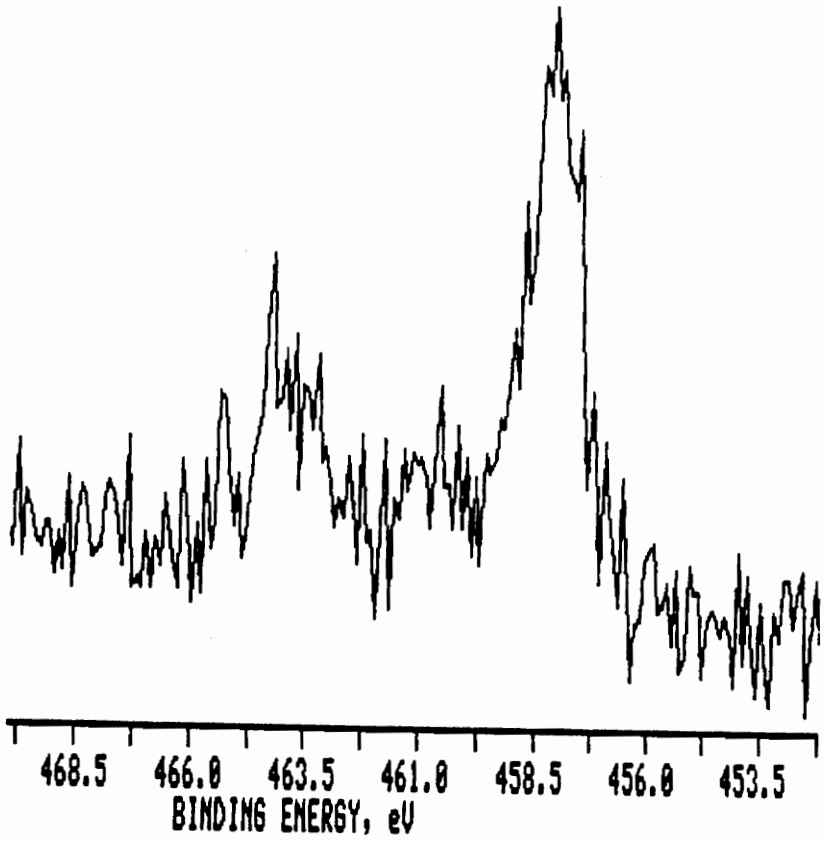

Figure 40. A narrow scan XPS spectrum of titanium on a PVC-adsorbed titanium surface.

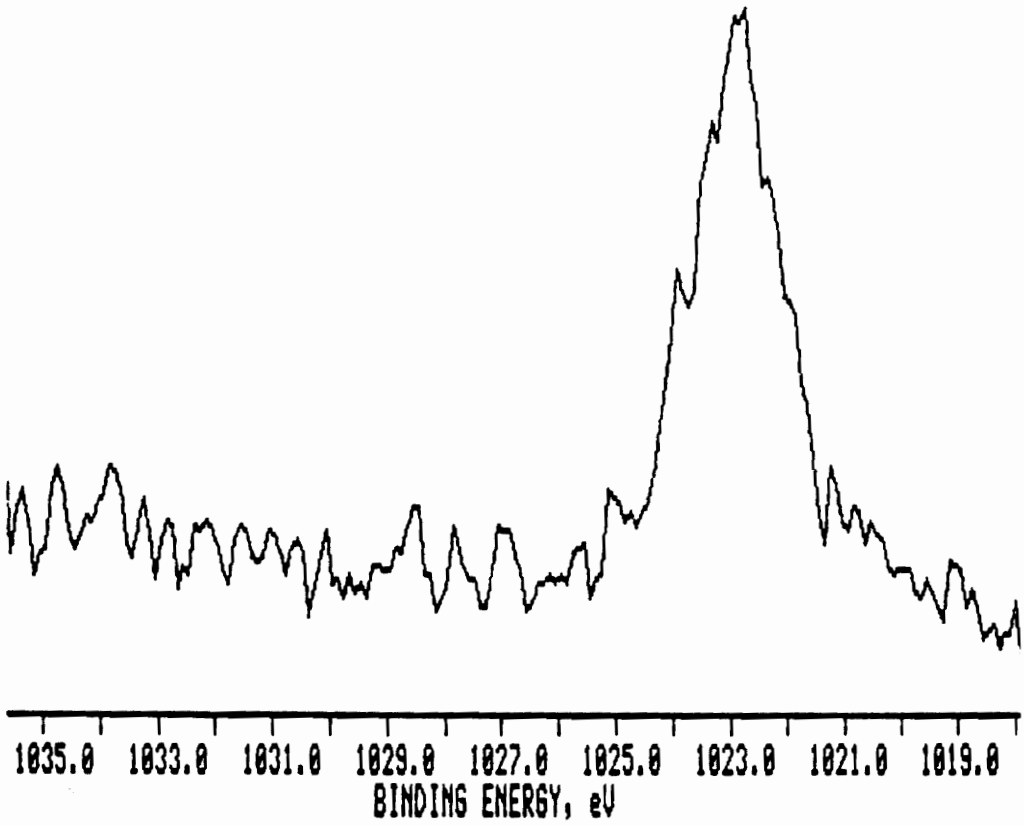

Figure 41. A narrow scan XPS spectrum of zinc on a PVC-adsorbed zinc surface.

spectra are all similar to their typical oxide spectra. This also indicates that there are no significant reactions between the adsorbed PVC and the metal surfaces in the adsorption tests.

The above evaluations suggest that the PVC adsorption test is reliable.

(b). Acidity of the metal oxide surfaces

Figure 42 shows the extent of PVC adsorption (Cl/F ratio) from a 0.1 wt% PVC solution for 15 minutes on different metal oxide surfaces. The amount of PVC adsorbed is in the order of Zn > Ti > Al . Because PVC is an acidic probe [55], the greater the adsorption of PVC, the lower the acidity of the metal oxide surface. Therefore, the relative acidity of the metal oxides is in the order of Al > Ti > Zn. This order also is in agreement with results measured for the corresponding metal oxide powders [137].

5.1.2. Evaluation of the sample preparation method

As described in the experimental chapter, to profile a BDS component gradient interphase formed on a metal surface, the surface of the interphase which contacted with the metal surface, was obtained by

(1). drying a BDS coating formed from a solution casted on the metal surface;

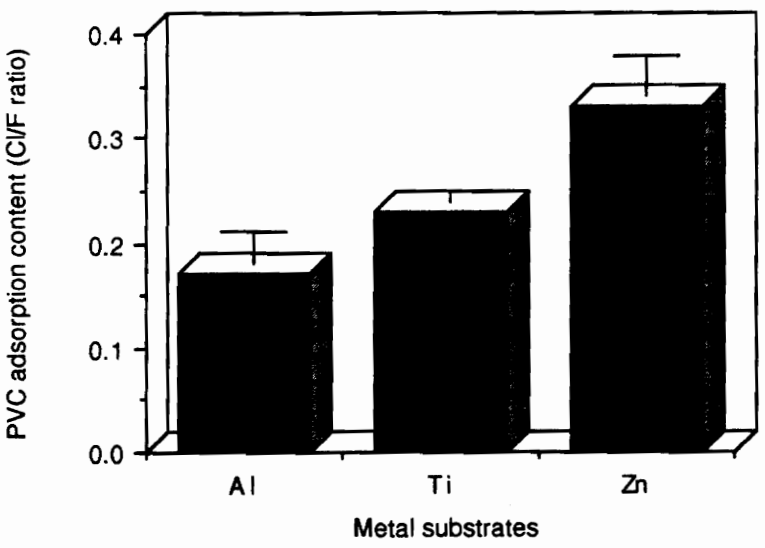

Figure 42. Characterization of metal surfaces by PVC adsorption tests through XPS measurement

(2). treating the sample in 50 °C water; and

(3). peeling-off the coating from the metal surface.

Each step of the experiment may introduce errors into the final profile results. Factors which may affect the final results include a residual solvent effect which comes from incomplete drying at the time the sample was taken out of the vacuum oven, a water treatment effect which comes from the water penetrating into the polymer/metal interface, and the effect of polymer remaining on the metal side after the coating was peeled-off.

5.1.2.1. Residual solvent effect

The residual solvent may have an effect on the final profile results by accelerating BDS component rearrangement in the post-drying steps. Figure 43 shows the relation between silicon concentration at the interface of the BDS side (15° take-off angle) and the drying time. In the first seven hours, the samples were dried at room temperature under vacuum < 1 torr. After that, the samples were dried at 85 °C under the same vacuum. It is shown that during the first seven hours, the silicon concentrations are relatively low. This may be because there is residual solvent at the interphase of the polymer coating at the time the coating was put in water. The residual solvent makes the coating soft enough so that when water penetrates into the interface of the polymer/metal substrate, the water causes rearrangement of the BDS copolymer with imide segments (polar segments) facing to the water. This rearrangement lowers the silicon concentration at the interface.

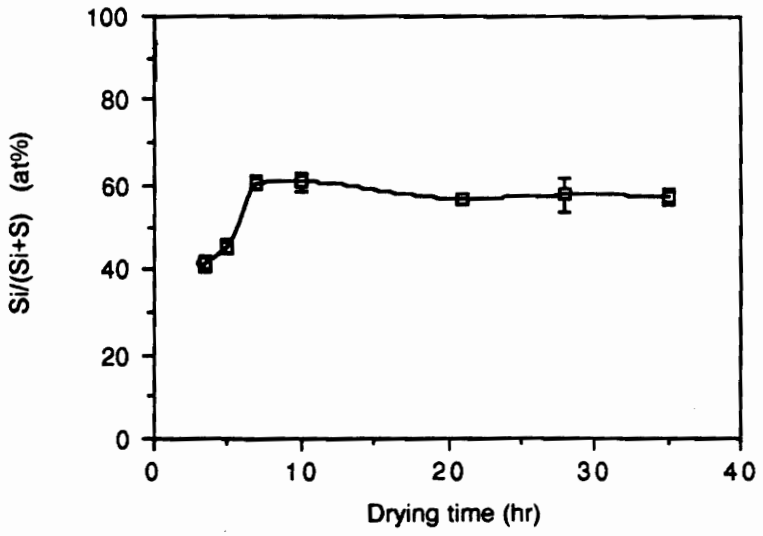

Figure 43. The effect of residual solvent on the siloxane segregation at the BDS coating/aluminum interfaces

After the initial seven hour drying period, the silicon interfacial concentration is constant with drying time. This constant silicon concentration suggests that the drying was almost completed, that the coating was solidified and that the residual solvent effect is minimized. Usually, a sample was dried at room temperature for seven hours and then at 85 °C for another 24 hours in a typical sample preparation for the component segregation study. This is enough to minimize the residual solvent effect.

5.1.2.2. Water treatment effect

The water treatment effect was already mentioned above. In the early stage of drying, the silicon interfacial concentration was relatively low compared to that in the later stage of drying. This phenomenon actually may come from the combined effects of water treatment and the residual solvent as mentioned above. After the BDS coating was extensively dried, the water treatment does not have any effect on the silicon concentration at the interface. This can be further confirmed by a water treatment test. A completely dried BDS coating was treated in 50 °C deionized water for 10 minutes. The surface composition of the BDS coating before and after the treatment is shown in Table XII. It is shown that the silicon concentration of a coating does not change with the water treatment. This further confirms that there is no influence on the silicon interfacial concentration by the water treatment step after the coating was dried according to the procedure described above.

5.1.2.3. The effect of polymer remaining on the metal side

Table XII. BDS coating surface tests in water.

Testing time (min.)	Si/(Si+S) % Take-off angle 15°	35°	75°
0.0	98.3±1.0	93.7±2.1	87.0±2.5
10.0	98.3±1.1	94.2±1.8	88.0±2.3

Polymer remaining on the metal side also may affect the interfacial component profile. Table XIII shows that compared to the original metal surfaces, the composition of the metal surfaces after peeling off the coatings does not change significantly. This means there is no significant amount of polymer remaining on the metal sides after the coatings were peeled off and the effect of polymer remaining on the metal side can be ignored.

5.1.3. Interphases formed from component segregation on different metal surfaces

Figure 44 shows the silicon concentration profile for the BDS coating surface (against the air) and for the polymer/aluminum interface (polymer side). It is shown that the interface has a much lower silicon concentration than that of the surface. It is clearly indicated that there is a composition gradient at the polymer/aluminum interface. This gradient region is the component gradient interphase. Another interesting point is that the silicon concentration is the highest at the interface and then decreases with depth to the polymer bulk. This can not be explained in terms of a polarity effect of the metal oxide. A metal oxide surface is usually considered as a high energy (polar) surface, while the siloxane component is a lower energy (less polar) component compared to the imide component. The siloxane component should not be enriched on a metal surface. Instead, the imide component should be enriched on the metal surface. To understand the component segregation mechanism, other metals, i.e., titanium and zinc, were used in the experiments.

Table XIII. Surface composition of metal substrates.

Metal substrates	Atomic concentration (%) C	O	Si	S	metal
Al (b.)	29.3	45.3	0.0	-	25.4
(a.)	31.0	45.0	0.4	0.3	22.2
Ti (b.)	28.3	55.5	1.8	0.0	13.7
(a.)	34.0	50.9	1.9	0.2	10.4
Zn (b.)	38.0	43.8	0.6	0.0	17.1
(a.)	42.1	39.8	0.3	0.2	16.8

(b.) ---- Before coating.

(a.) ---- After coatings peeled off.

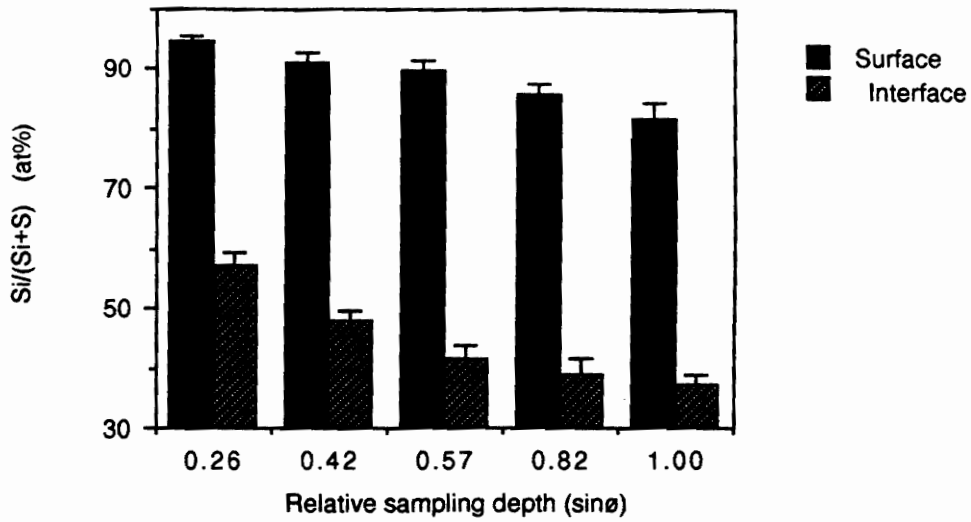

Figure 44. Component segregation of BDS copolymer at the coating surface and the coating/aluminum interface.

Figure 45 shows the interfacial silicon concentration (15° take-off angle) on different metal surfaces. It is shown that the interfacial silicon concentration is in the order of Al > Ti > Zn. Figure 46 is a plot of the interfacial profile results in terms of the silicon interfacial excess (R). The interfacial excess R is calculated from the equation

$$R = [(\text{Si at\%})_{\text{interface}} - (\text{Si at\%})_{\text{bulk}}]/ (\text{Si at\%})_{\text{bulk}} \qquad [14]$$

where Si at% is the silicon relative concentration obtained from the interphase (profiled from the interface side) or from the bulk (43.2 at%). It is shown that on aluminum and titanium oxide surfaces, at the smallest sampling depths (closest to the metal surface), the silicon interfacial excess is positive. This means that silicon is enriched at the interface on aluminum and titanium surfaces. At higher sampling depths, the silicon interfacial excess R does not approach zero (or equal to the bulk composition) but becomes negative on both aluminum and titanium. This means the total composition is dominated by imide segments at the layer next to the siloxane layer which is closer to the metal surface. More interesting is the fact that the silicon interfacial excess on the zinc oxide surface is always negative for all sampling depths. This was not observed for aluminum and titanium.

To understand the component segregation mechanism, interactions between the oxide surfaces and the components of the BDS copolymer should be considered. The BDS copolymer, as illustrated in Scheme I, is composed of both imide segments and siloxane segments. There are a small number of ring-opened imide segments with carboxylic acid groups as shown in the ATR-IR spectrum (see Fig. 24). Thus a

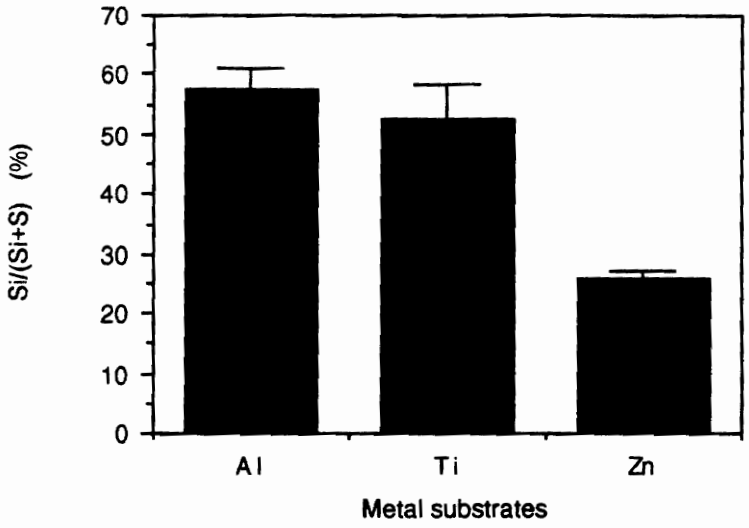

Figure 45. Influence of metal substrates on siloxane segregation of the BDS copolymer at interfaces.

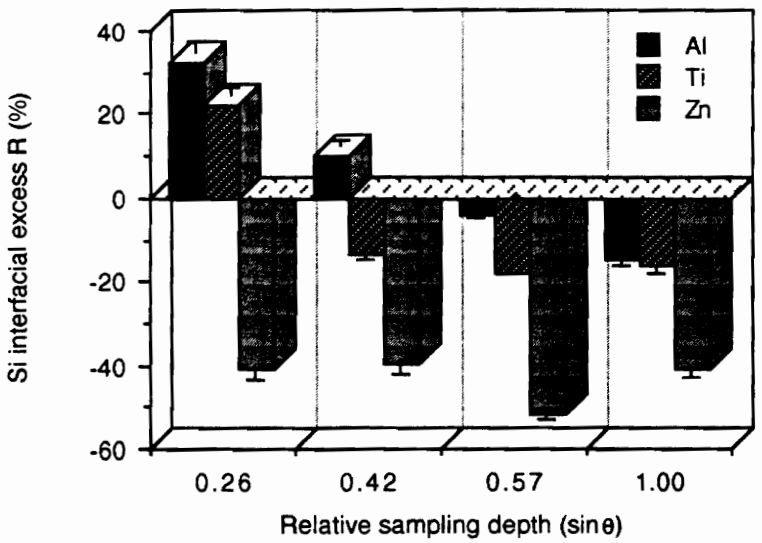

Figure 46. Silicon excess at interfaces of BDS polymer/metal substrates.

small number of imide segments are acidic. On the other hand, the end groups of the siloxane segments are amino groups which makes a small number of siloxane segments basic. If the metal oxide is acidic, the siloxane segments will trend to be adsorbed to the oxide surface and enriched on the surface; if the metal surface oxide is basic, the imide segments will trend to be adsorbed to the surface and the siloxane segments will be depleted on the surface. Fig. 45 shows the interfacial silicon concentration on different metal oxide surfaces with the order of Al > Ti > Zn. The relative acidities of the metal oxide surfaces are in the same order of Al > Ti > Zn. These results exactly agree with the hypothesis above. This argument suggests that the cause of the component segregation of BDS copolymer on metal surfaces may be the influence of the acid/base interactions between the components of the BDS copolymer and the metal oxide surfaces.

5.2. Interphases Formed from Polymer Penetration

5.2.1. Characterization of the porous aluminum surface

Porous aluminum surfaces were obtained from PAA (phosphoric acid anodizing) treatment. Figure 47 shows the porous structure of an aluminum surface obtained from PAA pretreatment at room temperature with a constant electric current of 6.5 mA/cm^2. The average size of the pores is about 100 nm. Figure 48 shows the cross-section of the porous oxide layer. It is seen that the pores run through the oxide layer. The oxide layer thickness can be altered by controlling anodizing voltage and anodizing time. Figures 49 to 52 are AES profiles of the oxide layer prepared at different anodizing voltages for 5 minutes. It is shown that the

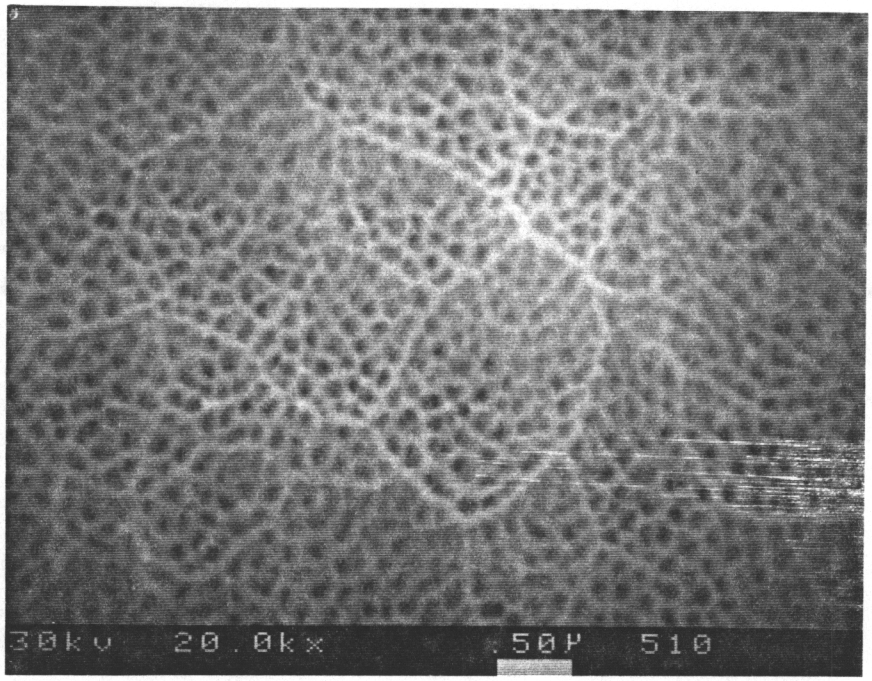

Figure 47. A SEM photograph of an aluminum porous surface.

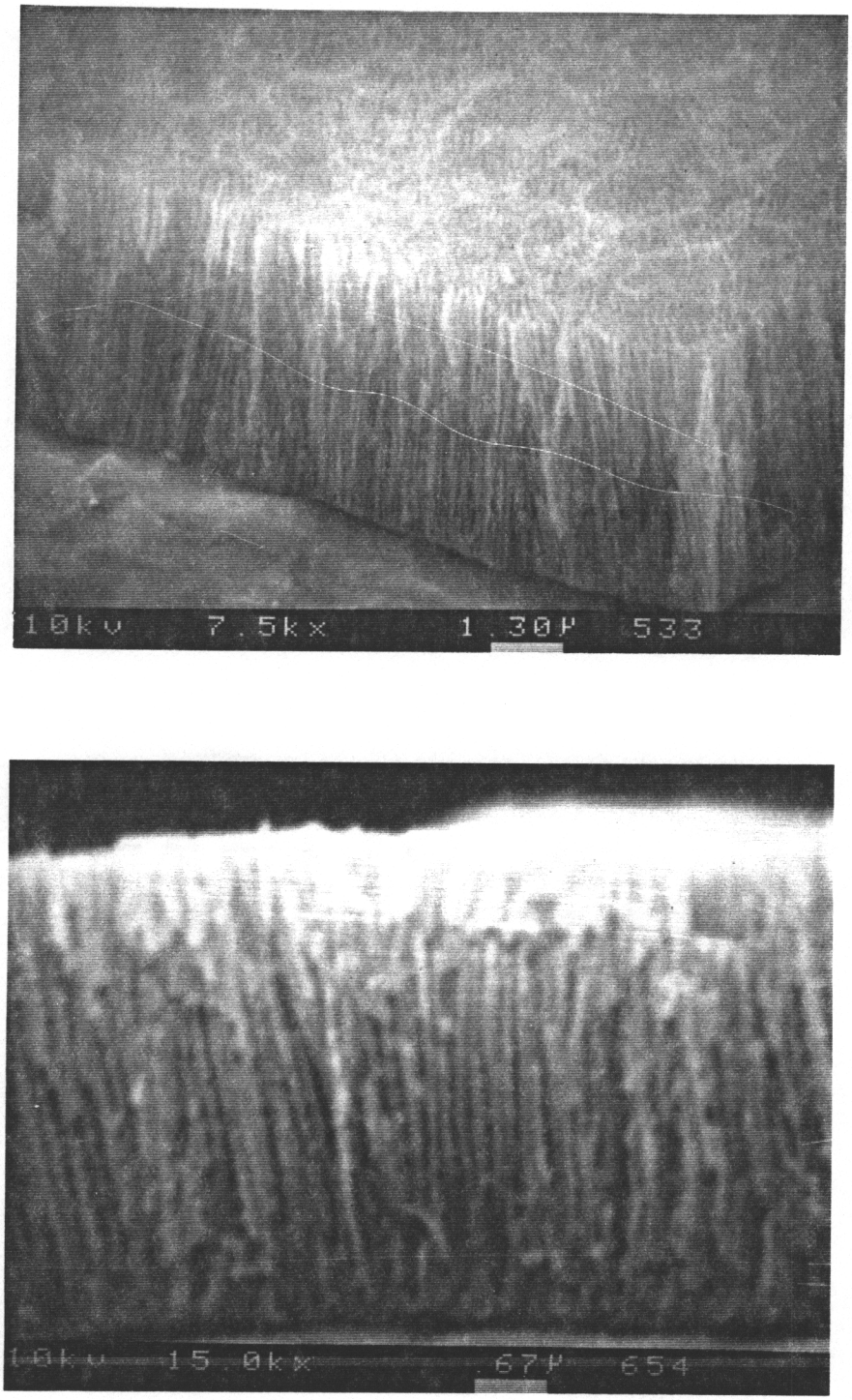

Figure 48. A SEM photograph of a porous oxide layer cross-section of an aluminum surface.

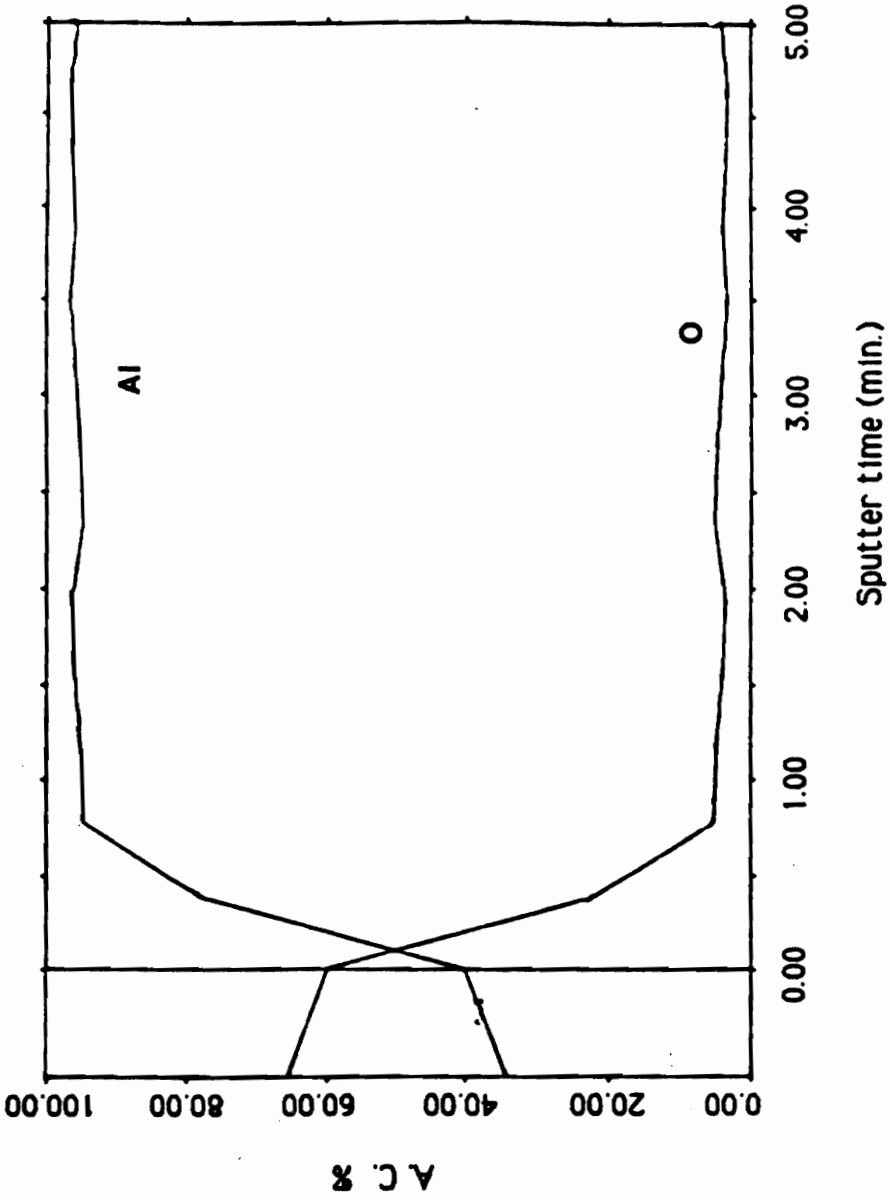

Figure 49. AES oxide layer profile of a non-anodized aluminum surface.

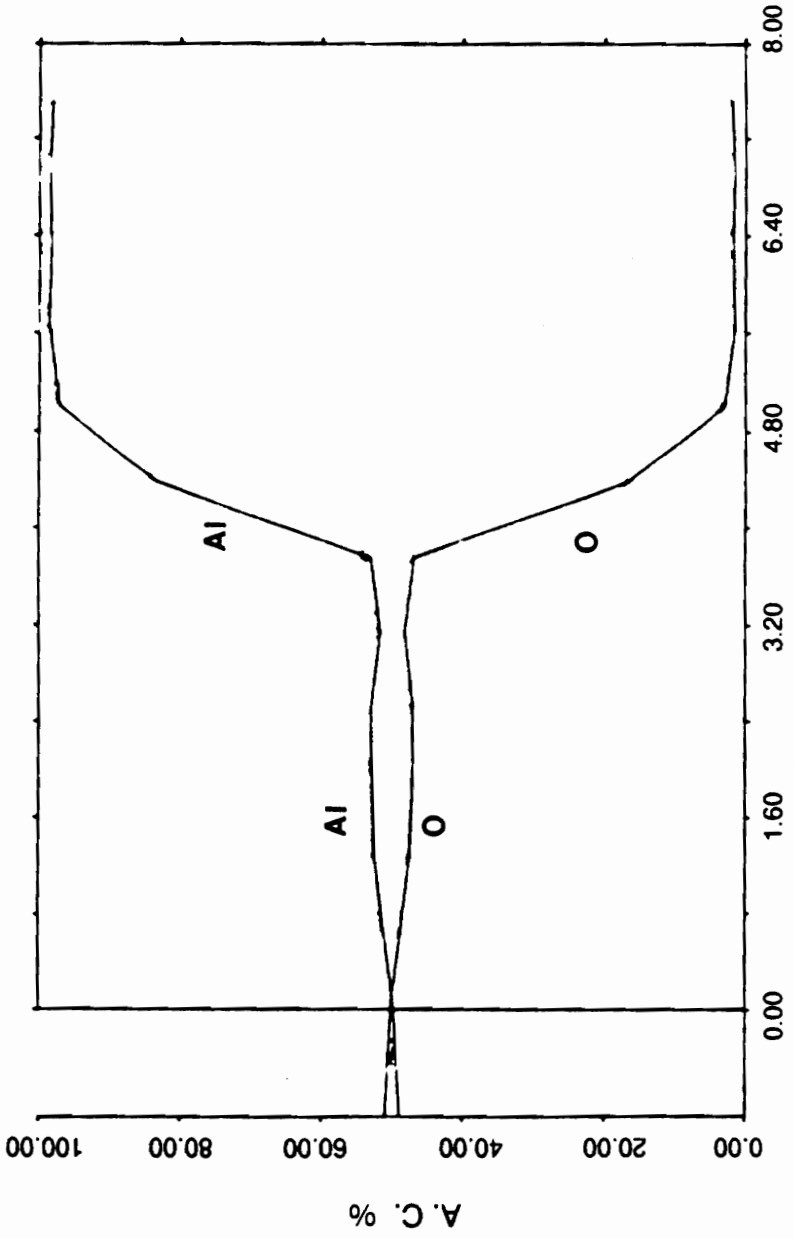

Figure 50. AES oxide layer profile of a 10 volt PAA-pretreated aluminum surface.

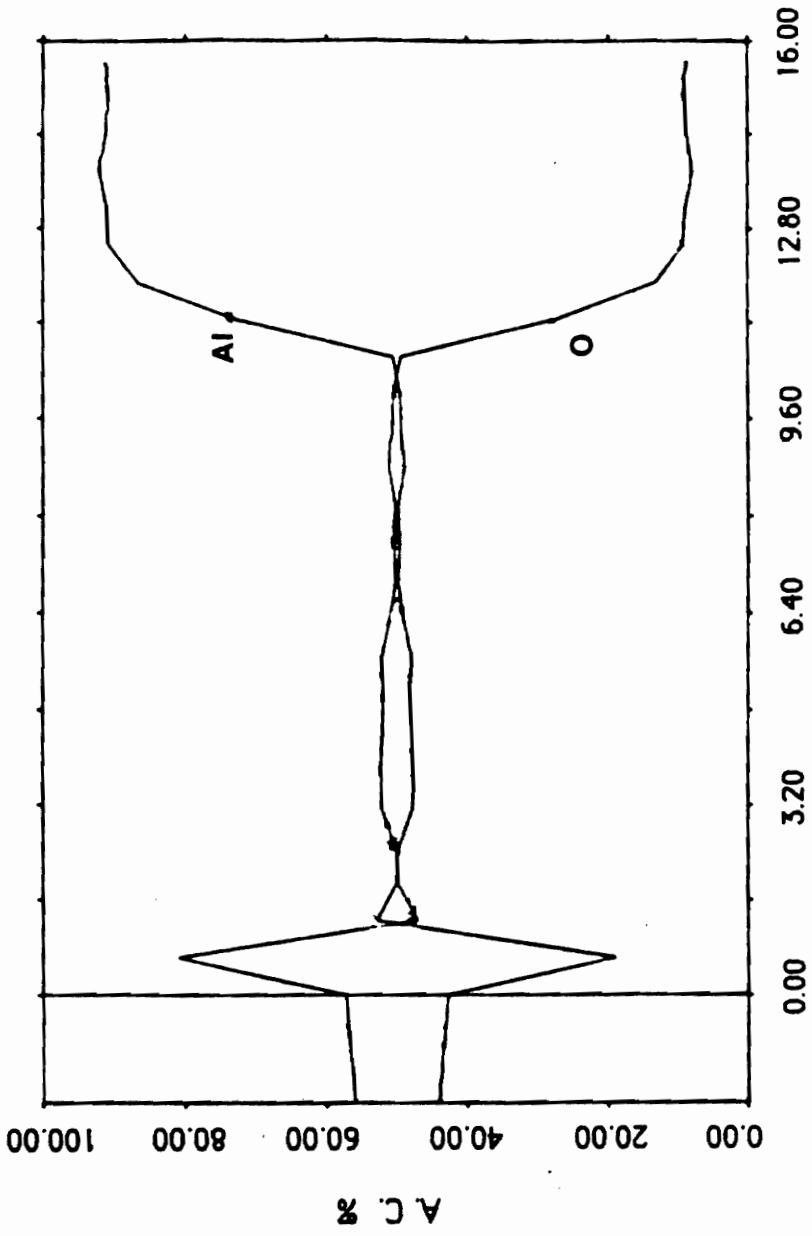

Figure 51. AES oxide layer profile of a 30 volt PAA-pretreated aluminum surface.

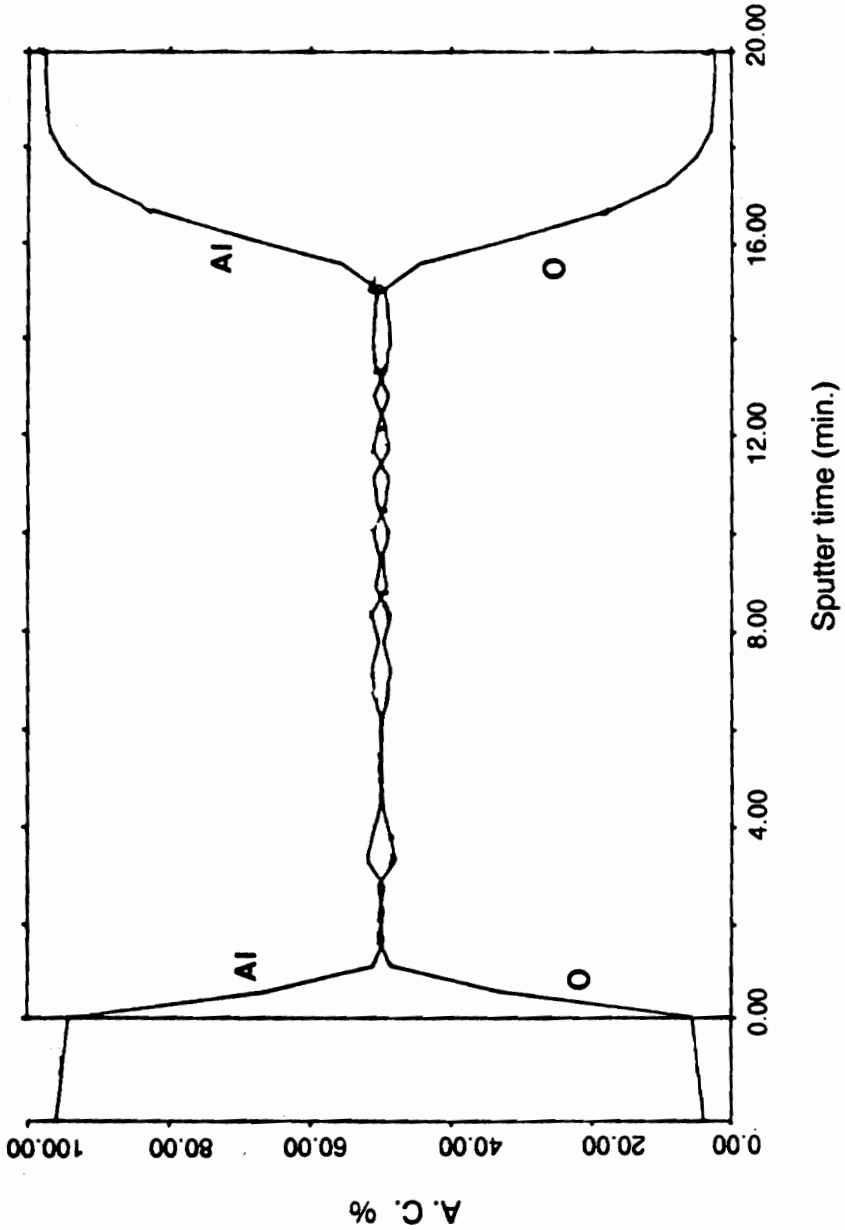

Figure 52. AES oxide layer profile of a 60 volt PAA-pretreated aluminum surface.

time for sputtering through the oxide layer (from the beginning of sputtering to a point at which the oxygen concentration approached to the base line) is longer for samples prepared at higher anodizing voltage than at lower anodizing voltage. The oxide layer thickness increased with increased anodizing voltage. Table XIV summarizes the sputtering time results from the figures.

5.2.2. Interphase formation through BDS penetration

When the porous (anodized) aluminum surfaces were coated with BDS solution, the solution may have penetrated into the pores. After solidification, the penetrated polymer may form an interphase with the aluminum oxide. Figures 53 and 54 show AES profiles across the polymer/nonporous aluminum oxide and polymer/porous aluminum oxide interfaces. The nonporous aluminum oxide surface is the surface without PAA pretreatment. The porous aluminum oxide surface is the surface obtained from anodizing at 30 V for 5 minutes. The profiles were obtained by sputtering from the metal side. The appearance of the carbon signal in both figures indicates break through to the polymer layer during sputtering. The period of time between the point that the carbon signal starts to increase and the cross point of the carbon-aluminum signal lines (Al at% = C at%) is experimentally defined as the interphase sputter time. Comparing Fig. 53 with Fig. 54, it is seen that it takes much longer to sputter through the polymer-oxide layer for the porous oxide sample than for the nonporous oxide sample. The interphase sputter times are summarized in Table XV. It is shown that the interphase sputter time is almost doubled for the sample on the porous surface compared to the sample on the nonporous surface. This means that polymer penetration into the porous oxide layer has occurred. This

Table XIV. Oxide layer profile of PAA pretreated aluminum surfaces.

Anodizing voltage (v)	Sputter time (min.)
0.0	0.8
10.0	5.0
30.0	12.7
60.0	18.4

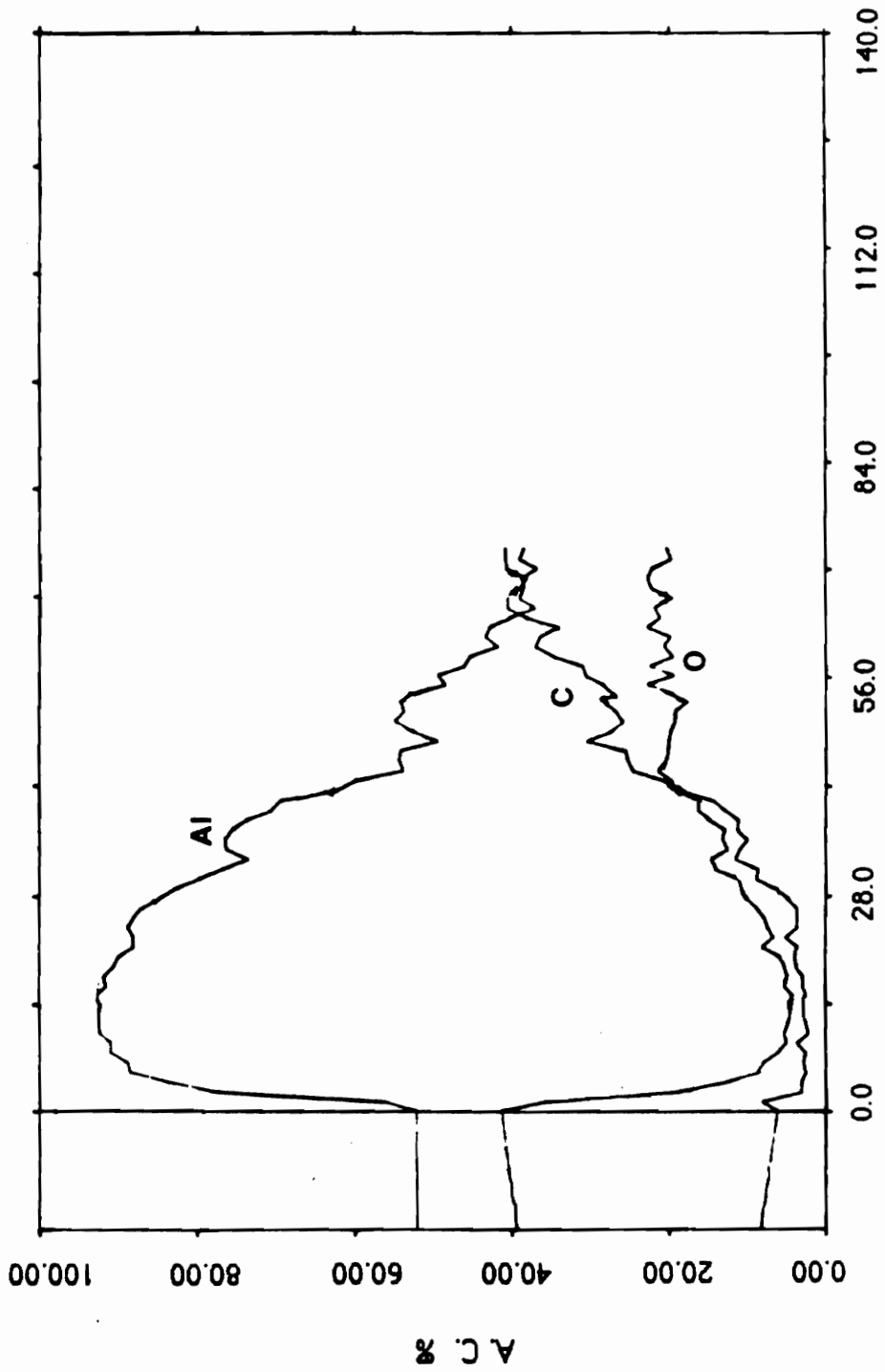

Figure 53. AES interphase profile across a bond line of the BDS coating/nonporous aluminum substrate.

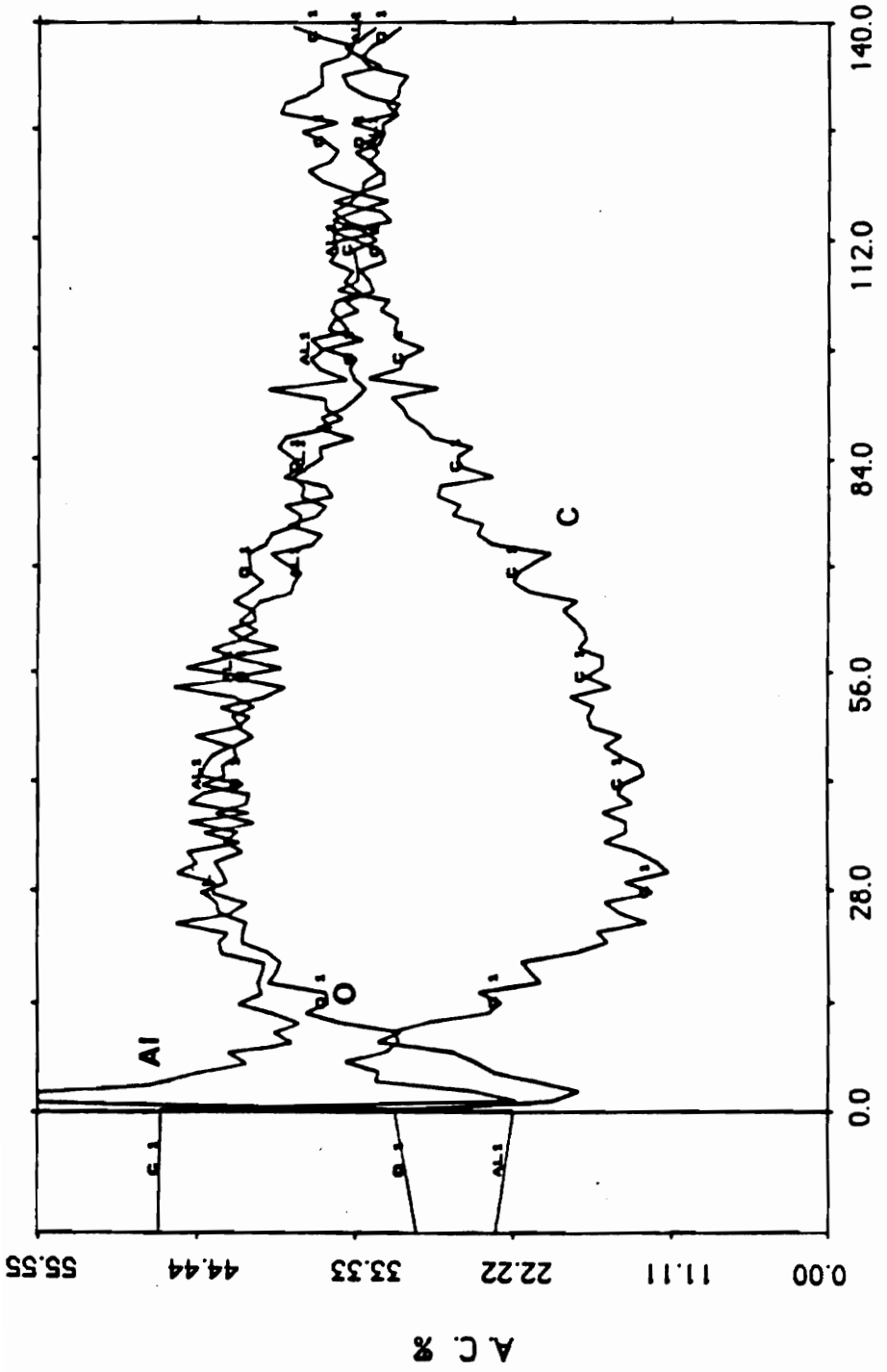

Figure 54. AES interphase profile across a bond line of the BDS coating/porous aluminum substrate.

Table XV. Interphase profile across bond lines of BDS coating/aluminum substrates.

Anodizing time (min.)	Sputter time (min.)	
	Oxide surface	Interphase
0.0	0.8	46.7
5.0	12.7	86.0

penetration forms a polymer-metal oxide interphase. The formation of the interphase is expected to have a significant influence on the adhesion between the polymer coating and the metal substrate.

VI. SUMMARY

This research was divided into two sections. In the first section, surfaces of BDS [BTDA (3,3',4,4'-benzophenonetetracarboxylic dianhydride) - DDS (3,3'-diaminodiphenyl sulfone) - PSX (polydimethylsiloxane) copolymer] coatings formed from a solution were modified through surface pretreatment in a strong alkaline solution. The relation between surface property changes and adhesion property changes of the coating surfaces was studied. In the second section, interfacial profile studies on bond lines of the BDS polymer/smooth metal substrates and the BDS polymer/porous aluminum substrate were conducted.

In the surface modification studies, pH contact angle titration, ATR-IR (attenuated total reflectance infrared) spectroscopy and angular dependent XPS (X-ray photoelectron spectroscopy) were used to characterize the coating surfaces. Water contact angle measurements and peel tests were used in evaluating the influence of the surface pretreatment on the wettability and adhesion strength of the coating surfaces. The surface pretreatment of the BDS coatings etched away the top siloxane surface layer, activated the surfaces through exposing and creating polar functional groups, particularly carboxylic acid groups, and roughened the coating surfaces. These changes resulted in significant improvements for the coating surfaces in wettability and in adhesion to polar adhesives.

Interfacial profiles on the bond lines of the BDS polymer/smooth metal substrates were obtained by XPS angular dependent measurements on the polymer sides of the bond interfaces obtained from peeling off of the polymer coatings with no significant polymer remaining on the metal surfaces. It was found that component

gradients of the BDS copolymer existed at the bond lines of the polymer/metal substrates. Therefore, component gradient interphases were formed at the bond lines. The component gradients were different on different metal oxide surfaces with the siloxane interfacial excess in the order Al > Ti > Zn. The relative acidities of the metal oxide surfaces were characterized by PVC (poly(vinyl chloride)) adsorption tests quantified by XPS measurements and were in the order Al > Ti > Zn. The cause for the BDS component segregation was suggested to be the influence of acid-base interactions between components of the BDS copolymer and the metal surface oxides.

Interfacial profiles of the bond lines of the BDS copolymer/porous aluminum substrates were obtained by AES (Auger electron spectroscopy) profiling through the bond lines from the metal side. The BDS polymer dilute solution penetrated into the porous aluminum surfaces and therefore formed polymer-metal oxide mixture interphases at the bond lines.

VII. SUGGESTED FUTURE STUDIES

Additional investigations recommended here may be useful as research in this area continues.

A BDS surface after pretreatment in an alkaline solution possesses carboxylic acid groups. The quantification of the acid groups can be done through pH contact angle titration with a NaOH solution under controlled conditions [86]. This quantification can be used in kinetic studies of the acid group creation during the modification. The well characterized surface may now serve as a model surface in the study of influence of acid-base interaction on adhesion.

The cause for the BDS component segregation on metal oxide surfaces was suggested as the influence of acid-base interactions between components of BDS copolymer and the metal oxide surfaces. This may be further confirmed by adsorption studies with model compounds.

Kinetic studies of the interphase formation by the penetration of the BDS copolymer solution or hot melts into porous aluminum surfaces may be an exciting topic for future research. These studies may include influence of oxide pore size, polymer molecular weight, applied pressure and temperature, on the penetration kinetics. The interphases made for the kinetic studies, i.e., interphases with different polymer penetration depths, may be used to study the influence of the interphase formation on adhesion strength, durability and water resistance.

REFERENCES

1. H. Vogel and C. S. Marvel, J. Polym. Sci., 5, 511 (1961).

2. P. M. Hergenrother and H. M. Levine, J. Polym. Sci., A-3, 1665(1965).

3. P. M. Hergenrother, Macromolecules, 14, 898 (1981).

4. J. A. Kruez, A. L. Endry, and F. P. Gay et al., J. Polym. Sci., A-1, 4, 2607(1966).

5. P. M. Hergenrother, in "Encyclopedia of Polymer Science and Engineering", 1, 5(1985).

6. G. N. Babu, in "Polyimides: Synthesis Characterization and Applications", Vol. 1, K. L. Mittal, ed., p.51, Plenum press, New York (1982).

7. K. W. Lee, S. P. Kowalczyk and J. M. Shaw, Macromolecules, 23, 2097(1990).

8. G. C. Davis, B. A. Heath, and G. Gildenblat, in "Polyimides: Synthesis Characterization and Applications", Vol. 2, K. L. Mittal, ed., p847, Plenum Press, New York (1984).

9. J. D. Summers, "Siloxane Modified Engineering Polymers: Synthesis and Characteristics", Ph. D. Dissertation, Virginia Polytechnic Institute & State University, Blacksburg, VA (1988).

10. L. M. Siperko and R. R. Thomas, J. Adhesion Sci. Technol., 3, 157(1989).

11. W. J. Ward and T. J. McCarthy, in "Encyclopedia of Polymer Science and Engineering", Volume Suppl. Vol., J. I. Kroschwitz ed., p.674, John Wiley & Sons, New York (1990).

12. A. J. Kinloch, J. Materials Sci., 15, 2141(1980).

13. J. G. Williams, "Fracture Mechanics of Polymers", p. 93, Halsted Press, New York (1984).

14. K. L. Mittal, Electro. Component. Sci. Technol., 3, 21(1976).

15. M. Tirrell, in "Opportunities & Research Needs in Adhesion Science and Technology" Conference at Stanford University, G. G. Fuller and K. L. Mittal ed., 1-23, Hitex Publication (1988).

16. N. A. DeBruyne, Nature, 180, 262(1957).

17. L. E. Raraty and D. Tabor, Proceedings of the Royal Society, A-245, 184(1958).

18. M. J. Barbaris, Nature, 215, 383(1967).

19. K. L. Mittal, in "Polymer Science and Technology", Vol. 9A, L. H. Lee ed., p. 129, Plenum Press, New York (1975).

20. G. J. McHargue, J. Adhesion Sci. Technol., 2, 369(1988).

21. L. T. Drzal, in "Summary of the Workshop Held on the Role of the Polymer Substrate Interphase in Structural Adhesion", Air Force Materials Laboratory Technical Report AFML-TR-77-129, (1977).

22. S. Bloeck, E. Hofling, and A. Jengic, Adhasion, 16, 39(1972).

23. R. M. Vasenin, "Adhesion, Fundamentals and Practics", p. 29, McLaten & Son, London (1969).

24. R. M. Vasenin, Adhesives Age, 8, 21(1965).

25. D. E. Packham , J. Appl. Polymer Sci., 18, 3237(1974).

26. D. E. Packham , J. Appl. Polymer Sci., 18, 3249(1974).

27. J. R. Evans and D. E. Packham, in "Adhesion-1", K. W. Allen ed., p. 297, Applied Science Publishers, London (1977).

28. J. R. Evans and D. E. Packham, J. Adhesion, 9, 267(1978).

29. J. R. Evans and D. E. Packham, J. Adhesion, 10, 39(1979).

30. J. R. Evans and D. E. Packham, J. Adhesion, 10, 177(1979).

31. J. S. Solomon, D. Hanlin, and N. T. McDevitt, in "Adhesion and Adsorption of Polymers", Part A, L. H. Lee ed., p. 103, Plenum Press, New York (1980).

32. A. Rantell, Trans. Inst. Metal Finish, 47, 197(1969).

33. K. Kato, Polymer, 8, 33(1967).

34. K. Kato, Polymer, 9, 419(1968).

35. M. Matsunaga, Y. Haguida and K. Ito, Metal Finish, 66, 80(1968).

36. K. Heynmann, Production Finish, 19, 38(1966).

37. L. E. Perrins and K. Pettett, Plastics and Polymers, 39, 391(1971).

38. E. H. Andrews and A. J. Kinloch, Proc. Roy. Soc., A332, 385(1973).

39. E. H. Andrews and A. J. Kinloch, Proc. Roy. Soc., A332, 401(1973).

40. A. N. Gent and J. Schultz, J. Adhesion, 3, 281(1972).

41. W. C. Wake, "Adhesion and the Formulation of Adhesions", p. 69, Applied Sci. Publishers, London (1976).

42. S. S. Voyutskii, "Autohesion and Adhesion of High Polymers", John Wiley and Sons, New York (1963).

43. R. M. Vasenin, Adhesives Age, 8, 30(1965).

44. J. N. Anand and H. J. Karam, J. Adhesion, 1, 16(1969).

45. R. P. Campion, J. Adhesion, 7, 1(1975).

46. B. V. Deryaguin, Research, 8, 70(1955).

47. A. Roberts, in "Adhesion-1", K. W. Allen ed., p. 207, Applied Science Publishers, London (1977).

48. C, Kemball, in "Adhesion", D. D. Eley ed., p.19, Oxford University Press, London (1966).

49. A. J. Staverman, in "Adhesion and Adhesives", Vol. 1, R. Houwink ed., p.9, Elsevier, Amsterdam (1965).

50. W. C. Wake, Royal Institute of Chemistry Lecture Series 4, 1(1966).

51. J. R. Huntsberger, in "Treatise on Adhesion and Adhesives", Vol.1, R. L. Patrick ed., p.119, Marcel Dekker, New York (1967).

52. M. J. Jaycock and G. D. Parfitt, "Chemistry of Interfaces", p.235, John Wiley & Sons, New York (1986).

53. F. M. Fowkes, J. Phys. Chem., 66, 382(1962).

54. F. M. Fowkes, J. Adhesion, 4, 155(1972).

55. F. M. Fowkes and M. A. Mostafa, Ind. Eng. Chem. Prod. Res. Dev., 17, 3(1978).

56. F. M. Fowkes, in "Adhesion and Adsorption of Polymers", A, L. H. Lee ed., p.42, Plenum Press, New York (1980).

57. F. M. Fowkes, in "Corrosion Control by Organic Coatings", NACE, H. Leidheiser, Jr. ed., p.1, Plenum Press, New York (1981).

58. F. M. Fowkes, D. W. Dwight, and D. A. Cole et al., J. Non-Crystalline Solids, 120, 47(1990).

59. F. M. Fowkes and D. W. Dwight, J. Adhesion Sci. Technol. 1, 7(1987).

60. L. Kozma and I. Olefjord, Mater. Sci. Technol., 3, 860(1987).

61. F. Nitschke, J. Adhesion Sci. Technol., 4, 41(1990).

62. J. S. Mijovic and J. A. Koutsky, Polym. Plast. Technol. Eng., 9, 139(1977).

63. J. Leu and K. F. Jensen, Mater. Res. Soc. Symp. Proc., 153, 181(1989).

64. Y. Momose, M. Noguchi and Okazaki, Nucl. Instrum. Methods Phys. Res., Section B, B39, 805(1989).

65. D. W. Fake, J. M. Newton, and J. F. Watts et al., Surf. Interface Anal., 10, 416(1987).

66. F. Kokai, H. Saito and T. Fujioka, Proc. SPIE-Int. Sco. Opt. Eng., 1190, 95(1989).

67. Y. Novis, J. J. Pireaux and A. Brezini et al., J. Appl. Phys., 64, 365(1988).

68. K. Allmer, A. Hult and B. Raanby, J. Polym. Sci., Part A, 27, 3419(1989).

69. K. Allmer, A. Hult and B. Raanby, J. Polym. Sci., Part A, 27, 3405(1989).

70. J. K. Hirvonen, Annu. Rev. Mater. Sci., 19, 401(1989).

71. P. Bertrand, Y. DePuydt and J. M. Beuken et al., Nucl. Instrum. Methods Phys. Res., Section B, B19-20, 887(1987).

72. H. C. Kim, J. H. Song, and G. L. Wikes et al., J. Appl. Polym. Sci., 38, 1515(1989).

73. P. Boulanger, J. Riga and J. Delhale et al., Polymer, 29, 797(1988).

74. H. Yasuda, J. Macromol. Sci. Chem., A10, 383(1976).

75. H. V. Boegin, "Plasma Science and Technology", Cornell University Press, Ithaca, New York (1982).

76. E. Ruckenstein and D. B. Chung, J. Coll. Interf. Sci., 123, 170(1988).

77. D. Cohn, A. S. Hoffman and B. D. Ratner, J. Appl. Polym. Sci., 33, 1(1987).

78. S. Lenka, P. L. Nayak and I. B. Moharity, ibid., 33, 21(1987).

79. M. T. Razzak, K. Otsuhata and Y. Tabata, ibid., 33, 2345(1987).

80. M. H. Rao, K. N. Rao and H. T. Lokhande et al., ibdi., 33, 2707(1987).

81. G. M. Whitesides, J. R. Rasmussen, and E. R. Stedronsky, J. Am. Chem. Soc., 99, 4736(1977).

82. G. M. Whitesides, J. R. Rasmussen, and D. E. Bergbreiter, ibid., 99,

4746(1977).

83. G. M. Whitesides and M. D. Wilson, ibid., 110, 8718(1988).

84. G. M. Whitesides and M. D. Wilson, and G. S. Ferguson, ibid., 112, 1244(1990).

85. G. M. Whitesides and C. D. Bain, ibid., 110, 5897(1988).

86. G. M. Whitesides, S. R. Holmes-Farley and R. Stephen et al., Langmuir, 1, 725(1985).

87. G. M. Whitesides, S. R. Holmes-Farley and R. Stephen, ibid., 4, 921(1988).

88. G. M. Whitesides, S. R. Holmes-Farley, and R. H. Reamey et al., ibid., 3, 799(1987).

89. G. M. Whitesides and S. R. Holmes-Farley, ibid., 3, 62(1987).

90. D. W Dwight and W. M. Riggs, J. Coll. Interf. Sci., 47, 650(1974).

91. D. J. Barker, D. M. Brewis and R. H. Dahm rt al., Polymer, 19, 856(1978).

92. J. Jansta, Electrochim. Acta, 26, 233(1981).

93. T. Masuda and M. H. Litt, J. Polym. Sci. Polym. Chem., 12, 489(1974).

94. H. W. Gibson and F. C. Bailey, Macromolecules, 13, 34(1980).

95. K. J. Kuhn, B. Hahn and V. Percec et al., Appl. Spectrosc., 41, 843(1987).

96. M. W. Urban and E. Salazar-Rojas, Macromolecules, 21, 372(1988).

97. H. Y. Erbil, J. Appl. Polym. Sci., 33, 1397(1987).

98. J. L. Koenig, E. G. Chatzi and S. L. Tidvick, Polym. Prepr. Am. Chem. Soc. Div. Polym. Chem., 28, 13(1987).

99. B. D. Ratner and T. A. Horbett, J. Coll. Interf. Sci., 83, 630(1981).

100. J. J. Engel and R. N. Fitzwater, in "Adhesion and Cohesion", T. Weiss ed., p.89, Elsevier, Amsterdam, (1962).

101. G. P. Anderson, S. J. Bennett and K. L. DeVries, "Analysis and Testing of Adhesive Bonds", p.82, Academic Press, New York (1977).

102. S. H. Lee and E. Ruckenstein, J. Coll. Interf. Sci., 120, 529(1987).

103. C. S. P. Sung, C. B. Hu, and E. W. Merrill, Polym. Prepr., 19, 20(1978).

104. R. L. Schmitt, J. A. Gardella, and J. H. Magill et al., Macromolecules, 18, 2675(1985).

105. Z. Wang, and D. Chen, "Polymeric Adhesives", p.294, Shanghai Sci. Technol. Publisher, Shanghai (1988).

106. S. Pawlenko, "Organosilicone Chemistry", p.46, Awlter Degruyter, Berlin (1986).

107. K. Meguro, J. Adhesion Sci. Technol., 4 , 393(1990).

108. E. J. Berger, ibid., 4, 373(1990).

109. J. F. Watts and E. M. Gibson, in "Adhesion 90", Proceeding the 4th International Conference, 5-1, University of Cambridge, England (1990).

110. D. H. K. Pan and W. M. Prest, Jr., J. Appl. Phys., 58, 2861(1985).

111. H. R. Thomas and J. J. O'Malley, Macromolecules, 12, 323(1979).

112. H. R. Thomas, G. M. Lee and J. J. O'Malley, ibid., 12, 996(1979).

113. H. R. Thomas and J. J. O'Malley, ibid., 14, 1316(1981).

114. R. W. Perala and E. W. Merrill, J. Coll. and Interf. Sci., 101, 120(1984).

115. J. D. Minford, SAMPE Qarterly, 9 (4), 18(1978).

116. N. A. DeBruyne, Aero Research Technical Notes, No. 168, p.1 (1956).

117. H. Schonhorn, C. Frisch and T. K. Kwei, J. Appl. Phys., 37, 4967(1966).

118. J. A. Marceau, SAMPE Quarterly, 9, (4), 1(1978).

119. R. J. Good, in "Adsorption at Interfaces", K. L. Mittal ed., Am. Chem. Soc. Symposium Series 8, p. 28, Am. Chem. Soc., Washington (1975).

120. D. K. Owens and R. C. Wendt, J. Appl. Polymer Sci., 13, 1740(1969).

121. J. A. Filbey, "Factors Affecting the Durability of Ti-6Al-4V/Epoxy Bonds", Ph. D. Dissertation, Virginia Polytechnic Institute & State University, Blacksburg, VA (1987).

122. C. U. Ko, "Effect of Surface Treatment on the Mechanical Properties of the Polysulfone-Al/Li Bonded System Including Thin Film Studies of Moisture Intrusion and the Viscoelastic Response of the Interphase Region", Ph. D. Dissertation, Virginia Polytechnic Institute & State University, Blacksburg, VA (1988).

123. G. D. Davis and J. D. Venables, in "Durability of Structural Adhesives", A. J. Kinloch ed., Chap. 2, p.43, Applied Sci. Publishers, London (1983).

124. E. A. Ledbury, A. G. Miller and P. D. Peters et al., in "Proceedings of the 12th National SAMPE Technical Conf.", p.935, SAMPE, Azusa, CA (1980).

125. W. Brockmann, O. D. Hennemann and H. Kollek et al., Int. J. Adhesion Adhesives, 6, 115(1986).

126. J. A. Marceau, in "Adhesive Bonding of Aluminum Alloys", E. W. Thrall and R. W. Shannon ed., p.51, Marcel Dekker, New York (1985).

127. K. K. Knock and M. C. Locke, in "Adhesion Aspects of Polymeric Coatings", K. L. Mittal ed., p.301, Plenum Press, New York (1983).

128. Standard Practice for Preparation of Aluminum Surface for Structural Adhesive Bonding (phosphoric acid anodization), ASTM D 3933-80 (1980).

129. G. M. Whitesides and C. D. Bain, J. Phys. Chem., 93, 1670(1989).

130. M. P. Seah and W. A. Dench, Surface Interface Anal., 1, 2(1979).

131. J. D. Andrade, S. M. Ma and R. N. King, J. Elec. Chem. Spect. Related Phen., 17, 181(1979).

132. E. Cartier and P. Pfluger, Appl. Phys., A 44, 43(1987).

133. P. D. Frayer, in "Polyimides", Vol. 1, K. L. Mittal ed., p.273, Plenum Press, New York (1982).

134. R. M. Silverstein, G. Clayton Bassler and T. C. Morrill, "Spectrometric Indentification of Organic Compounds", 4th edition, p.121, John Wiley & Sons, New York (1981).

135. R. C. Weast, M. J. Astle and W. H. Beyer, "CRC Handbook of Chem. Phys.", 67th edition, F-32, CRC Press, Florida (1987).

136. R. A. Dickie, J. E. DeVries and J. W. Holubka, J. Adhesion Sci. Technol. 3, 89(1989).

137. J. C. Bolger, in "Adhesion Aspect of Polymer Coatings", K. L. Mittal ed., p.3, Plenum Press, New York (1981).

VITA

The author, Tingdong Lin, was born in Zhanjiang city, Guangdong, China on February 21, 1961. The son of Mr. and Mrs. Shangqin Lin, he lived in Lianjiang county and attended school there for nine years. One year ahead of graduation, he passed a national college admission examination and was admitted to Zhongshan University, Guangzhou, China, and majored in chemistry. He spent four years for his degree of Bachelor of Science. He continued his study at the same university for another three years for his first degree of Master of Science majoring in polymer chemistry.

Graduated in 1985, he worked in an adhesive research group in the National Center for Analysis and Measurement, Guangzhou, China, as an associate researcher in developing pressure sensitive adhesives and water based adhesives.

In August, 1986, he entered the physical chemistry program at the University of Miami, Florida, the U. S. A. He was a vice-chairman of the Friendship Club of Chinese Students and Scholars and was given the "excellent leadership" award there. Two years later, he left the University with a non-thesis Master of Science degree. He began graduate work in chemistry at Virginia Polytechnic Institute and State University in August, 1988. He studied polymer/metal adhesion under the guidance of Dr. J. P. Wightman. He has presented poster papers on his research at the 13th annual meeting of the Adhesion Society and the 64th Colloid and Surface Science Symposium in 1990. He is a member of the Adhesion Society.

He was married to Yanmei Zhang, Shoagun, Guangdong, China, on December 21, 1988. His first daughter Virginia Qi Lin was born in Blacksburg, Virginia, on September 9, 1990.